RESONATING-GROUP METHOD FOR NUCLEAR MANY-BODY PROBLEMS*

Y. C. TANG and M. LeMERE

School of Physics, University of Minnesota
Minneapolis, Minnesota 55455, U.S.A.

and

D. R. THOMPSON**

Institut für Theoretische Physik der Universität
Tübingen, D-7400 Tübingen, Germany

*Work supported in part by the U. S. Department of Energy under Contract No. E(11-1)-1764.

**Alexander von Humboldt Stiftung Fellow.

DISCLAIMER

Contents

Abstract

The resonating-group method is a microscopic method which uses fully antisymmetric wave functions, treats correctly the motion of the total center of mass, and takes cluster correlation into consideration. In this review, we discuss the formulation of this method for various nuclear many-body problems, and describe a complex-generator-coordinate technique which has been employed to evaluate matrix elements required in resonating-group calculations. Several illustrative examples of bound-state, scattering, and reaction calculations, which serve to demonstrate the usefulness of this method, are presented. Finally, by utilizing the results of these calculations, we discuss the role played by the Pauli principle in nuclear scattering and reaction processes.

1. Introduction

The method of the resonating-group structure or the resonating-group method (RGM) was proposed in 1937 by Wheeler [1], based on the viewpoint that nucleons in nuclei spend fractions of their time in various substructures or clusters. In the forties and fifties, this method was extensively employed by especially the groups at the University of London [2] to study the problems of nuclear scattering and reactions. The results thus obtained generally agreed fairly well with experiment. However, because of computational difficulties, only very light systems could be investigated, namely, those systems which involve two s-shell nuclei in both the incident and the outgoing channels.

This method was given a physical interpretation in 1958 by Wildermuth and Kanellopoulos [3]. These authors contended that, because of the on-the-average attractive nature of the nuclear forces, there exist in nuclei relatively long-range correlations which manifest themselves through the formation of nucleon clusters [4,5]. In particular, they have emphasized the important role played by the Pauli exclusion principle which causes these cluster correlations to become the strongest in the nuclear surface region. Using such a cluster picture, commonly referred to as the nuclear cluster model, they have qualitatively and semi-quantitatively explained the essential features of many nuclear systems [6,7]. The mathematical formulation of the cluster model is, however, basically the same as that of the resonating-group method; in this review we shall, therefore, make no distinction between these two descriptions.

To give a general idea of what the resonating-group method is, we should

state that it is a microscopic method which explicitly takes cluster correlations into account. It has certain important features which distinguish itself from other methods commonly used in nuclear-physics studies. These features are as follows:

(i) It employs totally antisymmetric wave functions and, therefore, takes the Pauli exclusion principle fully into account.

(ii) It utilizes a nucleon-nucleon potential which explains reasonably well the two-nucleon low-energy scattering data.

(iii) It treats correctly the motion of the total center of mass.

(iv) It considers nuclear bound-state, scattering, and reaction problems from a unified viewpoint.

(v) It can be used to study cases where the particles involved in the incoming and outgoing channels are arbitrary composite nuclei.

Because of these features, resonating-group calculations are generally rather difficult to perform, especially when the number of nucleons involved in the system is large. Thus, even though there was a substantial number of such calculations done in the sixties [8], these were mostly simple extensions and modifications of previously reported works. Indeed, it was frequently remarked [9] that the requirement of antisymmetrization causes insurmountable computational difficulties and, therefore, the resonating-group method cannot be expected to be useful in studying systems containing more than eight nucleons. This is, of course, no longer true. With the development of generator-coordinate techniques for continuum studies since about 1970 [10-13], it now becomes possible to perform scattering calculations for rather large systems, such as the scattering of ^{16}O by ^{40}Ca [14] and so on. In fact, it is certain that even microscopic reaction calculations, such as $^{18}O(p,t)^{16}O$,

are feasible, and these calculations will undoubtedly be performed in the near future.

The formulation of the resonating-group method is described in sect. 2. This description will be relatively brief, because a detailed account of it has recently been given elsewhere [5]. Section 3 is devoted to the discussion of a complex-generator-coordinate technique [11,12,15,16], which was developed to facilitate the computation of the various matrix elements involved in resonating-group calculations. In this technique, the essential idea is to express the wave function as a linear superposition of antisymmetrized products of single-particle wave functions or Slater determinants. Then, by employing well-developed methods of dealing with product functions, one can usually carry out the analytical calculation of these matrix elements in a relatively straightforward manner.

Results of representative bound-state, scattering, and reaction calculations are presented in sect. 4. Here the purpose is not only to demonstrate the general utility of the resonating-group method in treating nuclear problems, but also to show how one can obtain better agreement with experiment by systematically improving the resonating-group trial wave function.

From the results of resonating-group calculations, one obtains information concerning the effects of the Pauli principle in nuclear systems. In sect. 5, we shall describe its influence on the effective local interaction between two composite clusters, and discuss the relationship between this principle and the various direct-reaction processes commonly employed in phenomenological studies.

Concluding remarks are given in sect. 6. Here also, we shall mention some possible problems which should be considered in the future by the resonating-group approach.

2. Formulation of the resonating-group method

2.1. Reformulation of the Schrödinger equation

As a starting point, we rewrite the time-independent Schrödinger equation

$$(H - E_T)\Psi = 0 \tag{1}$$

in the form of a projection equation

$$\langle \delta\Psi \mid H - E_T \mid \Psi \rangle = 0. \tag{2}$$

In eqs. (1) and (2), E_T is the total energy of the system and H is a Galilean-invariant Hamiltonian operator given by

$$H = \sum_{i=1}^{N} \frac{1}{2M} \underline{p}_i^2 + \sum_{i<j=1}^{N} V_{ij} - T_{cm} , \tag{3}$$

with N being the number of nucleons, T_{cm} being the kinetic-energy operator of the total center-of-mass, and V_{ij} being a nucleon-nucleon potential chosen to fit the two-nucleon scattering data especially in the low-energy region.

If $\delta\Psi$ represents a completely arbitrary variation in the space of all many-nucleon functions, then it is clear that eqs. (1) and (2) are entirely equivalent. The advantage of eq. (2) is that, as has been emphasized in ref. [5], this equation does allow one to conveniently treat the incoming and outgoing channels in a symmetrical way, which is an important consideration in the formulation of a flexible many-body nuclear-reaction theory. In addition, of course, eq. (2) provides a convenient basis for approximate, variational calculations in practical problems.

We shall now briefly discuss the general properties of the projection

equation (2). Let us make for ψ the ansatz

$$\psi = \sum_r a_r \phi_r + \int a_p \phi_p \, dp \equiv \sum_k a_k \phi_k \quad , \tag{4}$$

where the coefficients a_r and a_p are the discrete and continuous linear variational amplitudes for the basis functions ϕ_r and ϕ_p, respectively. The choice of the basis functions ϕ_k is arbitrary — they must be linearly independent, but need not be orthogonal to one another. Indeed, this latter point is an essential one, because only by choosing in general a nonorthogonal set of functions can one expect to introduce the incoming and outgoing channels symmetrically into the theory. Now, one can easily show [5] that, due to the hermiticity of H and the fact that all variational parameters are contained linearly in ψ , any two solutions ψ_m and ψ_n of eq. (2) are orthonormalized if all degeneracies are removed, and the Hamiltonian H can be represented by a real diagonal matrix, i.e.,

$$\langle \psi_m \mid \psi_n \rangle = \delta(m,n) \tag{5}$$

and

$$\langle \psi_m \mid H \mid \psi_n \rangle = E_T^m \, \delta(m,n) \quad , \tag{6}$$

where δ (m,n) represents the Kronecker δ-function if m is a discrete index and the Dirac δ-function if m is a continuous index. These relations are in fact true, even when one restricts the number of linear variation parameters or, in other words, when one works only in a restricted function-space. This is important, because in practical problems one certainly cannot expect to always use a set of basis functions which span the complete function-space.

A proper choice of the basis-function set is dictated by the requirement that in practical calculations one must severely limit the number of ϕ_k in the trial function ψ . In this respect, it is important to realize that the Pauli principle, expressed by the antisymmetrization of the wave function, has the effect of reducing greatly the differences between apparently different nonorthogonal wave functions when the nucleons are close to one another. From this it follows that, at relatively low excitation energies, the number of many-nucleon configurations which one needs for approximate calculations can usually be made so small that such calculations become quantitatively feasible.

2.2. Basis wave functions in cluster representation

As was mentioned in the Introduction, the cluster model has been quite successful in explaining qualitatively the features of many nuclear systems. It seems desirable, therefore, to adopt as basis functions generalized cluster wave functions [5] which describe the motion of a system of two or more clusters. Thus, in the resonating-group method one adopts a trial function ψ which has the following schematic form:

$$\psi = \mathcal{A}\Big\{ \sum_i \Phi(A_i)\Phi(B_i)F_i(\underset{\sim}{R}_i) + \sum_j \Phi(A_j)\Phi(B_j)\Phi(C_j)F_j(\underset{\sim}{R}_{j1},\underset{\sim}{R}_{j2}) + \sum_k \Phi(A_k)\Phi(B_k)\Phi(C_k)\Phi(D_k)F_k(\underset{\sim}{R}_{k1},\underset{\sim}{R}_{k2},\underset{\sim}{R}_{k3}) + \cdots + \sum_m c_m \mathcal{F}_m \Big\} \mathcal{Z}(\underset{\sim}{R}_{cm}) \qquad (7)$$

In the above equation, $\mathcal{A}$ is an antisymmetrization operator given by

$$\mathcal{A} = \sum_P (-1)^p P \quad , \tag{8}$$

where the sum extends over all permutations P which can be carried out on the nucleon coordiantes, and p is the number of interchanges that make up the permutation P. The functions Φ describe the internal behaviour of the clusters, while $Z(\underset{\sim}{R}_{cm})$ is a normalizable function describing the total c.m. motion. The functions $F_i(\underset{\sim}{R}_i)$, $F_j(\underset{\sim}{R}_{j1}, \underset{\sim}{R}_{j2})$, $F_k(\underset{\sim}{R}_{k1}, \underset{\sim}{R}_{k2}, \underset{\sim}{R}_{k3})$, and so on are relative-motion functions in two-, three-, four-, and more-cluster configurations, with $\underset{\sim}{R}_i$ and so on being Jacobi coordinates defined with respect to the centers of mass of the various clusters. The distortion functions $\mathcal{A}\left[\mathcal{G}_m Z(\underset{\sim}{R}_{cm})\right]$ are chosen to improve the wave function in the strong-interaction region; they vanish for large internucleon and intercluster distances.

We should mention that, with the exception of the functions $\mathcal{A}\left[\mathcal{G}_m Z\right]$, the other basis functions are contained implicitly in the generalized cluster functions (channel functions) in eq. (7). Consider, for example, a two-cluster term

$$\psi_2 = \mathcal{A}\left[\Phi(A)\Phi(B)F(\underset{\sim}{R})\, Z(\underset{\sim}{R}_{cm})\right] \tag{9}$$

This term can be written in a parameter representation as

$$\psi_2 = \int \mathcal{A}\left[\Phi(A)\Phi(B)\delta(\underset{\sim}{R} - \underset{\sim}{R}'')\, Z(\underset{\sim}{R}_{cm})\right] F(\underset{\sim}{R}'')\, d\underset{\sim}{R}'' \quad , \tag{10}$$

where $\underset{\sim}{R}''$ is a parameter coordinate on which the operator $\mathcal{A}$ does not act.

From the form of eq. (10), it can be seen that $\mathcal{A}\left[\phi(A)\phi(B)\delta(\underset{\sim}{R}-\underset{\sim}{R}'')\mathcal{Z}(\underset{\sim}{R}_{cm})\right]$ represents a continuous set of basis functions and $F(\underset{\sim}{R}'')$ represents a continuous set of variational amplitudes.

The basis functions chosen here are not orthogonal to each other.* As has been pointed out previously, this does not cause any basic difficulty, because the solutions of the projection equation are always mutually orthogonal if all degeneracies are removed. In addition, we should mention that this basis set is certainly overcomplete. This also does not pose any problem, since for practical calculations it is always necessary to use only a small number of channel and distortion functions in the expansion for ψ .

The variation $\delta\psi$ specifies the function space used in the calculation. This function space is defined through arbitrary variations of the linear functions F_i, F_j, $\cdots$, and the linear amplitudes c_m contained in the trial function ψ of eq. (7). By substituting the expressions for $\delta\psi$ and ψ into the projection equation (2), one then obtains a set of coupled integro-differential and integral equations which these linear functions and linear amplitudes satisfy. This will be discussed further in the next subsection.

As is obvious, the computation will in general become quite complicated if the function space is taken to be rather large. Thus, in practice, one must limit the extension of this space by using relatively simple forms for ψ , chosen according to physical intuition and energetical arguments. For instance, in the five-nucleon case, one might start by taking just one term in eq. (7), which represents a $n + \alpha$ cluster configuration with the α particle in its ground state. This results in the so-called

*It should be noted that even basis functions $\mathcal{A}\left[\phi(A)\phi(B)\delta(\underset{\sim}{R}-\underset{\sim}{R}'')\mathcal{Z}(\underset{\sim}{R}_{cm})\right]$ with different values of $\underset{\sim}{R}''$ are not orthogonal to each other.

single-channel approximation without specific distortion (see subsection 4.2a of ref. [5]). Because the α particle has a low compressibility and is, therefore, not easily distortable, one does find that this approximation can yield satisfactory results in the low-excitation region [17]. If one proceeds further to consider higher energies at which the α particle can be broken up, then one should improve the calculation by including also the d + t cluster configuration, with both the deuteron and the triton in their ground states. Thus one sees that, in the resonating-group approach, one makes successive improvements until the calculation becomes computationally infeasible. When such a stage is reached, then one may have to adopt more phenomenological means, such as the introduction of imaginary potentials and so on.

2.3. Derivation of coupled equations

In this subsection, we show how to derive the coupled equations which the linear variational functions and amplitudes satisfy. The derivation will be performed by assuming that the clusters have no internal angular momentum. This assumption is made merely for clarity in presentation; in actual calculations, the cluster internal angular momenta must of course be explicitly taken into consideration.

2.3a. Single-channel calculation without specific distortion

We start our discussion by considering the simplest case, namely, the case in which there is only one two-cluster open channel and where the specific distortion effect is neglected. In this case, the wave function is written as

$$\psi = \mathcal{A}\left[\phi(A)\phi(B)F(\underline{R})\,Z(\underline{R}_{cm})\right]$$

$$= \int \mathcal{A}\left[\phi(A)\phi(B)\delta(\underline{R}-\underline{R}'')Z(\underline{R}_{cm})\right]F(\underline{R}'')\,d\underline{R}'' \qquad (11)$$

By writing the variation of ψ also in a parameter representation, i.e.,

$$\delta\psi = \int \mathcal{A}\left[\phi(A)\phi(B)\,\delta(\underline{R}-\underline{R}')\,Z(\underline{R}_{cm})\right]\delta F(\underline{R}')\,d\underline{R}', \qquad (12)$$

we obtain then from the projection equation (2) the following equation:

$$\int \left[\mathcal{H}(\underline{R}',\underline{R}'') - E_T\,\mathcal{N}(\underline{R}',\underline{R}'')\right]F(\underline{R}'')\,d\underline{R}'' = 0, \qquad (13)$$

where

$$\mathcal{H}(\underline{R}',\underline{R}'') = \left\langle \phi(A)\phi(B)\delta(\underline{R}-\underline{R}')Z(\underline{R}_{cm}) \,|\, H \,|\, \mathcal{A}\left[\phi(A)\phi(B)\delta(\underline{R}-\underline{R}'')Z(\underline{R}_{cm})\right]\right\rangle, \qquad (14)$$

$$\mathcal{N}(\underline{R}',\underline{R}'') = \left\langle \phi(A)\phi(B)\delta(\underline{R}-\underline{R}')Z(\underline{R}_{cm}) \,|\, \mathcal{A}\left[\phi(A)\phi(B)\delta(\underline{R}-\underline{R}'')Z(\underline{R}_{cm})\right]\right\rangle, \qquad (15)$$

with the Dirac-bracket notation denoting an integration over all spatial coordinates and a summation over all spin and isospin coordinates. Note that, in eqs. (14) and (15), the antisymmetrization operator $\mathcal{A}$ occurs only on the ket side of the Dirac bracket; this is permissible, since this operator is a hermitian operator which commutes with the Hamiltonian operator H and satisfies the relation

$$\mathcal{A}^2 = (N_A + N_B)!\ \mathcal{A} \quad , \tag{16}$$

with N_A and N_B being the numbers of nucleons in the clusters A and B, respectively.

To proceed, let us write

$$\mathcal{A} = \mathcal{A}' \mathcal{A}_A \mathcal{A}_B \quad , \tag{17}$$

where $\mathcal{A}_A$ and $\mathcal{A}_B$ are, respectively, antisymmetrization operators for the nucleons in clusters A and B, and $\mathcal{A}'$ is an antisymmetrization operator which interchanges nucleons in different clusters. Then, eq. (15) can be written as

$$\mathcal{N}(\underset{\sim}{R}', \underset{\sim}{R}'') = \left\langle \phi(A)\phi(B)\delta(\underset{\sim}{R}-\underset{\sim}{R}')Z(\underset{\sim}{R}_{cm}) \middle| \mathcal{A}' \left[\hat{\phi}(A)\hat{\phi}(B)\delta(\underset{\sim}{R}-\underset{\sim}{R}'')Z(\underset{\sim}{R}_{cm}) \right] \right\rangle , \tag{18}$$

with

$$\hat{\phi}(A) = \mathcal{A}_A\, \phi(A) \quad , \tag{19}$$

and

$$\hat{\phi}(B) = \mathcal{A}_B\, \phi(B) \quad . \tag{20}$$

By defining further

$$\mathcal{A}' = 1 + \mathcal{A}'' \quad , \tag{21}$$

we can separate $\mathcal{N}(\underset{\sim}{R}', \underset{\sim}{R}'')$ into two parts, i.e.,

$$\mathcal{N}(\underset{\sim}{R}', \underset{\sim}{R}'') = \mathcal{N}_D(\underset{\sim}{R}', \underset{\sim}{R}'') + \mathcal{N}_E(\underset{\sim}{R}', \underset{\sim}{R}'') \quad , \tag{22}$$

where the direct part $\mathcal{N}_D$ is

$$\mathcal{N}_D(\underline{R}',\underline{R}'') = \langle \phi(A)\phi(B)\delta(\underline{R}-\underline{R}')\mathcal{Z}(\underline{R}_{cm}) | \hat{\phi}(A)\hat{\phi}(B)\delta(\underline{R}-\underline{R}'')\mathcal{Z}(\underline{R}_{cm})\rangle \quad (23)$$

and the exchange part $\mathcal{N}_E$ is

$$\mathcal{N}_E(\underline{R}',\underline{R}'') = \langle \phi(A)\phi(B)\delta(\underline{R}-\underline{R}')\mathcal{Z}(\underline{R}_{cm}) | \mathcal{A}''[\hat{\phi}(A)\hat{\phi}(B)\delta(\underline{R}-\underline{R}'')\mathcal{Z}(\underline{R}_{cm})]\rangle \quad (24)$$

For $\mathcal{N}_D$ we now perform the integration over the relative coordinate $\underline{R}$. The result is

$$\mathcal{N}_D(\underline{R}',\underline{R}'') = \langle \phi(A)\phi(B)\mathcal{Z}(\underline{R}_{cm}) | \hat{\phi}(A)\hat{\phi}(B)\mathcal{Z}(\underline{R}_{cm})\rangle_{\underline{R}} \delta(\underline{R}'-\underline{R}'') , \quad (25)$$

where the notation $\langle \ \rangle_{\underline{R}}$ is introduced to indicate integration over internal spatial coordinates of the clusters and the total c.m. coordinate, summation over all spin and isospin coordinates, but no integration over the relative coordinate $\underline{R}$. For convenience, we shall adopt the normalization condition

$$\langle \phi(A)\phi(B)\mathcal{Z}(\underline{R}_{cm}) | \hat{\phi}(A)\hat{\phi}(B)\mathcal{Z}(\underline{R}_{cm})\rangle_{\underline{R}} = 1 \quad (26)$$

With this particular normalization, the quantity $\mathcal{N}_D$ then takes on the simple form

$$\mathcal{N}_D(\underline{R}',\underline{R}'') = \delta(\underline{R}'-\underline{R}'') . \quad (27)$$

Similarly, one can separate $\mathcal{H}(\underline{R}', \underline{R}'')$ also into two parts, i.e.,

$$\mathcal{H}(\underline{R}', \underline{R}'') = \mathcal{H}_D(\underline{R}', \underline{R}'') + \mathcal{H}_E(\underline{R}', \underline{R}'') \quad , \tag{28}$$

with

$$\mathcal{H}_D(\underline{R}', \underline{R}'') = \langle \phi(A)\phi(B)\delta(\underline{R}-\underline{R}')\mathcal{Z} \,|\, H \,|\, \hat{\Phi}(A)\hat{\Phi}(B)\delta(\underline{R}-\underline{R}'')\mathcal{Z} \rangle \tag{29}$$

and

$$\mathcal{H}_E(\underline{R}', \underline{R}'') = \langle \phi(A)\phi(B)\delta(\underline{R}-\underline{R}')\mathcal{Z} \,|\, H \,|\, \mathcal{A}''[\hat{\Phi}(A)\hat{\Phi}(B)\delta(\underline{R}-\underline{R}'')\mathcal{Z}] \rangle \tag{30}$$

The expression for $\mathcal{H}_D$ can be simplified by noting that the Galilean-invariant Hamiltonian H of eq. (3) can be written as

$$H = H_A + H_B + H' \quad , \tag{31}$$

where H_A and H_B are, respectively, the internal Hamiltonians of the clusters A and B, and H' is a Hamiltonian for the relative motion, given by

$$H' = -\frac{\hbar^2}{2\mu}\nabla_{\underline{R}}^2 + V' \quad , \tag{32}$$

with μ being the reduced mass of the two clusters and

$$V' = \sum_{i \in A} \sum_{j \in B} V_{ij} \tag{33}$$

The two-nucleon potential V_{ij} will in general contain all types of exchange operators; however, since totally antisymmetrized wave functions are used in resonating-group calculations, we can always replace the space-exchange operator P^r_{ij} wherever it appears, by the operator $-P^\sigma_{ij} P^\tau_{ij}$ with P^σ_{ij} and P^τ_{ij} being the spin- and isospin-exchange operators, respectively. When this is done, we can then define a direct (local) potential $V_D(\underline{R})$ as

$$V_D(\underline{R}) = \langle \phi(A)\phi(B)\mathcal{Z}(\underline{R}_{cm}) \mid V' \mid \hat{\phi}(A)\hat{\phi}(B)\mathcal{Z}(\underline{R}_{cm}) \rangle_{\underline{R}} \qquad (34)$$

The cluster internal energies E_A and E_B are obtained by computing the expectation values of the Hamiltonians H_A and H_B, i.e.,

$$E_\lambda = \langle \phi(A)\phi(B)\mathcal{Z} \mid H_\lambda \mid \hat{\phi}(A)\hat{\phi}(B)\mathcal{Z} \rangle_{\underline{R}} \quad . \quad (\lambda = A, B) \qquad (35)$$

Using eqs. (26) and (31) - (35), we finally obtain

$$\mathcal{H}_D(\underline{R}', \underline{R}'') = \left[-\frac{\hbar^2}{2\mu} \nabla^2_{\underline{R}'} + V_D(\underline{R}') + E_A + E_B \right] \delta(\underline{R}' - \underline{R}'') \qquad (36)$$

By utilizing this expression and the expression for $\mathcal{N}_D(\underline{R}', \underline{R}'')$ of eq. (27), one sees that eq. (13) can be written more explicitly as

$$\left[-\frac{\hbar^2}{2\mu} \nabla^2_{\underline{R}'} + V_D(\underline{R}') - E \right] F(\underline{R}') + \int K(\underline{R}', \underline{R}'') F(\underline{R}'') \, d\underline{R}'' = 0 \qquad (37)$$

where E is the relative energy of the two clusters in the c.m. system, given by

$$E = E_T - E_A - E_B \tag{38}$$

and $K(\underline{R}', \underline{R}'')$ is an energy-dependent kernel function given by

$$K(\underline{R}', \underline{R}'') = \mathcal{H}_E(\underline{R}', \underline{R}'') - E_T \mathcal{N}_E(\underline{R}', \underline{R}'') \tag{39}$$

From this equation, it is seen that, if the two clusters are considered as structureless, then the effective interaction between them must be both non-local and energy-dependent.

From the above discussion, one also sees that if the antisymmetrization between nucleons in different clusters is neglected or, in other words, if the antisymmetrization operator $\mathcal{A}'$ is set as unity, then the kernel functions $\mathcal{H}_E$ and $\mathcal{N}_E$ will be equal to zero. In this crude approximation, the effective intercluster potential will therefore just be the direct potential V_D[18] (see Appendix A).

Next, we consider very briefly the case where the trial function is represented by a single three-cluster term [19], i.e.,

$$\psi = \mathcal{A}\left[\phi(A)\phi(B)\phi(C)F(\underline{R}_1, \underline{R}_2)Z(\underline{R}_{cm})\right] \tag{40}$$

Concerning this wave function, there is one important point which should be mentioned; that is, this trial function can also describe the behaviour of some two-cluster configurations. Consider the nucleus ^{6}Li as an example. Here the three-cluster n + p + α channel includes the two-cluster d + α channel. This is so, because the function $F(\underline{R}_1, \underline{R}_2)$ can assume a product form consisting of the deuteron bound-state function and the d + α

relative-motion function. Similarly, one can easily see that the $n + {}^5Li$ and $p + {}^5He$ channels are also included. On the other hand, the $t + {}^3He$ channel cannot be properly described by the wave function of eq. (40). This means that, if one wishes to consider the breakup reaction $^3He(t,np)\alpha$, then one must, in addition, introduce a two-cluster $t + {}^3He$ term into the resonating-group formulation.

By expressing ψ and $\delta\psi$ in parameter representations and using the projection equation (2), we obtain

$$\int [\mathcal{H}(\underline{R}_1', \underline{R}_2', \underline{R}_1'', \underline{R}_2'') - E_T \mathcal{N}(\underline{R}_1', \underline{R}_2', \underline{R}_1'', \underline{R}_2'')] F(\underline{R}_1'', \underline{R}_2'') d\underline{R}_1'' d\underline{R}_2'' = 0 , \quad (41)$$

where

$$\mathcal{H}(\underline{R}_1', \underline{R}_2', \underline{R}_1'', \underline{R}_2'') = \langle \Phi(A)\Phi(B)\Phi(C)\delta(\underline{R}_1 - \underline{R}_1')\delta(\underline{R}_2 - \underline{R}_2') \mathcal{Z}$$

$$| H | \mathcal{A} [\Phi(A)\Phi(B)\Phi(C)\delta(\underline{R}_1 - \underline{R}_1'')\delta(\underline{R}_2 - \underline{R}_2'') \mathcal{Z}] \rangle , \quad \cdots (42)$$

$$\mathcal{N}(\underline{R}_1', \underline{R}_2', \underline{R}_1'', \underline{R}_2'') = \langle \Phi(A)\Phi(B)\Phi(C)\delta(\underline{R}_1 - \underline{R}_1')\delta(\underline{R}_2 - \underline{R}_2') \mathcal{Z}$$

$$| \mathcal{A} [\Phi(A)\Phi(B)\Phi(C)\delta(\underline{R}_1 - \underline{R}_1'')\delta(\underline{R}_2 - \underline{R}_2'') \mathcal{Z}] \rangle , \quad \cdots (43)$$

and $\underline{R}_1'$, $\underline{R}_2'$, $\underline{R}_1''$, and $\underline{R}_2''$ are parameter coordinates which are not acted

upon by the antisymmetrization operator $\mathcal{A}$. Proceeding now in exactly the same manner as described above in the two-cluster case, we can again write eq. (41) in the following more explicit form:

$$\left[-\frac{\hbar^2}{2\mu_1} \nabla^2_{\underset{\sim}{R}'_1} - \frac{\hbar^2}{2\mu_2} \nabla^2_{\underset{\sim}{R}'_2} + V_D(\underset{\sim}{R}'_1, \underset{\sim}{R}'_2) - E \right] F(\underset{\sim}{R}'_1, \underset{\sim}{R}'_2)$$

$$+ \int K(\underset{\sim}{R}'_1, \underset{\sim}{R}'_2, \underset{\sim}{R}''_1, \underset{\sim}{R}''_2) F(\underset{\sim}{R}''_1, \underset{\sim}{R}''_2) \, d\underset{\sim}{R}''_1 d\underset{\sim}{R}''_2 = 0 \qquad (44)$$

where μ_1 and μ_2 are reduced masses, and E is the relative energy of the clusters given by

$$E = E_T - E_A - E_B - E_C \, , \qquad (45)$$

with E_A, E_B, and E_C being cluster internal energies.

If one is concerned with bound and sharp resonance states, then eq. (44) may be approximately solved by using the Ritz variational procedure employing trial wave functions which vanish in the asymptotic regions. For the consideration of three-body breakup reactions, some possibilities to utilize the derived direct potential $V_D(\underset{\sim}{R}'_1, \underset{\sim}{R}'_2)$ and energy-dependent kernel functions $K(\underset{\sim}{R}'_1, \underset{\sim}{R}'_2, \underset{\sim}{R}''_1, \underset{\sim}{R}''_2)$ have been recently discussed by Schmid [19] . It should be mentioned, however, that these functions have, in general, quite complicated structures. Thus, together with the fact that three-body boundary conditions are also complicated, we are of the opinion that for future progress to be realized in solving the breakup problem, more advanced mathematical techniques and computational innovations must first be made.

2.3b. Single-channel calculation with specific distortion

For some systems, the specific distortion effect may play an important role. This occurs in the d + α case [20, 21], for example, where the high compressibility of the deuteron cluster means that this cluster may be strongly distorted when it overlaps appreciably with the α cluster. Therefore, for a proper consideration of such systems, it will be necessary to introduce square-integrable distortion functions into the formulation such that the behaviour in the region of strong interaction may be adequately described.

Let us assume, for simplicity in discussion, that only one distortion function is introduced. The trial function is then given by

$$\psi = \psi_0 + c_1 \mathcal{A} [\mathcal{S}_1 z(\underset{\sim}{R}_{cm})] , \tag{46}$$

where ψ_0 is a channel function of the form given by eq. (11) and c_1 is a linear variational amplitude. By performing independent variations $\delta\psi_0$ and $\mathcal{A}[\mathcal{S}_1 z]\delta c_1$, the projection equation becomes

$$\langle \delta\psi_0 | H - E_T | \psi_0 \rangle + c_1 \langle \delta\psi_0 | H - E_T | \hat{\mathcal{S}}_1 z \rangle = 0 , \tag{47}$$

$$\langle \hat{\mathcal{S}}_1 z | H - E_T | \psi_0 \rangle + c_1 \langle \hat{\mathcal{S}}_1 z | H - E_T | \hat{\mathcal{S}}_1 z \rangle = 0 , \tag{48}$$

with

$$\hat{\mathcal{S}}_1 = \mathcal{A} \mathcal{S}_1 \tag{49}$$

Solving eq. (48) for c_1 and substituting the resultant expression into eq. (47) yields

$$\langle \delta\psi_0 \mid H + \tilde{V} - E_T \mid \psi_0 \rangle = 0 \quad , \tag{50}$$

where

$$\tilde{V} = - \frac{(H-E_T) \mid \hat{\mathcal{S}}_1 z \rangle \langle \hat{\mathcal{S}}_1 z \mid (H-E_T)}{\langle \hat{\mathcal{S}}_1 z \mid H - E_T \mid \hat{\mathcal{S}}_1 z \rangle} \tag{51}$$

By using eq. (26) and the normalization condition

$$\langle \mathcal{S}_1 z \mid \hat{\mathcal{S}}_1 z \rangle = 1 \quad , \tag{52}$$

we can write eq. (50) more explicitly as follows:

$$\left[-\frac{\hbar^2}{2\mu} \nabla^2_{\underline{R}'} + V_D(\underline{R}') - E \right] F(\underline{R}')$$

$$+ \int \left[K(\underline{R}', \underline{R}'') + K_1(\underline{R}', \underline{R}'') \right] F(\underline{R}'') \, d\underline{R}'' \quad , \tag{53}$$

where

$$K_1(\underline{R}', \underline{R}'') = - \frac{\lambda(\underline{R}') \lambda^*(\underline{R}'')}{\hat{E}_1 - E_T} \quad , \tag{54}$$

with

$$\lambda(\underline{R}') = \langle \phi(A)\phi(B)\delta(\underline{R}-\underline{R}')z \mid H - E_T \mid \hat{\mathcal{S}}_1 z \rangle \tag{55}$$

and $\hat{E}_1$ being the expectation value of H with respect to the distortion function, given by

$$\hat{E}_1 = \langle \mathcal{S}_1 z \mid H \mid \hat{\mathcal{S}}_1 z \rangle . \tag{56}$$

Thus, one sees that the addition of a distortion function introduces an extra nonlocal, energy-dependent, separable term into the effective internuclear potential.

It is a simple procedure to generalize to the case where many distortion functions are added to ψ_0 . The only complication arises because the functions $\mathcal{A}[\mathcal{S}_m z]$ are not orthogonal to each other. But this complication can be easily overcome by transforming to a basis set of orthonormal functions [see eq. (52)] which diagonalize the Hamiltonian H in the subspace spanned by the original distortion functions $\mathcal{A}[\mathcal{S}_m z]$.

2.3c. Coupled-channel calculation

We discuss in this subsection the resonating-group formulation of a two-channel problem. Here the trial function ψ has the form

$$\psi = \psi_f + \psi_g , \tag{57}$$

where

$$\psi_f = \mathcal{A}\left[\phi(A)\phi(B)F(\underset{\sim}{R}_f)\mathcal{Z}(\underset{\sim}{R}_{cm})\right] \tag{58}$$

and

$$\psi_g = \mathcal{A}\left[\phi(C)\phi(D)\,G(\underline{R}_g)\,Z(\underline{R}_{cm})\right] . \tag{59}$$

In the above equations, the ϕ's are cluster internal functions, chosen to satisfy the normalization condition (see p. 114 of ref. [5])

$$\left\langle \phi(A)\phi(B)Z(\underline{R}_{cm}) \middle| \hat{\phi}(A)\hat{\phi}(B)Z(\underline{R}_{cm}) \right\rangle_{\underline{R}_f}$$

$$= \left\langle \phi(C)\phi(D)Z(\underline{R}_{cm}) \middle| \hat{\phi}(C)\hat{\phi}(D)Z(\underline{R}_{cm}) \right\rangle_{\underline{R}_g} = 1 . \tag{60}$$

By substituting ψ and $\delta\psi$, expressed in parameter representations, into the projection equation, we obtain the following coupled equations:

$$\int \hat{K}_{ff}(\underline{R}'_f, \underline{R}''_f)\,F(\underline{R}''_f)\,d\underline{R}''_f + \int K_{fg}(\underline{R}'_f, \underline{R}''_g)\,G(\underline{R}''_g)\,d\underline{R}''_g = 0 , \tag{61}$$

$$\int \hat{K}_{gg}(\underline{R}'_g, \underline{R}''_g)\,G(\underline{R}''_g)\,d\underline{R}''_g + \int K_{gf}(\underline{R}'_g, \underline{R}''_f)\,F(\underline{R}''_f)\,d\underline{R}''_f = 0 , \tag{62}$$

where

$$\hat{K}_{ff}(\underline{R}'_f, \underline{R}''_f) = \left\langle \phi(A)\phi(B)\,\delta(\underline{R}_f - \underline{R}'_f)\,Z \mid H - E_T \mid \right.$$

$$\left. \mathcal{A}\left[\phi(A)\phi(B)\delta(\underline{R}_f - \underline{R}''_f)\,Z\right] \right\rangle , \tag{63}$$

$$\hat{K}_{gg}(\underline{R}'_g, \underline{R}''_g) = \langle \phi(C)\phi(D)\delta(\underline{R}_g - \underline{R}'_g)\mathcal{Z} \mid H - E_T \mid \mathcal{A}\left[\phi(C)\phi(D)\delta(\underline{R}_g - \underline{R}''_g)\mathcal{Z}\right] \rangle , \tag{64}$$

$$K_{fg}(\underline{R}'_f, \underline{R}''_g) = \langle \phi(A)\phi(B)\delta(\underline{R}_f - \underline{R}'_f)\mathcal{Z} \mid H - E_T \mid \mathcal{A}\left[\phi(C)\phi(D)\delta(\underline{R}_g - \underline{R}''_g)\mathcal{Z}\right] \rangle , \tag{65}$$

$$K_{gf}(\underline{R}'_g, \underline{R}''_f) = \langle \phi(C)\phi(D)\delta(\underline{R}_g - \underline{R}'_g)\mathcal{Z} \mid H - E_T \mid \mathcal{A}\left[\phi(A)\phi(B)\delta(\underline{R}_f - \underline{R}''_f)\mathcal{Z}\right] \rangle , \tag{66}$$

with $\underline{R}'_f$, $\underline{R}''_f$, $\underline{R}'_g$, and $\underline{R}''_g$ being parameter coordinates. If we now use the procedure described in subsection 2.3a, then it is easily seen that these coupled equations may be reduced to the following more familiar form:

$$\left[-\frac{\hbar^2}{2\mu_f}\nabla^2_{\underline{R}'_f} + V_{Df}(\underline{R}'_f) - E_f\right] F(\underline{R}'_f) + \int K_{ff}(\underline{R}'_f, \underline{R}''_f) F(\underline{R}''_f)\, d\underline{R}''_f + \int K_{fg}(\underline{R}'_f, \underline{R}''_g) G(\underline{R}''_g)\, d\underline{R}''_g = 0 , \tag{67}$$

$$\left[-\frac{\hbar^2}{2\mu_g}\nabla^2_{\underline{R}'_g} + V_{Dg}(\underline{R}'_g) - E_g\right] G(\underline{R}'_g) + \int K_{gg}(\underline{R}'_g, \underline{R}''_g) G(\underline{R}''_g)\, d\underline{R}''_g + \int K_{gf}(\underline{R}'_g, \underline{R}''_f) F(\underline{R}''_f)\, d\underline{R}''_f = 0 , \tag{68}$$

where μ_f and μ_g are, respectively, the reduced masses of the clusters in channels f and g, V_{Df} and V_{Dg} are direct potentials, E_f and E_g are relative energies given by

$$E_f = E_T - E_A - E_B \ , \tag{69}$$

$$E_g = E_T - E_C - E_D \ , \tag{70}$$

and K_{ff} and K_{gg} are energy-dependent kernel functions given by

$$K_{ff}(\underline{R}_f', \underline{R}_f'') = \langle \phi(A)\phi(B)\delta(\underline{R}_f - \underline{R}_f')\mathcal{Z} \,|\, H - E_T \,|\, \mathcal{A}''[\hat{\phi}(A)\hat{\phi}(B)\delta(\underline{R}_f - \underline{R}_f'')\mathcal{Z}] \rangle , \tag{71}$$

$$K_{gg}(\underline{R}_g', \underline{R}_g'') = \langle \phi(C)\phi(D)\delta(\underline{R}_g - \underline{R}_g')\mathcal{Z} \,|\, H - E_T \,|\, \mathcal{A}''[\hat{\phi}(C)\hat{\phi}(D)\delta(\underline{R}_g - \underline{R}_g'')\mathcal{Z}] \rangle . \tag{72}$$

From the expressions for these kernel functions, one sees that

$$K_{ff}(\underline{R}_f', \underline{R}_f'') = K_{ff}^*(\underline{R}_f'', \underline{R}_f') \ , \tag{73}$$

$$K_{gg}(\underline{R}_g', \underline{R}_g'') = K_{gg}^*(\underline{R}_g'', \underline{R}_g') \ , \tag{74}$$

$$K_{fg}(\underline{R}_f', \underline{R}_g'') = K_{gf}^*(\underline{R}_g'', \underline{R}_f') \ . \tag{75}$$

These relations follow, of course, from the hermiticity of the Hamiltonian operator.

By solving eqs. (67) and (68) subject to appropriate boundary conditions, one obtains information concerning various scattering and reaction processes.

For example, if the channels f and g denote, respectively, the d + t channel and the n + α channel, then performing a two-channel calculation in the manner described here will yield results for the scattering processes t(d,d)t and α(n,n)α, and the reaction process α(n,d)t.

The above-described two-channel formulation can be improved by the addition of one or more distortion functions. This will, of course, results in a more complicated set of coupled equations. The procedure to derive these equations is, however, essentially the same as that described in subsection 2.3b ; therefore, we shall not further go into it here.

3. Complex-generator-coordinate technique

3.1. General remarks

In resonating-group calculations, the major task is to compute the kernel functions given, for example, by eqs. (63)-(66). For these computations, one needs to carry out a substantial number of multi-dimensional spatial integrations. Because of the complicated nature of the resonating-group trial wave function caused by the requirement of total antisymmetrization and correct treatment of the c.m. motion, these integrations are generally rather tedious to perform, especially when the number of nucleons involved in the system is large. Indeed, this was the main reason which led a number of people to comment in the past that the resonating-group method is impracticable for any system containing more than eight nucleons.

The integration technique which was extensively used a few years ago is the so-called cluster-coordinate technique [5,22] . In this technique, one introduces as spatial variables of integration the internal and relative coordinates of the clusters and the total c.m. coordinate. This seems to be a natural set of integration variables to use, because the resonating-group trial wave function is explicitly expressed in terms of these coordinates. Then, by choosing functions of Gaussian dependence for both the spatial part of the wave function and the spatial part of the nucleon-nucleon potential, multi-dimensional integrals can be evaluated analytically.

The evaluation of matrix elements by the cluster-coordinate technique is, however, usually a quite tedious procedure. The main reason for this is that the Gaussian functions will have exponents which contain cross

terms in the cluster internal coordinates. For example, let us consider a translationally invariant α-cluster wave function of the form

$$\bar{\Phi}(\alpha) = \exp\left[-\frac{1}{2}\alpha \sum_{i=1}^{4} \underset{\sim}{\rho}_i^2\right] , \tag{76}$$

which depends on the internal coordinates $\underset{\sim}{\rho}_1$, $\underset{\sim}{\rho}_2$, and $\underset{\sim}{\rho}_3$, defined as

$$\underset{\sim}{\rho}_i = \underset{\sim}{r}_i - \underset{\sim}{R}_\alpha , \qquad (i = 1, 2, 3) \tag{77}$$

with $\underset{\sim}{R}_\alpha$ being the c.m. coordinate of the α cluster. Because the coordinate $\underset{\sim}{\rho}_4$ is not an independent variable, the exponent

$$\begin{aligned} -\frac{\alpha}{2}\sum_{i=1}^{4} \underset{\sim}{\rho}_i^2 &= -\frac{\alpha}{2}\left[\underset{\sim}{\rho}_1^2 + \underset{\sim}{\rho}_2^2 + \underset{\sim}{\rho}_3^2 + (-\underset{\sim}{\rho}_1 - \underset{\sim}{\rho}_2 - \underset{\sim}{\rho}_3)^2\right] \\ &= -\frac{\alpha}{2}\left(2\underset{\sim}{\rho}_1^2 + 2\underset{\sim}{\rho}_2^2 + 2\underset{\sim}{\rho}_3^2 + 2\underset{\sim}{\rho}_1\cdot\underset{\sim}{\rho}_2 + 2\underset{\sim}{\rho}_1\cdot\underset{\sim}{\rho}_3 + 2\underset{\sim}{\rho}_2\cdot\underset{\sim}{\rho}_3\right) \end{aligned} \tag{78}$$

contains such cross terms. Therefore, to compute the multi-dimensional integrals which involve integrands of Gaussian functions multiplied by polynomials of spatial coordinates, one must first diagonalize the quadratic terms in the exponents by applying linear coordinate transformations. For systems containing a relatively small number of nucleons ($N_A + N_B \lesssim 8$), this is not too difficult. However, when one deals with systems which contain a rather large number of nucleons, this diagonalization procedure can become very tedious due to the antisymmetrization of the wave function, because for every permutation of nucleons in different clusters, one has to introduce a different coordinate transformation. In addition, it is clear that the

cluster-coordinate technique is also not particularly suited for reaction calculations. This is so, since the natural choices for internal and relative coordinates in the incoming and outgoing channels are obviously not the same.

Because of these difficulties mentioned above, the cluster-coordinate technique has begun to lose favour and we shall, therefore, not discuss it here. Rather, we shall describe in this section another technique, the complex-generator-coordinate technique (CGCT), which uses as integration variables the nucleon coordinates themselves and which is especially useful for reaction calculations and for systems involving a rather large number of nucleons. This technique has been developed and extensively used by many authors [11, 12, 15, 16, 23, 24] within the last few years. As was mentioned in the Introduction, the main idea is to express the trial wave function as an integral of antisymmetrized products of single-particle functions and then make use of well-developed techniques in shell-model calculations to carry out an analytical evaluation of the required matrix elements.

In subsection 3.2, we give a general description of the complex-generator-coordinate technique. Then, in subsection 3.3, we consider a special case in which the internal behaviour of each cluster is described by a harmonic-oscillator shell-model wave function or a linear superposition of such wave functions. This special case is interesting, because with such internal functions the complex-generator-coordinate technique becomes particularly convenient.

Even with the complex-generator-coordinate technique, the derivation of the kernel functions is still a rather tedious process. Thus, it will be important to have a test which can be easily applied and which these functions must meet. Fortunately, in resonating-group calculations, a test satisfying

these criteria does exist. This is the so-called redundant-solution test which we shall describe in subsection 3.4.

3.2. Description of the complex-generator-coordinate technique

Let us consider a two-cluster function of the form

$$\Psi = \mathcal{A}\left[\phi(A)\phi(B)F(\underset{\sim}{R}_A - \underset{\sim}{R}_B)\mathcal{Z}(\underset{\sim}{R}_{cm})\right], \tag{79}$$

where

$$\phi(K) = \bar{\phi}(K)\xi_K(\nu_K, t_K) \tag{80}$$

with K = A or B and ξ_K being an appropriate spin-isospin function. The functions $\bar{\phi}(A)$ and $\bar{\phi}(B)$ are spatial parts of the cluster internal functions; they are assumed to be products of functions, with each function describing the motion of a nucleon with respect to the center of mass of the corresponding cluster. That is, we choose $\bar{\phi}(A)$ and $\bar{\phi}(B)$ to have the forms

$$\bar{\phi}(A) = \prod_{j=1}^{N_A} \varphi_j(\underset{\sim}{r}_j - \underset{\sim}{R}_A), \tag{81}$$

$$\bar{\phi}(B) = \prod_{k=N_A+1}^{N_A+N_B} \varphi_k(\underset{\sim}{r}_k - \underset{\sim}{R}_B), \tag{82}$$

with

$$\underset{\sim}{R}_A = \frac{1}{N_A}\sum_{j=1}^{N_A}\underset{\sim}{r}_j, \qquad \underset{\sim}{R}_B = \frac{1}{N_B}\sum_{k=N_A+1}^{N_A+N_B}\underset{\sim}{r}_k \tag{83}$$

The functions φ_j with j = 1 to N_A and φ_k with k = N_A + 1 to $N_A + N_B$ are chosen such that $\bar{\Phi}(A)$ and $\bar{\Phi}(B)$ describe properly the spatial behaviour of the clusters; they can be generated from an oscillator well, a Woods-Saxon well, or any other well which is appropriate.

Because of the presence of the cluster c.m. coordinates $\underset{\sim}{R}_A$ and $\underset{\sim}{R}_B$, the trial function ψ is not in the form of an antisymmetrized product of single-particle wave functions. However, by introducing an integral representation for ψ, we can show that the integrand can be represented in such a product form or, in other words, the integrand will contain no cross terms of the type $\underset{\sim}{r}_i \cdot \underset{\sim}{r}_j$. To show this, we rewrite ψ in the form

$$\psi = \int \mathcal{A}\left[\bar{\Phi}(A,\underset{\sim}{R}''_A)\bar{\Phi}(B,\underset{\sim}{R}''_B)\delta(\underset{\sim}{R}_A-\underset{\sim}{R}''_A)\delta(\underset{\sim}{R}_B-\underset{\sim}{R}''_B)\xi_A\xi_B\right]$$

$$\times F(\underset{\sim}{R}''_A-\underset{\sim}{R}''_B)\mathcal{Z}\left(\frac{N_A\underset{\sim}{R}''_A+N_B\underset{\sim}{R}''_B}{N}\right)d\underset{\sim}{R}''_A\,d\underset{\sim}{R}''_B \quad , \qquad (84)$$

with $\underset{\sim}{R}''_A$ and $\underset{\sim}{R}''_B$ being parameter coordinates and N = N_A + N_B being the total number of nucleons. In eq. (84) it is noted that the parameter coordinates are included in the arguments of the internal wave functions; this is purposedly done, in order to call attention to the fact that in $\bar{\Phi}(A,\underset{\sim}{R}''_A)$ and $\bar{\Phi}(B,\underset{\sim}{R}''_B)$ the parameter coordinates $\underset{\sim}{R}''_A$ and $\underset{\sim}{R}''_B$, instead of the cluster coordinates $\underset{\sim}{R}_A$ and $\underset{\sim}{R}_B$, are used [see eqs. (81) and (82)].

Consider now the term $\bar{\Phi}(K,\underset{\sim}{R}''_K)\delta(\underset{\sim}{R}_K-\underset{\sim}{R}''_K)$, with K = A or B, in eq. (84). If we represent $\delta(\underset{\sim}{R}_K-\underset{\sim}{R}''_K)$ as

$$\delta(\underset{\sim}{R}_K - \underset{\sim}{R}''_K) = \left(\frac{1}{2\pi}\right)^3 \int \exp\left[i\underset{\sim}{S}''_K \cdot (\underset{\sim}{R}_K - \underset{\sim}{R}''_K)\right] d\underset{\sim}{S}''_K \qquad (85)$$

then it can be easily shown that

$$\bar{\Phi}(K, \underset{\sim}{R}''_K)\,\delta(\underset{\sim}{R}_K - \underset{\sim}{R}''_K) = \left(\frac{1}{2\pi}\right)^3$$

$$\times \int \left[\prod_i \varphi_i(\underset{\sim}{r}_i - \underset{\sim}{R}''_K) \exp\left(i\frac{1}{N_K}\underset{\sim}{S}''_K \cdot \underset{\sim}{r}_i\right)\right] \exp\left(-i\underset{\sim}{S}''_K \cdot \underset{\sim}{R}''_K\right) d\underset{\sim}{S}''_K \qquad (86)$$

represents an integral over a product of single-particle wave functions with respect to the nucleon coordinates $\underset{\sim}{r}_i$. Using eq. (86) we obtain therefore for ψ the following expression:

$$\psi = \left(\frac{1}{2\pi}\right)^6 \int \mathcal{A}\left\{\left[\xi_A \prod_{j=1}^{N_A} \varphi_j(\underset{\sim}{r}_j - \underset{\sim}{R}''_A) \exp\left(i\frac{1}{N_A}\underset{\sim}{S}''_A \cdot \underset{\sim}{r}_j\right)\right]\right.$$

$$\left. \times \left[\xi_B \prod_{k=N_A+1}^{N} \varphi_k(\underset{\sim}{r}_k - \underset{\sim}{R}''_B) \exp\left(i\frac{1}{N_B}\underset{\sim}{S}''_B \cdot \underset{\sim}{r}_k\right)\right]\right\}$$

$$\times \exp\left(-i\underset{\sim}{S}''_A \cdot \underset{\sim}{R}''_A - i\underset{\sim}{S}''_B \cdot \underset{\sim}{R}''_B\right) F(\underset{\sim}{R}''_A - \underset{\sim}{R}''_B)$$

$$\times Z\left(\frac{N_A \underset{\sim}{R}''_A + N_B \underset{\sim}{R}''_B}{N}\right) d\underset{\sim}{S}''_A\, d\underset{\sim}{S}''_B\, d\underset{\sim}{R}''_A\, d\underset{\sim}{R}''_B \qquad (87)$$

This shows that, by introducing parameter coordinates $\underset{\sim}{R}''_A$ and $\underset{\sim}{R}''_B$ and generator coordinates $\underset{\sim}{S}''_A$ and $\underset{\sim}{S}''_B$, the wave function ψ can be represented as an integral over antisymmetrized products of single-particle wave functions or Slater determinants.

By making the transformation

$$\underset{\sim}{R}'' = \underset{\sim}{R}''_A - \underset{\sim}{R}''_B \ ,$$

$$\underset{\sim}{R}''_{cm} = \frac{1}{N} \left(N_A \underset{\sim}{R}''_A + N_B \underset{\sim}{R}''_B \right) , \tag{88}$$

and by expressing $\delta\psi$ in a similar form involving parameter coordinates $\underset{\sim}{R}'_A$ and $\underset{\sim}{R}'_B$ and generator coordinates $\underset{\sim}{S}'_A$ and $\underset{\sim}{S}'_B$, we obtain explicit expressions for the kernel functions $\mathcal{H}(\underset{\sim}{R}', \underset{\sim}{R}'')$ and $\mathcal{N}(\underset{\sim}{R}', \underset{\sim}{R}'')$ [see eqs. (14) and (15)]. Consider the kernel function $\mathcal{H}(\underset{\sim}{R}', \underset{\sim}{R}'')$, for example. Because the operator H contains a sum of one- and two-particle operators, this kernel function has the form of an integral over the generator coordinates $\underset{\sim}{S}'_A$, $\underset{\sim}{S}'_B$, $\underset{\sim}{S}''_A$, $\underset{\sim}{S}''_B$ and the parameter coordinates $\underset{\sim}{R}'_{cm}$, $\underset{\sim}{R}''_{cm}$ ($\underset{\sim}{R}'$ and $\underset{\sim}{R}''$ are not integrated over), with its integrand consisting of a sum of products of matrix elements

$$\langle \hat{\varphi}_i | \hat{\varphi}_j \rangle \ , \quad \langle \hat{\varphi}_i | O_p | \hat{\varphi}_j \rangle \ , \quad \langle \hat{\varphi}_i \hat{\varphi}_j | O_{pq} | \hat{\varphi}_l \hat{\varphi}_m \rangle ,$$

where the $\hat{\varphi}_i$'s are one-particle functions depending on the generator and parameter coordinates. The orthogonality relations between the $\hat{\varphi}_i$'s in the same cluster will usually reduce very drastically the number of terms which need to be evaluated.

Even though our discussion above was based on a two-cluster wave function, it is clear that one can easily generalize it to a wave function which describes the behaviour of a system composed of a large number of clusters.

3.3. Special case — cluster internal functions in harmonic-oscillator shell-model representation

Even though the technique described above is useful when the cluster internal functions have the general form given by eqs. (81) and (82), it becomes especially convenient when the internal structure of each cluster is described by a translationally invariant harmonic-oscillator shell-model function of the lowest configuration or a sum of such functions, with each of them specified by a different value for the oscillator width parameter. In this subsection, we shall consider first the simpler case where one such oscillator internal function is used, i.e.,

$$\bar{\Phi}(K) = \prod_{i} h_i(\underset{\sim}{r}_i - \underset{\sim}{R}_K) \exp\left[-\tfrac{1}{2}\alpha_K(\underset{\sim}{r}_i - \underset{\sim}{R}_K)^2\right] , \tag{89}$$

with α_K being the oscillator width parameter for cluster K (K = A or B) and the functions h_i being polynomials in single-partial spatial coordinates. With this choice and upon performing the transformation

$$\underset{\sim}{Q}''_K = \frac{1}{N_K \alpha_K} \underset{\sim}{S}''_K - i\,\underset{\sim}{R}''_K , \tag{90}$$

the wave function Ψ of eq. (87) can then be written in the following form:

$$\psi = \left(\frac{N_A\alpha_A}{2\pi}\right)^3\left(\frac{N_B\alpha_B}{2\pi}\right)^3$$

$$\times \int \mathcal{A}'\Big\{ \mathcal{A}_A\Big[\xi_A \prod_{j=1}^{N_A} h_j(\underline{r}_j - \underline{R}_A'')\exp\Big[-\tfrac{1}{2}\alpha_A(\underline{r}_j - i\underline{Q}_A'')^2\Big]\Big]$$

$$\times \mathcal{A}_B\Big[\xi_B \prod_{k=N_A+1}^{N} h_k(\underline{r}_k - \underline{R}_B'')\exp\Big[-\tfrac{1}{2}\alpha_B(\underline{r}_k - i\underline{Q}_B'')^2\Big]\Big]\Big\}$$

$$\times F(\underline{R}_A'' - \underline{R}_B'')\exp\Big[\tfrac{1}{2}N_A\alpha_A(\underline{R}_A'' - i\underline{Q}_A'')^2 + \tfrac{1}{2}N_B\alpha_B(\underline{R}_B'' - i\underline{Q}_B'')^2\Big]$$

$$\times Z\left(\frac{N_A\underline{R}_A'' + N_B\underline{R}_B''}{N}\right) d\underline{Q}_A''\, d\underline{Q}_B''\, d\underline{R}_A''\, d\underline{R}_B'' \,, \qquad (91)$$

where we have further made use of the relation given by eq. (17). The above equation for ψ can be reduced by noting that, because the internal function is chosen to have the lowest configuration in a harmonic-oscillator well, the arguments $(\underline{r}_j - \underline{R}_A'')$ of h_j and $(\underline{r}_k - \underline{R}_B'')$ of h_k can be replaced, respectively, by the arguments $(\underline{r}_j - \underline{C}_A'')$ and $(\underline{r}_k - \underline{C}_B'')$, with $\underline{C}_A''$ and $\underline{C}_B''$ being any constant vectors independent of the nucleon spatial coordinates.* Thus, by using eq. (88) and the transformation

*Even more general choices can be made. For example, $\underline{C}_A''$ and $\underline{C}_B''$ may be chosen as any symmetric functions of the nucleon spatial coordinates.

$$\underset{\sim}{S}'' = \alpha_A \underset{\sim}{Q}_A'' - \alpha_B \underset{\sim}{Q}_B'' ,$$

$$\underset{\sim}{S}_{cm}'' = \frac{1}{N} \left(N_A \alpha_A \underset{\sim}{Q}_A'' + N_B \alpha_B \underset{\sim}{Q}_B'' \right) , \tag{92}$$

and by choosing

$$Z(\underset{\sim}{R}_{cm}'') = \exp\left(- \frac{N_A \alpha_A + N_B \alpha_B}{2} \underset{\sim}{R}_{cm}''^2 \right) , \tag{93}$$

we can easily perform the integration over the variables $\underset{\sim}{R}_{cm}''$ and $\underset{\sim}{S}_{cm}''$, and obtain the following simplified expression:

$$\Psi = \left(\frac{N_A N_B}{2\pi N} \right)^3 \int \mathcal{A}' \left[\hat{\Phi}'(A; \underset{\sim}{S}'', \underset{\sim}{R}'') \hat{\Phi}'(B; \underset{\sim}{S}'', \underset{\sim}{R}'') \right] \Gamma(\underset{\sim}{S}'', \underset{\sim}{R}'') F(\underset{\sim}{R}'') \, d\underset{\sim}{S}'' \, d\underset{\sim}{R}'' , \tag{94}$$

where

$$\Gamma(\underset{\sim}{S}'', \underset{\sim}{R}'')$$

$$= \exp\left[- \frac{1}{2} \frac{N_A N_B (N_A \alpha_A + N_B \alpha_B)}{N^2 \alpha_A \alpha_B} \left(\underset{\sim}{S}'' + i \frac{N_B \alpha_A + N_A \alpha_B}{N} \underset{\sim}{R}'' \right)^2 \right] , \tag{95}$$

and

$$\hat{\Phi}'(A; \underset{\sim}{S}'', \underset{\sim}{R}'') = \mathcal{A}_A \left[\xi_A \prod_{j=1}^{N_A} h_j \exp\left[- \tfrac{1}{2} \alpha_A (\underset{\sim}{r}_j - \underset{\sim}{\eta}_A'')^2 \right] \right] ,$$

$$\hat{\Phi}'(B; \underset{\sim}{S}'', \underset{\sim}{R}'') = \mathcal{A}_B \left[\xi_B \prod_{k=N_A+1}^{N} h_k \exp\left[- \tfrac{1}{2} \alpha_B (\underset{\sim}{r}_k - \underset{\sim}{\eta}_B'')^2 \right] \right] , \tag{96}$$

with

$$\underset{\sim}{\eta}_A'' = \frac{i N_B}{N \alpha_A} \left[\underset{\sim}{S}'' + i \frac{N_A}{N} (\alpha_B - \alpha_A) \underset{\sim}{R}'' \right] ,$$

$$\underset{\sim}{\eta}_B'' = - \frac{i N_A}{N \alpha_B} \left[\underset{\sim}{S}'' - i \frac{N_B}{N} (\alpha_B - \alpha_A) \underset{\sim}{R}'' \right] . \qquad (97)$$

The meaning of the function $\hat{\Phi}'(K; \underset{\sim}{S}'', \underset{\sim}{R}'')$, with K = A or B, is clear; it is a shell-model function of the lowest configuration in a harmonic-oscillator well of width parameter α_K, with the center of the well located at the point $\underset{\sim}{\eta}_K''$. Since it is seen from eq. (97) that $\underset{\sim}{\eta}_K''$ is a complex quantity, we have therefore chosen to call the technique described here a complex-generator-coordinate technique.

As is seen from eq. (94), the wave function ψ has a Hill-Wheeler form [10,25-28], with $\mathcal{A}' [\hat{\Phi}'(A; \underset{\sim}{S}'', \underset{\sim}{R}'') \hat{\Phi}'(B; \underset{\sim}{S}'', \underset{\sim}{R}'')]$ being the intrinsic or generating function and $\Gamma(\underset{\sim}{S}'', \underset{\sim}{R}'') F(\underset{\sim}{R}'')$ being the weight function.

If one makes the assumption that α_A is equal to α_B, then the expressions for $\underset{\sim}{\eta}_A''$ and $\underset{\sim}{\eta}_B''$ are simpler and the computation of the required matrix elements becomes also somewhat simplified. The power of the complex-generator-coordinate technique described here lies, however, in the fact that the computation does not become much more complicated even when the width parameters α_A and α_B are chosen to have different values. This is in contrast to the generator-coordinate method used by many other investigators [29-45]. In this latter method, a real generator coordinate (the distance vector between the centers of the harmonic-oscillator potential

wells) is used and the calculation of the matrix elements becomes straightforward only when α_A and α_B are assumed as equal (see, however, refs. [46, 47]), which is of course a frequently unrealistic assumption.

By carrying out the same procedure for the variation $\delta\psi$ which will contain a generator coordinate $\underline{S}'$, a parameter coordinate $\underline{R}'$, and two arbitrary constant vectors $\underline{C}'_A$ and $\underline{C}'_B$, one obtains then for the kernel function $\hat{K}(\underline{R}',\underline{R}'')$ [see eq. (13)] the expression

$$\hat{K}(\underline{R}',\underline{R}'') = \mathcal{H}(\underline{R}',\underline{R}'') - E_T \mathcal{N}(\underline{R}',\underline{R}'')$$

$$= \left(\frac{N_A N_B}{2\pi N}\right)^6 \int \Big\langle \Big[\xi_A \prod_{j=1}^{N_A} h_j(\underline{r}_j - \underline{C}'_A) \exp\left[-\tfrac{1}{2}\alpha_A(\underline{r}_j - \underline{\eta}'_A)^2\right]\Big]$$

$$\times \Big[\xi_B \prod_{k=N_A+1}^{N} h_k(\underline{r}_k - \underline{C}'_B) \exp\left[-\tfrac{1}{2}\alpha_B(\underline{r}_k - \underline{\eta}'_B)^2\right]\Big]$$

$$|H - E_T| \mathcal{A}' \Big\{ \mathcal{A}_A \Big[\xi_A \prod_{j=1}^{N_A} h_j(\underline{r}_j - \underline{C}''_A) \exp\left[-\tfrac{1}{2}\alpha_A(\underline{r}_j - \underline{\eta}''_A)^2\right]\Big]$$

$$\times \mathcal{A}_B \Big[\xi_B \prod_{k=N_A+1}^{N} h_k(\underline{r}_k - \underline{C}''_B) \exp\left[-\tfrac{1}{2}\alpha_B(\underline{r}_k - \underline{\eta}''_B)^2\right]\Big]\Big\} \Big\rangle$$

$$\times \Gamma^*(\underline{S}',\underline{R}')\,\Gamma(\underline{S}'',\underline{R}'')\,d\underline{S}'\,d\underline{S}'' , \qquad (98)$$

where

$$\underset{\sim}{\eta}_A' = \frac{i N_B}{N\alpha_A}\left[\underset{\sim}{S}' + i\,\frac{N_A}{N}(\alpha_B-\alpha_A)\underset{\sim}{R}'\right],$$

$$\underset{\sim}{\eta}_B' = -\frac{i N_A}{N\alpha_B}\left[\underset{\sim}{S}' - i\,\frac{N_B}{N}(\alpha_B-\alpha_A)\underset{\sim}{R}'\right]. \qquad (99)$$

From eq. (98) it is noted that in the expression for $\hat{K}(\underset{\sim}{R}',\underset{\sim}{R}'')$ there appear only products of complex functions, each depending on a single-particle (space, spin, and isospin) coordinate. Thus, the antisymmetrization procedure causes no great difficulty and the computation of $\hat{K}(\underset{\sim}{R}',\underset{\sim}{R}'')$ can be performed in a rather straightforward manner (for details, see refs. [12,48,49]). In addition, we should mention that the integration over the nucleon coordinates may be further facilitated by making use of the freedom associated with the choice of the vectors $\underset{\sim}{C}_A'$, $\underset{\sim}{C}_B'$, $\underset{\sim}{C}_A''$, and $\underset{\sim}{C}_B''$ appearing in the arguments of h_j and h_k. In the present case, it is appropriate to choose

$$\underset{\sim}{C}_A' = \underset{\sim}{C}_A'' = \frac{1}{2}\left(\underset{\sim}{\eta}_A'^{*} + \underset{\sim}{\eta}_A''\right),$$

$$\underset{\sim}{C}_B' = \underset{\sim}{C}_B'' = \frac{1}{2}\left(\underset{\sim}{\eta}_B'^{*} + \underset{\sim}{\eta}_B''\right). \qquad (100)$$

This particular choice is made, in order to take advantage of the orthonormality relations satisfied by the single-particle wave functions in a harmonic oscillator potential well.

Next, we discuss the more general case [16] where the cluster internal function is given by a sum of translationally-invariant harmonic-oscillator shell-model functions of the lowest configuration. That is, the internal functions are now chosen to be

$$\Phi(A) = \sum_{p=1}^{n_p} \Phi_p(A) \,,$$

$$\Phi(B) = \sum_{q=1}^{n_q} \Phi_q(B) \,, \qquad (101)$$

where

$$\Phi_p(A) = C_{Ap}\, \mathcal{A}_A \left\{ \xi_A \prod_{j=1}^{N_A} h_j(\underline{r}_j - \underline{R}_A) \exp\left[-\tfrac{1}{2} \alpha_{Ap} (\underline{r}_j - \underline{R}_A)^2 \right] \right\} ,$$

$$\Phi_q(B) = C_{Bq}\, \mathcal{A}_B \left\{ \xi_B \prod_{k=N_A+1}^{N} h_k(\underline{r}_k - \underline{R}_B) \exp\left[-\tfrac{1}{2} \alpha_{Bq} (\underline{r}_k - \underline{R}_B)^2 \right] \right\} , \qquad (102)$$

with α_{Ap} ($p = 1$ to n_p) and α_{Bq} ($q = 1$ to n_q) being a set of appropriately chosen width parameters, and C_{Ap} and C_{Bq} being appropriate amplitudes. We should mention that even though the internal functions given above are expressed explicitly in terms of oscillator functions, there is no severe restriction regarding the flexibility required in properly describing the internal behaviour of the clusters, because any cluster internal function may be well approximated by the linear superposition of a sufficiently large

number of oscillator cluster functions with different width parameters.

With $\Phi(A)$ and $\Phi(B)$ given by eqs. (101) and (102), eq. (13) then becomes

$$\sum_{p,r=1}^{n_p} \sum_{q,s=1}^{n_q} \int \hat{K}_{pq,rs}(\underset{\sim}{R}', \underset{\sim}{R}'') F(\underset{\sim}{R}'') d\underset{\sim}{R}'' = 0 , \tag{103}$$

where

$$\hat{K}_{pq,rs}(\underset{\sim}{R}', \underset{\sim}{R}'') = \langle \Phi_p(A) \Phi_q(B) \delta(\underset{\sim}{R} - \underset{\sim}{R}') Z(\underset{\sim}{R}_{cm}) \\ | H - E_T | \mathcal{A} [\Phi_r(A) \Phi_s(B) \delta(\underset{\sim}{R} - \underset{\sim}{R}'') Z(\underset{\sim}{R}_{cm})] \rangle . \tag{104}$$

As discussed above, a particular form for the function $Z(\underset{\sim}{R}_{cm})$ must be chosen in order to express $\hat{K}(\underset{\sim}{R}', \underset{\sim}{R}'')$ in the form of eq. (98). Since this choice involves the oscillator width parameters of the cluster wave functions [see eq. (93)], it is not clear in the present case how this choice should be made because different sets of width parameters appear on the bra and ket sides of eq. (104). However, by using the fact that the operator $(H - E_T)$ is Galilean-invariant, one can write eq. (104) as

$$\hat{K}_{pq,rs}(\underline{R}',\underline{R}'') = \frac{\langle \mathcal{Z}(\underline{R}_{cm}) \mid \mathcal{Z}(\underline{R}_{cm}) \rangle}{\langle \chi_{pq}(\underline{R}_{cm}) \mid \chi_{rs}(\underline{R}_{cm}) \rangle}$$

$$\times \langle \phi_p(A)\phi_q(B)\delta(\underline{R}-\underline{R}')\chi_{pq}(\underline{R}_{cm}) \mid H - E_T \mid$$

$$\mathcal{A}\left[\phi_r(A)\phi_s(B)\delta(\underline{R}-\underline{R}'')\chi_{rs}(\underline{R}_{cm})\right] \rangle \tag{105}$$

The arbitrary function $\chi_{pq}(\underline{R}_{cm})$ can now be chosen, in accordance with eq. (93) to be

$$\chi_{pq}(\underline{R}_{cm}) = \exp\left(-\frac{N_A\alpha_{Ap} + N_B\alpha_{Bq}}{2}\underline{R}_{cm}^2\right) \tag{106}$$

With this choice, the matrix element $\hat{K}_{pq,rs}(\underline{R}',\underline{R}'')$ can be written in the form of eq. (98), and its evaluation can be accomplished just as in the single-width-parameter case (n_p=n_q=1) discussed above.

3.4. Redundant-solution test

Even with the help of the CGCT, it is still rather tedious to derive explicit expressions for the required kernel functions. In this subsection, we discuss a redundant-solution test [50,51] which can be used to check the correctness of these functions, in the case where each of the clusters is described by a single harmonic-oscillator shell-model function in the lowest configuration and a common width parameter is used to characterize

all the clusters involved.

For simplicity in discussion, let us consider a single-channel two-cluster case* where the trial function is given by eq. (79). Under conditions mentioned above for the cluster internal functions, there exist then inter-cluster relative-motion functions $F^{red}(\underset{\sim}{R})$, called redundant solutions, for which

$$\psi^{red} = \mathcal{A}\left[\Phi(A)\Phi(B)F^{red}(\underset{\sim}{R})\mathcal{Z}(\underset{\sim}{R}_{cm})\right] = 0 \qquad (107)$$

In light systems, these redundant solutions can be readily determined by using the exact correspondence between oscillator cluster and oscillator shell models [5]. For example, in the $^3H + \alpha$ system, it can be easily shown that, to comply with the Pauli principle, the relative motion between the clusters must have at least three oscillator quanta of excitation. Thus, the redundant solutions are those which correspond to lower-order oscillations with number of quanta less than three, i.e., 1s, 1p, 1d, and 2s oscillator functions.

Because ψ^{red} is identically equal to zero, one obtains also

$$\langle\Phi(A)\Phi(B)\delta(\underset{\sim}{R}-\underset{\sim}{R}')\mathcal{Z}(\underset{\sim}{R}_{cm})\,|\,\mathcal{A}\left[\Phi(A)\Phi(B)F^{red}(\underset{\sim}{R})\mathcal{Z}(\underset{\sim}{R}_{cm})\right]\rangle = 0\,, \qquad (108)$$

and

$$\langle\Phi(A)\Phi(B)\delta(\underset{\sim}{R}-\underset{\sim}{R}')\mathcal{Z}(\underset{\sim}{R}_{cm})\,|\,H\,|\,\mathcal{A}\left[\Phi(A)\Phi(B)F^{red}(\underset{\sim}{R})\mathcal{Z}(\underset{\sim}{R}_{cm})\right]\rangle = 0. \qquad (109)$$

*A more general discussion for a multi-cluster system is given in ref. [52].

By using eqs. (14) and (15), these equations can be further written as

$$\int \mathcal{N}(\underline{R}', \underline{R}'') F^{red}(\underline{R}'') d\underline{R}'' = 0 \tag{110}$$

and

$$\int \mathcal{H}(\underline{R}', \underline{R}'') F^{red}(\underline{R}'') d\underline{R}'' = 0 \tag{111}$$

That is, the redundant solutions are the eigenfunctions of both the norm or overlap kernel $\mathcal{N}(\underline{R}', \underline{R}'')$ and the Hamiltonian kernel $\mathcal{H}(\underline{R}', \underline{R}'')$, with eigenvalues equal to zero. Thus, the correctness of these two kernel functions can be ascertained by simply examining their eigenvalue spectra and counting the number of times which eigenvalues equal to zero occur.

One may also demonstrate the existence of redundant solutions in another interesting way. Consider as an example the n + ^{40}Ca case [49], where the redundant solutions are 1s, 1p, 1d, and 2s harmonic-oscillator functions. If one now takes eq. (37), makes the partial-wave expansion

$$F(\underline{R}') = \sum_{l} \frac{1}{R'} f_l(R') P_l(\cos\theta') , \tag{112}$$

$$K(\underline{R}', \underline{R}'') = \frac{1}{R'R''} \sum_{l} \sum_{m} k_l(R', R'') Y_{lm}(\theta', \phi') Y^{*}_{lm}(\theta'', \phi'') , \tag{113}$$

and solves numerically the resultant integrodifferential equation

$$\left\{ \frac{\hbar^2}{2\mu}\left[\frac{d^2}{dR'^2} - \frac{\ell(\ell+1)}{R'^2} \right] + E - V_D(R') \right\} f_\ell(R')$$

$$= \int_0^\infty k_\ell(R',R'')\, f_\ell(R'')\, dR'' \,, \qquad (114)$$

then the redundant solutions may be exhibited at any value of E by plotting $f_\ell(R')$ obtained using different values for the integration step size h_i in the numerical procedure. If the various kernel functions are correctly derived, then the functions $f_\ell(R')$ for $\ell \leq 2$ should differ at small values of R' but remain the same in the asymptotic region. On the other hand, for $\ell > 2$, $f_\ell(R')$ should be independent of h_i for all values of R'. In fig. 1 we illustrate the $\ell = 2$ and 3 solutions for n + ^{40}Ca scattering obtained by using h_i equal to 0.3 and 0.4 fm. As is seen, these curves do behave in exactly the way as discussed above, thus indicating that the kernel functions given in the appendix of ref. [49] have indeed been correctly derived.

When α_A is not equal to α_B, redundant solutions do not exist. However, the eigenvalue spectra of $\mathcal{N}(\underline{R}',\underline{R}'')$ and $\mathcal{H}(\underline{R}',\underline{R}'')$ are still expected to be similar to those in the equal-width-parameter case, which follows from the fact that the Pauli principle tends to reduce greatly the differences between apparently different structures [5]. For example, the $\ell = 0$ eigenvalues of $\mathcal{N}(\underline{R}',\underline{R}'')$ for the α + ^{16}O system are equal to 0.0, 0.0, 0.0015, 0.0204, 0.244, 0.514, 0.715, $\cdots$ in the case where $\alpha_A = 0.32$ fm^{-2} for the ^{16}O cluster and $\alpha_B = 0.514$ fm^{-2} for the α cluster, which are rather close to the corresponding values of 0,0, 0, 0, 0.229,

0.510, 0.718, ··· in the equal width-parameter case. Thus, even though there is, strictly speaking, no redundant-solution test in the unequal-width-parameter case, one can still examine the eigenvalue spectra to gain some confidence about the correctness of the derived kernel functions.

In the $\alpha_A \neq \alpha_B$ case, the absence of redundant solutions is replaced by the presence of spurious resonances which occur with definite characteristic energies [53, 54]. Take the $^3H + \alpha$ system as an example. Now, instead of two $\ell = 0$ redundant solutions, there appear two relatively sharp spurious resonances in the $\ell = 0$ phase shift [55]. These spurious resonances do not represent the existence of true resonance states in the compound system, and their presence can be easily suppressed either by the adoption of a least-square variational procedure [56, 57] or by the introduction of a phenomenological imaginary potential into the resonating-group formulation [58].

4. Bound-state, scattering, and reaction calculations

In this section, we show the usefulness of the resonating-group method in treating nuclear many-body problems by discussing the results of some bound-state, scattering, and reaction calculations. These calculations are selected mainly for illustrative purposes; however, they do serve to indicate the importance of including various features, such as specific distortion effects, reaction channels, etc., in a practical calculation.

4.1. Bound- and resonance-state calculations

4.1a. Cluster states in ^{17}O, ^{18}F, ^{19}F, and ^{20}Ne

As first example, we describe a recent study* on the nuclei ^{17}O, ^{18}F, ^{19}F, and ^{20}Ne in which one of the main purposes was to investigate bound and resonance states in these nuclei which have predominantly a light-ion plus ^{16}O cluster configuration. In this study, the trial wave function used is given by eq. (79), with the cluster internal functions assumed to have the form given by eqs. (80) and (89). The width parameters are then chosen to yield the various empirically determined rms matter radii; that is,

$$\alpha_A = 0.32 \ fm^{-2} \tag{115}$$

---

*A study of this type, but with a different nucleon-nucleon potential and with the exchange-Coulomb kernel approximated by a procedure described in ref. [49], was given in ref. [24].

for the ^{16}O cluster, and

$$\alpha_B = 0.20,\ 0.37,\ \text{and}\ 0.514\ \text{fm}^{-2} \tag{116}$$

for the d, ^3H or ^3He, and α clusters, respectively.

The nucleon-nucleon potential is taken to be [59, 60]

$$V_{ij} = \left[V_R + \tfrac{1}{2}(1+P_{ij}^{\sigma}) V_t + \tfrac{1}{2}(1-P_{ij}^{\sigma}) V_s \right] \left[\tfrac{1}{2}u + \tfrac{1}{2}(2-u) P_{ij}^{r} \right]$$

$$- \frac{1}{2\hbar} V_\lambda \exp\left[-\lambda (\underline{r}_i - \underline{r}_j)^2\right] (\underline{\sigma}_i + \underline{\sigma}_j) \cdot (\underline{r}_i - \underline{r}_j) \times (\underline{p}_i - \underline{p}_j)$$

$$+ \frac{e^2}{|\underline{r}_i - \underline{r}_j|} \tfrac{1}{2}(1+\tau_{iz}) \tfrac{1}{2}(1+\tau_{jz}) , \tag{117}$$

where

$$V_R = V_{0R} \exp\left[-K_R (\underline{r}_i - \underline{r}_j)^2\right],$$

$$V_t = -V_{0t} \exp\left[-K_t (\underline{r}_i - \underline{r}_j)^2\right],$$

$$V_s = -V_{0s} \exp\left[-K_s (\underline{r}_i - \underline{r}_j)^2\right], \tag{118}$$

with

$$\begin{aligned} V_{0R} &= 200.0\ \text{MeV}, & K_R &= 1.487\ \text{fm}^{-2}, \\ V_{0t} &= 178.0\ \text{MeV}, & K_t &= 0.639\ \text{fm}^{-2}, \\ V_{0s} &= 91.85\ \text{MeV}, & K_s &= 0.465\ \text{fm}^{-2}. \end{aligned} \tag{119}$$

This particular nucleon-nucleon potential is chosen, since it yields a

satisfactory description of not only the two-nucleon low-energy scattering data but also the essential properties of the deuteron, triton, and α particle.

The exchange-mixture parameter u in eq. (117) is an adjustable parameter in the calculation. Its value is determined by fitting the light-ion separation energy in the lowest $\ell = 0$ state of the compound nucleus. For example, in the $\alpha + {}^{16}O$ case, one adjusts u until the calculation yields the experimental value [61] of 4.73 MeV for the α-particle separation energy in the ground state of ^{20}Ne. This adjustment is necessary, since in the present calculation various simplifications are made; in particular, the specific distortion effects are not explicitly taken into consideration. The resultant value of u so determined should be reasonably close to 1 which corresponds to a Serber exchange mixture. If this should turn out not to be the case, then adjusting u is too crude a procedure to compensate for these simplifications and a more elaborate calculation should be performed. Also, in eq. (117), the spin-orbit depth parameter V_λ and range parameter λ will be treated as phenomenological parameters; their values will be determined by using experimental data on the energy splittings of the lowest $\ell=2$ levels in the various compound systems.

Using the procedure described in subsection 2.3a and upon performing a partial-wave expansion, one obtains, in a particular (J,ℓ) state, the following integrodifferential equation for the radial function $f_{J\ell}(R')$:

$$\left\{ \frac{\hbar^2}{2\mu} \left[\frac{d^2}{dR'^2} - \frac{\ell(\ell+1)}{R'^2} \right] + E - V_N(R') - V_C(R') - \eta_{J\ell} V_{so}(R') \right\} f_{J\ell}(R')$$

$$= \int_0^\infty \left[k_\ell^N(R',R'') + k_\ell^C(R',R'') \right] f_{J\ell}(R'')\, dR'' \qquad (120)$$

where the quantity $\eta_{J\ell}$ is given by

$$\eta_{\ell+\frac{1}{2},\ell} = \ell \quad , \quad \eta_{\ell-\frac{1}{2},\ell} = -(\ell+1) \tag{121}$$

in the n + ^{16}O or ^{3}H + ^{16}O case, and

$$\eta_{\ell+1,\ell} = 2\ell \quad , \quad \eta_{\ell,\ell} = -2 \quad , \quad \eta_{\ell-1,\ell} = -2(\ell+1) \tag{122}$$

in the d + ^{16}O case. The functions V_N, V_C, and V_{so} represent the direct nuclear-central, the direct Coulomb, and the direct spin-orbit potentials, respectively, while the kernels k_ℓ^N and k_ℓ^C represent the nonlocal contributions arising from the exchange character of the nucleon-nucleon potential and the antisymmetrization procedure. In deriving the intercluster spin-orbit interaction, the simplification is made to omit the exchange terms by setting the antisymmetrization operator $\mathcal{A}'$ in eq. (17) as unity. Also, in the actual computation two additional approximations have been made: (i) the exchange-Coulomb kernel k_ℓ^C is determined by an approximate, but self-consistent procedure which is described in Appendix B, and (ii) the nucleon-nucleon spin-orbit range parameter λ is assumed to have a value approaching infinity. As a result of this latter approximation, the potential $V_{so}(R')$ is characterized by only a single parameter $J_\lambda = V_\lambda \lambda^{-5/2}$ which will then be determined by using experimental information as described above.

The values of u are equal to 0.924, 0.989, 0.907 and 0.881 in the n, d, ^{3}H, and α plus ^{16}O cases, respectively. The finding that u turns out to

have a largest value in the d + ^{16}O case can be attributed to the fact that the deuteron cluster has a high compressibility and, hence, can be easily distorted. As for the values of J_λ, they are, respectively, equal to 50.0, 20.8, and 12.4 MeV-fm^5 in the n + ^{16}O, d + ^{16}O, and ^{3}H + ^{16}O cases. Here one notes that these J_λ values are quite different in different systems, indicating that one must be careful in interpreting the intercluster spin-orbit potential in eq. (120). At the present moment, it seems appropriate to say that this potential should be considered as mainly phenomenological in nature and is constructed only to represent the average effect of the two-nucleon tensor potential.

Calculated levels in ^{17}O, ^{18}F, ^{19}F, and ^{20}Ne are shown in fig. 2, together with those experimental levels [61-66] which have predominantly n, d, ^{3}H, and α plus ^{16}O cluster configurations. In obtaining the resonance levels, the procedure used is to calculate the various phase shifts and locate energy positions at which the phase-shift curve has a largest, positive value for the slope. This is illustrated for the α + ^{16}O case in fig. 3, where one notes the presence of the 6^+ and 8^+ members of the ground $K^\pi = 0^+$ band, the $K^\pi = 0^-$ negative-parity band, and the excited $K^\pi = 0^+$ band. In fact, there is even an indication for the existence of an excited $K^\pi = 0^-$ band. The states in this latter band are, however, quite broad and, consequently, their presence will be hard to verify experimentally.

As is seen from fig. 2, there is a generally good agreement between calculation and experiment. This shows that, even with the simplest type of resonating-group calculations, one can still obtain valuable information concerning the existence of particular cluster states in nuclear systems.

A similar calculation in the $\alpha + {}^{16}O$ case has been performed by Matsuse et al [67]. By studying the reduced α-widths of the levels, they concluded that the states in the $K^{\pi} = 0^{-}$ band have a strong $\alpha + {}^{16}O$ molecule-like character, while the states in the ground-state band have rather shell-model like character with large (8,0) SU_3 component but can still be described fairly well within the framework of the resonating-group method using the simple trial function of eq. (79). In addition, these authors have examined various electromagnetic properties [67,68] and found generally satisfactory agreement between calculated and experimental results.

Using a bound-state approximation for resonance levels, Tomoda and Arima [69] have also studied the ^{20}Ne problem. They employed a model space which is constructed by combining the $(2s\text{-}1d)^4$ shell-model and the $\alpha + {}^{16}O$ cluster-model spaces. This is equivalent to extending the calculation described above by taking into account some specific distortion effects. As the consequence of the use of a larger model space, they have obtained from their calculation not only the above-mentioned rotational bands but also another $K^{\pi} = 0^{+}$ band which corresponds to the one found experimentally with band head at 6.72 MeV [70].

Similar calculations have been made in many other systems. These are described in refs. [21, 36, 71-82].

4.1b. 3α cluster structure of ^{12}C

For the illustration of a multi-cluster resonating-group calculation, we describe the investigation of Fukushima and Kamimura [83], in which the low-energy T = 0 states of ^{12}C are considered in the 3α cluster

representation. In this investigation, the trial wave function has the form of eq. (40), i.e.,

$$\Psi_{LM} = \mathcal{A}\left[\phi(\alpha 1)\phi(\alpha 2)\phi(\alpha 3)F_{LM}(\underset{\sim}{R}_1, \underset{\sim}{R}_2)\mathcal{Z}(\underset{\sim}{R}_{cm})\right], \tag{123}$$

where

$$\underset{\sim}{R}_1 = \underset{\sim}{R}_{\alpha 1} - \underset{\sim}{R}_{\alpha 2},$$

$$\underset{\sim}{R}_2 = \frac{1}{2}(\underset{\sim}{R}_{\alpha 1} + \underset{\sim}{R}_{\alpha 2}) - \underset{\sim}{R}_{\alpha 3}, \tag{124}$$

with $\underset{\sim}{R}_{\alpha 1}$, $\underset{\sim}{R}_{\alpha 2}$, and $\underset{\sim}{R}_{\alpha 3}$ being the centers of mass of the three α clusters. The internal function $\phi(\alpha 1)$ is taken to be

$$\phi(\alpha 1) = \exp\left[-\frac{1}{2}\alpha \sum_{i=1}^{4}(\underset{\sim}{r}_i - \underset{\sim}{R}_{\alpha 1})^2\right]\xi_{\alpha 1}, \tag{125}$$

with $\xi_{\alpha 1}$ being an appropriate spin-isospin function. The internal functions $\phi(\alpha 2)$ and $\phi(\alpha 3)$ are chosen to have similar forms, specified by the same width parameter α. The relative-motion function $F_{LM}(\underset{\sim}{R}_1, \underset{\sim}{R}_2)$ is determined by solving eq. (44). For bound and quasibound states, it is convenient to solve this equation approximately by expressing $F_{LM}(\underset{\sim}{R}_1, \underset{\sim}{R}_2)$ as

$$F_{LM}(\underset{\sim}{R}_1, \underset{\sim}{R}_2) = \sum_{i\ell_1, j\ell_2} B^{L}_{i\ell_1, j\ell_2} \times \left[\sum_{m_1 m_2} C(L, \ell_1, \ell_2; M, m_1, m_2)\chi^{i}_{\ell_1 m_1}(\underset{\sim}{R}_1)\bar{\chi}^{j}_{\ell_2 m_2}(\underset{\sim}{R}_2)\right], \tag{126}$$

where $C(L,\ell_1,\ell_2;M,m_1,m_2)$ is a Clebsch-Gordan coefficient, and $B^{L}_{i\ell_1,j\ell_2}$ are linear expansion coefficients to be obtained by a variational procedure. The functions $\chi^{i}_{\ell_1 m_1}(\underline{R}_1)$ and $\bar{\chi}^{j}_{\ell_2 m_2}(\underline{R}_2)$ are assumed, for computational convenience, to have the forms

$$\chi^{i}_{\ell_1 m_1}(\underline{R}_1) = R_1^{\ell_1} \exp(-\nu_i R_1^2) Y_{\ell_1 m_1}(\theta_1,\phi_1) \tag{127}$$

and

$$\bar{\chi}^{j}_{\ell_2 m_2}(\underline{R}_2) = R_2^{\ell_2} \exp(-\mu_j R_2^2) Y_{\ell_2 m_2}(\theta_2,\phi_2) \tag{128}$$

From eq. (126) it is seen that the total angular momentum J = L of a given ^{12}C state is obtained by coupling the orbital angular momentum ℓ_1 of the relative motion of the first two α clusters which form a ^{8}Be cluster to the orbital angular momentum ℓ_2 of the relative motion of the third α cluster with respect to the center of mass of the ^{8}Be core.

Because of computational problems, it is necessary to use a relatively small number of basis functions in eq. (126). As a consequence, the choice of the fixed nonlinear parameters α, ℓ_1, ℓ_2, ν_i, and μ_j becomes quite important. For the choice of α, it is found that a reasonable value which can be used for all ^{12}C states considered here is 0.55 fm^{-2}. This value is nearly equal to that which optimizes the energy expectation value of the α-particle Hamiltonian. Also, since in the present calculation a totally antisymmetrized trial function is used, one can adopt the simplification of setting $\ell_1 = 0$ in

$\chi^{\lambda}_{\ell_1 m_1}$.* This results in only a relatively minor overestimate of the calculated energies, but does limit the calculation to natural-parity states in ^{12}C. As to the choice of ν_λ and μ_j , four values for each of these parameters are adopted. These are given by ν_λ / α = 0.8, 0.45, 0.15 and 0.05 and $\mu_j / (\frac{4}{3}\alpha)$ = 0.8, 0.45, 0.15, and 0.05. The total number of basis functions for each J^π state is then 16. For the ^{12}C states considered in this calculation, this seems to be sufficient because an examination in which the number of ν_λ and μ_j is increased shows that only little energy gain can be further obtained.

Using a nucleon-nucleon potential of the form of eq. (117) with

$$\begin{aligned} V_{OR} &= 60 \text{ MeV} , & K_R &= 0.980 \text{ fm}^{-2} , \\ V_{Ot} &= V_{O\Delta} = 60 \text{ MeV} , & K_t &= K_\Delta = 0.309 \text{ fm}^{-2} , \\ u &= 0.82 , \end{aligned} \qquad (129)$$

which is similar to the Volkov no. 2 potential [84], Fukushima and Kamimura obtained a ^{12}C low-energy spectrum which is shown in fig. 4 together with the spectrum experimentally determined [85-87]. To facilitate a comparison between these two spectra, they have shifted the energy origin of the calculated spectrum such that the calculated and experimental 3α threshold

*For the $J^\pi = 4^+$ state, a somewhat different simplification is adopted. Here the assumption of $\ell_1 = 0$ when $\nu_\lambda < \frac{3}{4}\mu_j$ and $\ell_2 = 0$ when $\nu_\lambda \geq \frac{3}{4}\mu_j$ is used. Comparing to the case where ℓ_1 is always set as zero, one finds that this procedure yields a significant energy gain for the 4^+ state, but no energy gain for the states with $J^\pi = 0^+$ and 2^+ [83].

energies occur at the same vertical position. This adjustment is necessary, since with the wave function of eq. (125) the calculated binding energy of an α particle is 27.3 MeV which is somewhat smaller than the experimental value of 28.3 MeV.

From fig. 4 it is seen that there is a reasonable agreement between calculation and experiment. The fact that the states in the ground-state band are too closely spaced is a basic defect of the 3α model, with each α cluster in its lowest configuration. As has been pointed out by Takigawa and Arima [88], this defect can be remedied by a proper consideration of the effects caused by the spin-orbit component in the nucleon-nucleon potential.

Fukushima and Kamimura have also studied the electromagnetic properties of ^{12}C in various states and found good agreement with observed results. In view of the fact that the agreement between calculated and experimental energies is only fair, this finding is somewhat surprising. Thus, it will be interesting to conduct a further examination where an improved wave function is used. This can be achieved, for instance, by introducing different width parameters for the α clusters, including less symmetric α-cluster configurations, and so on.

Other microscopic multi-cluster calculations appearing in the literature are given in refs. [89-97].

4.2. Scattering calculations

4.2a. Scattering of light ions by ^{16}O

In this subsection, we discuss the scattering of light ions n,d, ^{3}He, and α by ^{16}O. The purpose is to show that even simple resonating-group

calculations can yield cross-section results which agree satisfactorily with experiment.

The formulation of the problem is given in subsection 4.1a. In the present investigation where one is concerned with experimental data in the positive-energy region, it will be necessary to take reaction channels into consideration. As is clear, the proper way to do this is to perform a many-channel resonating-group calculation as described in subsection 2.3c. However, this will involve a great deal of computational effort, because at relatively high energies one will have to contend with not only many reaction channels but also the problem of multi-cluster breakup. Therefore, for the calculations to be described here, we shall crudely take reaction effects into account by adopting the simple procedure of introducing a phenomenological imaginary potential into the theoretical formulation. In other words, we shall replace $V_N(R')$ in eq. (120) by $V_N(R') + iW(R')$. For $W(R')$ a surface-derivative Woods-Saxon form will be employed, i.e.,

$$W(R') = W_I \left[4 a_I \frac{d}{dR'} f_I(R') \right] \tag{130}$$

with

$$f_I(R') = \left\{ 1 + \exp\left[(R' - R_I)/a_I \right] \right\}^{-1} \tag{131}$$

The geometry parameters R_I and a_I are chosen by the criterion that the rms radius of the form factor $f_I(R')$ be approximately equal to that of the direct nuclear potential $V_N(R')$. Thus, we use

$$a_I = 0.6 \text{ fm} \tag{132}$$

and

$$R_I = 3.2,\ 4.6,\ 4.4,\ \text{and } 4.2 \text{ fm} \tag{133}$$

for n, d, ^{3}He, and α plus ^{16}O scattering, respectively. With these parameters fixed, the only adjustable quantity is the depth parameter W_I; this parameter is then adjusted at each energy to obtain a best fit with experimental differential-cross-section result.

A comparison between calculated and experimental [63,98-101] differential scattering cross sections for the various systems at indicated energies is shown in fig. 5. To obtain the calculated results, we have used values of W_I equal to 4.7, 6.6, 6.5, and 1.15 MeV for n, d, ^{3}He, and α + ^{16}O scattering, respectively. As is seen, the agreement is generally quite reasonable. The fit to experiment in the d + ^{16}O case seems to be somewhat less satisfactory than those in other cases. This can probably be explained by the fact that the single-Gaussian deuteron spatial wave function used in this calculation is not flexible enough to adequately describe the behaviour of this cluster [53] and that the important deuteron specific distortion effects have not been properly taken into consideration.

There is another interesting result which should be mentioned. In the n + ^{16}O case at 13.18 MeV, the reaction and integrated-elastic cross sections calculated with the value of W_I given above are equal to 639 and 883 mb, respectively, which compare well with the measured values of 730 ± 100 and 880 ± 90 mb quoted in ref. [98]. This indicates that, since in a resonating-group calculation the real central part of the effective

intercluster interaction is well accounted for, one can even use the elastic-scattering cross-section data to make a reasonable prediction of the total reaction cross section.

Calculated and experimental [102] results for the ratio $\sigma(\theta)/\sigma_c(\theta)$ in the $\alpha + {}^{16}O$ case at a higher energy of 19.2 MeV are compared in fig. 6. For the calculated result , we use a value of W_I = 2.0 MeV which yields a total reaction cross section of 927 mb. Here one sees that the agreement obtained is indeed quite satisfactory, with the only discrepancy being in the detailed structure of the interference minimum near 80^0.

At present, there exist resonating-group scattering calculations for many systems both heavier and lighter than the system described here. Some selective calculations are discussed in refs. [11, 12, 14-17, 24, 49, 53, 103-119] . In particular, we wish to point out that the calculation reported in ref. [16] is performed with the flexible cluster internal function given by eq. (101).

4.2b. $\alpha + \alpha$ scattering with specific distortion effect

The formulation of a scattering problem with specific distortion effect taken into consideration is described in subsection 2.3b. In the present calculation of $\alpha + \alpha$ scattering [60] , one writes the trial wave function as

$$\Psi = \Psi_0 + \sum_{i=1}^{n_d} \mathcal{A}\left[\tilde{\Phi}_i(\alpha 1)\,\tilde{\Phi}_i(\alpha 2)\,G_i(\underline{R})\,Z(\underline{R}_{cm})\right] , \qquad (134)$$

where n_d is the number of distortion functions. The function Ψ_0 represents the usual no-distortion approximation; it has the form

$$\Psi_0 = \mathcal{A}\left[\phi(\alpha 1)\,\phi(\alpha 2)\,F(\underset{\sim}{R})\,Z(\underset{\sim}{R}_{cm})\right] , \tag{135}$$

where $\phi(\alpha 1)$ or $\phi(\alpha 2)$ describes the internal structure of a free α-particle, given by

$$\phi(\alpha 1) = \left\{ \sum_{i=1}^{2} A_i \exp\left[-\tfrac{1}{2}\alpha_i \sum_{j=1}^{4} \left(\underset{\sim}{r}_j - \underset{\sim}{R}_{\alpha 1} \right)^2 \right] \right\} \xi_{\alpha 1} \tag{136}$$

and similarly for $\phi(\alpha 2)$. The parameters α_i and A_i ($i = 1,2$) are determined by minimizing the expectation value of the α-particle Hamiltonian; with the nucleon-nucleon potential of eqs. (117) - (119), their values are

$$\begin{aligned} A_1 &= 1.0 , & \alpha_1 &= 0.305 \text{ fm}^{-2} , \\ A_2 &= 16.057 , & \alpha_2 &= 0.708 \text{ fm}^{-2} , \end{aligned} \tag{137}$$

and the resultant values for the binding energy and the rms radius are equal to 25.39 MeV and 1.415 fm, respectively, which agree reasonably well with the corresponding experimental values.

The functions $\tilde{\phi}_i(\alpha 1)$ and $\tilde{\phi}_i(\alpha 2)$ are taken as

$$\tilde{\phi}_i(\alpha 1) = \exp\left[-\tfrac{1}{2}\tilde{\alpha}_i \sum_{j=1}^{4} \left(\underset{\sim}{r}_j - \underset{\sim}{R}_{\alpha 1} \right)^2 \right] \xi_{\alpha 1} ,$$

$$\tilde{\phi}_i(\alpha 2) = \exp\left[-\tfrac{1}{2}\tilde{\alpha}_i \sum_{j=5}^{8} \left(\underset{\sim}{r}_j - \underset{\sim}{R}_{\alpha 2} \right)^2 \right] \xi_{\alpha 2} , \tag{138}$$

with the choice of $\tilde{\alpha}_i$ to be discussed below. As for the function $G_i(\underset{\sim}{R})$ in the distortion-function term of Ψ , we make the following expansion:

$$G_i(\underset{\sim}{R}) = \sum_{\ell} \tilde{A}_{\ell i} \frac{1}{R} g_{\ell i}(R) P_\ell(\cos\theta) \tag{139}$$

where

$$g_{\ell i}(R) = R^{n+1} \exp(-\tilde{\beta}_i R^2) \tag{140}$$

with

$$\begin{aligned} n &= 4 \quad \text{for} \quad \ell = 0,2 \\ &= \ell \quad \text{for} \quad \ell \geq 4 \, . \end{aligned} \tag{141}$$

The choice of $\tilde{\beta}_i$ will also be discussed below. It should be noted that once appropriate sets of $(\tilde{\alpha}_i, \tilde{\beta}_i)$ are chosen, one can then determine the variational amplitudes $\tilde{A}_{\ell i}$ and the variational function $F(\underset{\sim}{R})$ by using the procedure given in subsection 2.3b.

The procedure for choosing the number n_d of distortion functions and the nonlinear parameters $\tilde{\alpha}_i$ and $\tilde{\beta}_i$ (i = 1 to n_d) is discussed in detail in refs. [21, 120]. In the $\alpha + \alpha$ case described here, it is found that, for a value of u in eq. (117) close to but less than 1, a choice of $n_d = 3$ is sufficient and the corresponding $(\tilde{\alpha}_i, \tilde{\beta}_i)$ sets can be taken as (0.7 fm^{-2}, 0.32 fm^{-2}), (0.7 fm^{-2}, 0.48 fm^{-2}), and (0.7 fm^{-2}, 0.64 fm^{-2}). The value of u is then chosen such that the resonance energy of the $\ell = 0$ state is correctly obtained. The result is u = 0.950.

In fig. 7 we show $\ell = 0,2$, and 4 $\alpha + \alpha$ phase shifts, calculated with u = 0.950, at c.m. energies from 0 to 20 MeV. The solid curves show the result obtained with the three distortion functions mentioned above,

while the dashed curves show the no-distortion ($n_d = 0$) result. The empirical data points are those of refs. [121-125]. As is seen, there is a good over-all agreement between the calculated result with $n_d = 3$ and the empirical result. In the $\ell = 4$ states, the calculated phase shifts are generally somewhat too small. This can probably be attributed to the fact that, in this calculation, a rather simple nucleon-nucleon potential, containing only a weakly repulsive core, has been adopted.

By studying the results of distortion calculations in different systems [21, 126, 127], one can make the following general comments: (i) specific distortion effects of a nucleus are more important the higher its compressibility, (ii) a nucleus is more distorted the larger the number of nucleons in the other nucleus which causes the distortion, (iii) except near energies where resonances occur, specific distortion effects decrease with increasing energy, (iv) except for resonance effects and odd-even effects, the influence of distortion decreases with increasing orbital angular momentum, and (v) distortion appears to be stronger in "Pauli-favoured" states [127]. Based on these comments, one anticipates then that for the scattering of neutrons by doubly-closed-shell nuclei ^{4}He, ^{16}O, and ^{40}Ca, the effects of specific distortion should be relatively unimportant and a simple resonating-group calculation of the type used in subsection 4.2a should be adequate. That this is indeed so is shown in fig. 8 where one sees that results calculated without specific distortion effects [60] do compare very favourably with experimental results [98, 128-130].

Other calculations involving specific distortion effects are described in refs. [20, 21, 126, 127, 131-135].

4.3. Reaction calculations

4.3a. $^3He(d,p)^4He$ reaction

As an example of a coupled-channel study, we consider a calculation in the five-nucleon system where both the d + ^{3}He (or d + ^{3}H) channel (channel f) and the p + α (or n + α) channel (channel g) are included [136]. For this calculation, the formulation of subsection 2.3c is used and reaction effects, arising from the presence of other open channels, are approximately taken into account by the use of phenomenological imaginary potentials.

The trial wave function in the channel-spin 1/2 state is given by eq. (57) with*

$$\psi_f = \mathcal{A}\left[N_f^{-1/2}\, \Phi_3 \Phi_d \xi_f F(\underset{\sim}{R}_f) Z(\underset{\sim}{R}_{cm})\right] \tag{142}$$

and

$$\psi_g = \mathcal{A}\left[N_g^{-1/2}\, \Phi_\alpha \xi_g G(\underset{\sim}{R}_g) Z(\underset{\sim}{R}_{cm})\right] \tag{143}$$

In the above equations, ξ_f and ξ_g denote appropriate spin-isospin functions [22], and Φ_3, Φ_d, and Φ_α describe the spatial behaviour of

---

*Because of the adoption of a central nucleon-nucleon potential in the calculation, the spin-3/2 channel of the d + ^{3}He system is not coupled to the p + α channel; for this reason, we shall not discuss here the calculation in the spin-3/2 channel.

the three-nucleon cluster (^{3}He or ^{3}H), the deuteron cluster, and the α cluster, respectively. The quantities $N_f^{-\frac{1}{2}}$ and $N_g^{-\frac{1}{2}}$ are included so that the normalization condition of eq. (60) is satisfied.

The functions Φ_α and Φ_3 are assumed as

$$\Phi_\alpha = \exp\left[-\tfrac{1}{2}\alpha \sum_{j=1}^{4} (\underline{r}_j - \underline{R}_\alpha)^2\right] \tag{144}$$

and

$$\Phi_3 = \exp\left[-\tfrac{1}{2}\gamma \sum_{j=1}^{3} (\underline{r}_j - \underline{R}_3)^2\right], \tag{145}$$

where the parameters α and γ are chosen to yield the correct rms matter radii for the respective nuclei, i.e.,

$$\alpha = 0.514 \text{ fm}^{-2} \tag{146}$$

and

$$\begin{aligned} \gamma &= 0.378 \text{ fm}^{-2} \quad \text{for } ^3\text{H} \\ &= 0.367 \text{ fm}^{-2} \quad \text{for } ^3\text{He} \ . \end{aligned} \tag{147}$$

For the diffuse deuteron cluster, it is necessary to use a more flexible cluster function

$$\Phi_d = \sum_{i=1}^{3} A_i \exp\left[-\tfrac{1}{2}\alpha_i \sum_{j=4}^{5} (\underline{r}_j - \underline{R}_d)^2\right]. \tag{148}$$

The parameters A_i and α_i are determined by minimizing the expectation value of the deuteron Hamiltonian; the result is

$$A_1 = 1.0 \quad , \qquad \alpha_1 = 0.07284 \text{ fm}^{-2} \quad ,$$
$$A_2 = 3.631 \quad , \qquad \alpha_2 = 0.3657 \text{ fm}^{-2} \quad ,$$
$$A_3 = 5.746 \quad , \qquad \alpha_3 = 1.4696 \text{ fm}^{-2} \quad . \qquad (149)$$

With the wave functions of eqs. (144) - (149), we obtain from eqs. (69) and (70) a value of $(E_g - E_f) = 20.45$ MeV which is reasonably close to the experimental value of 18.35 MeV.

The nucleon-nucleon potential used has the form of eq. (117), with

$$V_R = 0 \quad ,$$
$$V_{0t} = 66.92 \text{ MeV} \quad , \qquad K_t = 0.415 \text{ fm}^{-2} \quad ,$$
$$V_{0\Delta} = 29.05 \text{ MeV} \quad , \qquad K_\Delta = 0.292 \text{ fm}^{-2} \quad . \qquad (150)$$

The spin-orbit component is, for simplicity in calculation, omitted by setting $V_\lambda = 0$. As for the exchange-mixture parameter u, it is chosen such that the calculation yields a good fit to the $n + \alpha$, p-wave phase shifts obtained using the central part of the optical potential found by Satchler et al [137] from a phenomenological study of the experimental data. The resultant value is $u = 0.95$.*

As discussed in subsection 2.3c, two coupled integrodifferential equations for the relative-motion functions $F(R'_f)$ and $G(R'_g)$ can be

*This is the value of u in the channel-spin 1/2 state. For reasons explained in ref. [136] , the value of u used in the channel-spin 3/2 state is 1.10.

derived. Upon performing a partial-wave expansion and solving the resultant equations subject to appropriate boundary conditions, one can then obtain the partial-wave S-matrix and, subsequently, the differential scattering and reaction cross sections.

In fig. 9 we show a comparison between calculated coupled-channel (solid line) and single-channel (dashed line) differential scattering cross sections for d + ^{3}H scattering at 2.02 MeV. The experimental data shown are those of ref. [138]. Here one sees that the coupled-channel result is not only considerably improved over the single-channel result [115] but also in good agreement with experiment. This shows that a systematic improvement of the resonating-group calculation by expanding the trial-function space can indeed quickly lead to a satisfactory explanation of observed phenomena.

The calculated $\alpha(p,d)^3$He differential reaction cross section at E_p = 68 MeV is shown by the solid curve in fig. 10. To account approximately for the many-body breakup channels not considered explicitly, we have again introduced into the formulation phenomenological imaginary potentials, with the geometry parameters chosen according to the criterion given in subsection 4.2a and the depth parameters chosen by fitting cross-section data in elastic-scattering channels. As is seen from this figure, the agreement with experimental data [139] is fairly satisfactory. The presence of deep minima and the slight underestimate in the calculated cross section are likely due to the fact that in the nucleon-nucleon potential employed there are no noncentral components.

From fig. 10 it is also noted that the differential reaction cross section has a decreasing trend in the forward angular region, but begins

to increase when θ passes about 90^{o}. As has been studied in careful detail [140], the reason for this is that, at a relatively high energy, the reaction proceeds mainly through different mechanisms in the forward and backward angular regions. Thus, in the forward angular region it proceeds mainly through a one-nucleon pickup process, while in the backward angular region it proceeds mainly through a two-nucleon pickup process. Both of these processes are automatically included in the coupled-channel calculation described here, because in this calculation a totally anti-symmetrized wave function is employed.

Other reaction calculations using the resonating-group approach are reported in refs. [141-146].

4.3b. $^{4}He(d,t)^{3}He$ reaction

For resonating-group calculations at relatively high energies where many rearrangement and breakup channels are open, it is practically impossible to take all these channels explicitly into consideration. Thus, in these calculations, one is compelled to adopt the procedure of utilizing only a small number of open channels in the trial function and taking into account the remaining channels by introducing phenomenological imaginary potentials into the formulation.

At lower energies, the number of open channels is much smaller. Consequently, if one makes the assumption that breakup processes proceed entirely through a sequential-decay mechanism [147], then it becomes possible to perform resonating-group calculations with essentially all these channels taken into account. In this subsection, we describe such a calculation, made by Schütte *et al* [148], on the reaction $^{4}He(d,t)^{3}He$.

The purpose of this calculation is to explain quantitatively the violation of the Barshay-Temmer theorem [149,159] for this reaction. This theorem is based on strict isospin symmetry of nuclear forces; it predicts that the differential reaction cross section and the analyzing power should, respectively, be symmetric and antisymmetric with respect to 90^0 in the c.m. system. These predictions are, however, not quite borne out by experiments which show a rather strong asymmetry in the cross section at E_f = 15.7 MeV* and a smaller but definite asymmetry at higher energies [151].

Many channels are included in this calculation. These are: $d + \alpha$, $^5He(3/2^-) + p$, $^5Li(3/2^-) + n$, $^5He^*(1/2^-) + p$, $^5Li^*(1/2^-) + n$, $^3He + t$, $^5He^{**}(3/2^+) + p$, and $^5Li^{**}(3/2^+) + n$ channels. The nucleon-nucleon potential used contains soft repulsive cores, and spin-orbit and tensor components [152]. The Kohn-Hulthén variational procedure was used to compute the S-matrix for this problem.

According to the Barshay-Temmer theorem, isospin-conserving $^4He(d,t)^3He$ transitions are possible only to $t + ^3He$ channels with T = 0, S = 1, ℓ = even or T = 0, S = 0, ℓ = odd. These transitions will result in a symmetric differential reaction cross section. However, via the virtual excitation of the $^5He^{**}(3/2^+) + p$ and $^5Li^{**}(3/2^+) + n$ fragmentations, which are superpositions of T = 0 and T = 1 states, isospin-nonconserving $^4He(d,t)^3He$ transitions become also possible. With these latter transitions, one then

---

*The quantity E_f denotes the c.m. relative energy in the $d + \alpha$ channel.

obtains a differential reaction cross section which is not symmetric with respect to 90^{o} in the c.m. system.

In fig. 11 calculated and experimental [148, 153] differential reaction cross sections at E_f = 21.33 and 16.63 MeV are compared. As is seen, the agreement is quite satisfactory. The calculation reproduces the general features of the measured result, but does not quite yield the magnitude of the observed maximum asymmetry. This latter defect is probably caused by the use of a simplified description of the five-nucleon system in the calculation.

A comparison between calculation and experiment [154] for the analyzing power at E_f = 21.33 MeV is shown in fig. 12. Here it is found that the calculated derivations from antisymmetry are quite small ($< 10\%$), which is in agreement with experimental finding.

There are other calculations of the type described in this subsection. For these calculations the interested readers are referred to the review articles by Hackenbroich [155,156].

5. Effects of the Pauli principle

5.1. Introductory remarks

The importance of the Pauli principle, expressed by the presence of the antisymmetrization operator $\mathcal{A}$ in eq. (7), in well-known in nuclear-structure problems [3,157]. As has been discussed in detail in ref. [5], it serves to reduce greatly the difference between seemingly different structures and thereby resolve the apparent contradictions among existing nuclear models. In practical calculations, this has the consequence that, especially at relatively low excitation energies, one can frequently obtain satisfactory results by employing only a small number of many-nucleon configurations in the trial wave function.

The purpose of this section is to describe briefly the role played by the Pauli principle in nuclear scattering and reaction processes. Specifically, what will be discussed is its influence on the effective internuclear potential (i.e., the real-central part of the optical potential) and the connection between this principle and the various direct-reaction mechanisms commonly employed in phenomenological analyses [158].

5.2. Effective internuclear potential

5.2a. Odd-even ℓ-dependence and channel-spin dependence

One of the important findings from resonating-group calculations is that the phase-shift behaviour frequently exhibits a distinct odd-even dependence on the orbital angular momentum. This is demonstrated in fig. 13, where phase shifts as a function of ℓ are shown for various systems, all calculated at a wave number of 1.52 fm^{-1}. From this figure one sees that

the degree of odd-even or parity dependence is quite different in different systems, being rather strong in the $^3H + \alpha$ system, moderate in the $n + \alpha$ system, but distinctly weak in the $n + {}^{16}O$, $\alpha + {}^{16}O$, and $n + {}^{40}Ca$ systems.

The occurrence of the odd-even ℓ-dependence is a consequence of the Pauli principle. This is so, since it is shown in subsection 2.3a that if this principle were not taken into consideration or, in other words, if the operator $\mathcal{A}'$ in eq. (17) were set as unity, then the effective internuclear potential would just be equal to the direct potential V_D which has no ℓ-dependence and which will yield phase-shift points following a smooth trend with respect to the orbital angular momentum.

Also because of the Pauli principle, the nature of the odd-even ℓ-dependence may depend on the channel spin s. As an illustration, the phase-shift behaviour [159] of both the $^3H + {}^3He$ system and the $d + {}^3He$ system at 50 MeV is depicted in fig. 14. Here it is seen that in the $d + {}^3He$ system the zigzag pattern in the s = 3/2 state is exactly opposite to that in the s = 1/2 state, while in the $^3H + {}^3He$ system the zigzag patterns are similar in both channel-spin states.

The above finding in the $d + {}^3He$ system may be explained by noting that in the s = 3/2 state the neutron in the deuteron cluster cannot penetrate into the 1s-neutron hole of the ^3He cluster. This causes the ^3He cluster to act toward the deuteron like a spin and isospin saturated substructure, with the consequence that the $d + {}^3He$ system in this channel-spin state behaves very much like the $d + \alpha$ system. In the s = 1/2 state, on the other hand, the neutron can penetrate into the 1s-hole of ^3He to form a cluster similar to a diffuse α particle; thus, in this channel-spin state, the $d + {}^3He$ system has a similarity to the $p + \alpha$ system and even more so to

the more diffuse $^3H + \alpha$ system.

In an analogous manner, one can understand the situation in the $^3H + ^3He$ system. Here in both channel-spin states, a nucleon from one of the clusters can penetrate into the 1s-hole of the other cluster. Therefore, it is expected not only that the $^3H + ^3He$ effective interaction should be rather insensitive to the channel spin, but also that the system should behave similarly to the $d + \alpha$ system and to the $d + ^3He$ system in its $s = 3/2$ state. As is seen from fig. 14, this is indeed the case.

To demonstrate the presence of odd-even ℓ-dependence in a clearer way, we construct a local-potential model in which the clusters are considered as structureless and the interaction between them is represented by an effective potential $\tilde{V}_{\ell\lambda}$ given by

$$\tilde{V}_{\ell\lambda} = C_{\ell\lambda} V_{N\lambda} \,, \tag{151}$$

with λ denoting the channel-spin multiplicity (the index λ may be dropped if the considered system has a single λ-value), $V_{N\lambda}$ being the direct nuclear potential, and $C_{\ell\lambda}$ being an ℓ-dependent multiplicative parameter. In fig. 15, the results for $C_{\ell\lambda}$, obtained by fitting exactly the phase-shift values of the corresponding resonating-group calculations [49], are shown for the $n + ^{40}Ca$ and $^3H + \alpha$ systems at indicated energies. As is seen, this parameter is only weakly ℓ-dependent in the $n + ^{40}Ca$ system, but shows a strong zigzag pattern in the $^3H + \alpha$ system.

Next, we illustrate in the $n + ^6Li$ system another interesting consequence of the Pauli principle. By examining the phase-shift behaviour exhibited in figs. 13 and 14, one might predict that in this system the effective

potential $\tilde{V}_{\ell\lambda}$ should be stronger in odd-ℓ states, regardless of the channel-spin value. That this is not quite so can be seen from fig. 16 where the open circles and crosses represent the resonating-group result [111], while the solid lines are smooth curves drawn through phase-shift points calculated using the local-potential model of eq. (151) with $C_{\ell\lambda}$ taking on indicated values.. Here one sees that in the s = 1/2 state the odd-ℓ interaction is indeed stronger than the even-ℓ interaction, but the opposite is true in the s = 3/2 state. As to the reason for this apparent failure of the prediction made above, one notes that for this system there are in the nonclosed 1p shell two target nucleons which behave like a deuteron cluster. Since it follows again from the Pauli principle that a neutron can closely approach a deuteron in the s = 1/2 state but not so in the s = 3/2 state, one may come to the conclusion that the blocking effect, caused by these two 1p-nucleons, is much more important in the s = 3/2 state than in the s = 1/2 state. Therefore, this example serves to show that in predicting the relative strength of the effective interaction in odd-ℓ and even-ℓ states, one must always carefully investigate the dynamical structures of the clusters under consideration.

From fig. 16 one also notes that the ℓ = 0, s = 1/2 resonating-group phase-shift point seems to deviate somewhat from the zigzag trend followed by other s = 1/2 points. This is very likely related to the fact that, for this particular set of (ℓ, λ) value, there exists a Pauli-forbidden state in the resonating-group formulation. Indeed, deviations of this kind have also been found in n + α and other systems. This indicates, therefore, that to construct a useful semi-microscopic potential model, one may need

not only to adopt the odd-even feature described here, but also to introduce into the model either an orthogonality condition [160] or a Pauli repulsive core [161-163].

For a quantitative estimate of the importance of the Pauli principle, it is useful to express $C_{\ell\lambda}$ in eq. (151) as

$$C_{\ell\lambda} = C_{a\lambda} + (-1)^{\ell} C_{b\lambda} , \qquad (152)$$

where $C_{a\lambda}$ and $C_{b\lambda}$ are ℓ-independent parameters. Then, as is evident, the amount by which $C_{a\lambda}$ differs from 1 or $C_{b\lambda}$ differs from 0 is a measure of the effects of antisymmetrization. In table 1, the best values of $C_{a\lambda}$ and $C_{b\lambda}$ for various systems at 30 MeV are listed; these values are obtained by fitting as well as possible the corresponding resonating-group phase-shift results. From this table it is seen that, although the values of $C_{b\lambda}$ may become close to 0 for certain systems, the values of $C_{a\lambda}$ are all appreciably larger than 1, indicating that in scattering processes the Pauli principle is generally important.

At a relatively high energy, the behaviour of the differential scattering cross section in the backward angular region is strongly correlated with the magnitude (not the sign) of $C_{b\lambda}$ [164]. In fig. 17 we show a comparison [165] between the results obtained for $^3He + \alpha$ scattering at 44.5 MeV using the resonating-group method and the potential model of eqs. (151) and (152) with $C_{a\lambda} = 1.15$ and $C_{b\lambda} = 0$. Here it is seen that, although the agreement in the forward angular region is rather satisfactory, there is a strong disagreement at angles larger than about 90^0. In the $n + {}^{40}Ca$ system at 30 MeV, on the other hand, one sees from fig. 18 that,

because of the small magnitude of $C_{b\lambda}$, the agreement between the resonating-group result (solid dots) and the result obtained using the potential model with $C_{a\lambda} = 1.35$ and $C_{b\lambda} = 0$ (solid curve) is fairly reasonable even at rather large angles (the dashed curve in this figure is obtained by omitting antisymmetrization effects, i.e., by setting $C_{a\lambda} = 1$ and $C_{b\lambda} = 0$ in the potential model).

It should be remarked, however, that even when $C_{b\lambda}$ has a small magnitude, one may still observe significant effects in situations where partial-wave scattering amplitudes strongly cancel one another. Generally, these occur at backward angles when the scattering energies are relatively high. For instance, in a phenomenological potential-model study of nucleon scattering by ^{40}Ca at about 30 MeV [166], it was found that when $C_{b\lambda}$ is changed from 0 to -0.01, the scattering behaviour at angles larger than about 150^{o} is appreciably affected and the differential cross section at 180^{o} is increased by a factor of around 3.

Odd-even potential models have been successfully used to analyze experimental data of $p + {}^{3}He$ [139], $p + \alpha$ [139], $^{3}He + \alpha$ [167,168], and $\alpha + {}^{6}Li$ [169] scattering. In heavier systems such as $^{12}C + {}^{13}C$ [170,171] and $^{12}C + {}^{16}O$ [172], the application of such models has similarly yielded satisfactory agreement with measured results. In addition, a phenomenological study of the $^{16}O + {}^{20}Ne$ scattering data [173] has also indicated the need of an odd-even term in the effective internuclear potential.

The situation in the case of $\alpha + {}^{40}Ca$ scattering is not as clear. Thus, to explain the scattering behaviour in the backward angular region, Kondo et al [174] have found it desirable to introduce a small amount of odd-even ℓ-dependence into the real part of the optical potential. On

the other hand, Michel and Vanderpoorten [175] have been able to obtain excellent fits with experimental data over a wide energy range using parity-independent potentials. The fact that the same experimental result can be explained by different sets of potentials is just a manifestation of potential-model ambiguities, as has been pointed out especially by Wall [176]. Based on resonating-group findings in both $\alpha + {}^{16}O$ and $\alpha + {}^{40}Ca$ [80] systems and the discussion to be presented in the next subsection, we are of the opinion that the essential features of $\alpha + {}^{40}Ca$ scattering can very likely be properly accounted for without the incorporation of an odd-even ℓ-dependent component into the effective potential.

5.2b. General discussion

In the Born approximation, one can show that the ℓ-dependence contained in the effective internuclear potential is only of the odd-even type. This has been demonstrated in the $n + \alpha$ case [164]. There it was shown that, by separating the kernel function $K(\underline{R}', \underline{R}'')$ [see eq. (37)] into three parts, i.e.,

$$K = K_\alpha + K_\beta + K_\gamma \ , \tag{153}$$

with K_α, K_β, and K_γ being the knockout (incident neutron knocks out a target neutron), pickup (incident neutron picks up a ^3He cluster), and nucleon-rearrangement kernels, respectively, one can easily construct effective local potentials $\tilde{V}_\alpha$, $\tilde{V}_\beta$, and $\tilde{V}_\gamma$ which yield exactly the same Born scattering amplitudes as these kernel terms. The potential $\tilde{V}_\alpha$ is a Wigner-type potential, whereas the potentials $\tilde{V}_\beta$ and $\tilde{V}_\gamma$ are Majorana-type potentials. The total effective local interaction is,

therefore, given in the Born approximation by $V_D + \tilde{V}_\alpha + \tilde{V}_\beta + \tilde{V}_\gamma$, which clearly has an odd-even ℓ-dependence. As one goes to energy regions where the Born approximation is less valid, the ℓ-dependence in the effective internuclear interaction will of course become more complicated; however, it is reasonable to expect that the odd-even feature should still remain to be the main part of the orbital angular-momentum dependence.

For a more general discussion* [177], we consider now the effects of the Pauli principle on the effective interaction between two clusters A and B, with cluster A containing N_A nucleons and characterized by a width parameter α_A and cluster B containing N_B nucleons and characterized by a width parameter α_B [see eq. (89)]. Specifically, what we shall do is to study exchange effects associated with the normalization kernel $\mathcal{N}_E(\underset{\sim}{R}', \underset{\sim}{R}'')$ of eq. (24), which has the form

$$\begin{aligned} \mathcal{N}_E(\underset{\sim}{R}', \underset{\sim}{R}'') &= \sum_\chi \mathcal{N}_E^\chi(\underset{\sim}{R}', \underset{\sim}{R}'') \\ &= \sum_\chi P_\chi \exp\left(-a_\chi \underset{\sim}{R}'^2 - C_\chi \underset{\sim}{R}' \cdot \underset{\sim}{R}'' - a_\chi \underset{\sim}{R}''^2\right) \end{aligned} \qquad (154)$$

with χ being the number of nucleons interchanged between the clusters and P_χ being a polynomial in $\underset{\sim}{R}'^2$, $\underset{\sim}{R}' \cdot \underset{\sim}{R}''$, and $\underset{\sim}{R}''^2$. By using the complex-generator-coordinate technique described in sect. 3, one can derive general expressions for the coefficients a_χ and C_χ [48]. These expressions are

$$a_\chi = \frac{\mu_0^2}{4\chi} \frac{\chi^2\left[(\alpha_A-\alpha_B)^2 + \frac{2}{\mu_0}(N_A+N_B)\alpha_A\alpha_B\right] + N_A N_B\left(1-\frac{\chi}{\mu_0}\right)(\alpha_A+\alpha_B)^2}{N_A N_B(\alpha_A+\alpha_B) - \chi(N_A\alpha_A + N_B\alpha_B)} \qquad \cdots(155)$$

*A similar, but more restricted, discussion is given in ref. [178].

and

$$C_\chi = -\frac{\mu_0^2}{2\chi}\,\frac{\chi^2(\alpha_A-\alpha_B)^2 + N_A N_B\left(1-\frac{\chi}{\mu_0}\right)(\alpha_A+\alpha_B)^2}{N_A N_B(\alpha_A+\alpha_B) - \chi\left(N_A\alpha_A + N_B\alpha_B\right)} \tag{156}$$

where μ_0 denotes the reduced nucleon number, given by

$$\mu_0 = \frac{N_A N_B}{N_A + N_B} \tag{157}$$

It should be remarked that the kernel function $\mathcal{N}_E(\underset{\sim}{R}',\underset{\sim}{R}'')$ of eq. (30) contains the same exponential factors in the limit case where the nucleon-nucleon potential has a range approaching infinity ($K\to 0$ in eq. (16) of ref. [164]). Because of this, it is our opinion that a study of the normalization kernel $\mathcal{N}_E$ alone should yield a useful, semi-quantitative understanding of the effects of antisymmetrization.

For clarity in discussion, we make the simplification

$$\alpha_A = \alpha_B = \alpha \tag{158}$$

and assume $N_A > N_B$.* Then, by employing the procedure discussed in ref. [179], one can find effective local potentials $\tilde{V}_\chi(\underset{\sim}{R}')$ which yield,

*The conclusions reached with and without the simplification of $\alpha_A = \alpha_B = \alpha$ are very similar.

in the Born approximation, the same scattering amplitudes as the kernel terms $\mathcal{N}_E^{\chi}(\underset{\sim}{R}', \underset{\sim}{R}'')$. The result is as follows:

(i) $\chi < \mu_0$ — The effective potentials are Wigner-type potentials which yield large Born scattering amplitudes only at forward angles. These potentials are

$$\tilde{V}_{\chi}(\underset{\sim}{R}') = \tilde{P}_{\chi} \exp\left[-(k/k_{\chi})^2\right] \exp\left[-(R'/R_{\chi})^2\right] \tag{159}$$

with

$$k_{\chi} = \left[\frac{\mu_0(2\mu_0 - \chi)}{\chi}\alpha\right]^{1/2} \tag{160}$$

and

$$R_{\chi} = \left[\frac{4(\mu_0 - \chi)}{\chi(2\mu_0 - \chi)}\frac{1}{\alpha}\right]^{1/2} \tag{161}$$

(ii) $\chi > \mu_0$ — The effective potentials are Majorana-type potentials which yield large Born scattering amplitudes only at backward angles. These potentials are

$$\tilde{V}_{\chi}(\underset{\sim}{R}') = \tilde{P}_{\chi} \exp\left[-(k/k_{\chi})^2\right] \exp\left[-(R'/R_{\chi})^2\right] P^{R'} \tag{162}$$

with

$$k_{\chi} = \left[\frac{\mu_0 \chi}{2\mu_0 - \chi}\alpha\right]^{1/2} \tag{163}$$

and

$$R_x = \left[\frac{4(x-\mu_0)}{x(2\mu_0 - x)} \frac{1}{\alpha} \right]^{1/2} \tag{164}$$

Also, in eqs. (159) and (162), $\tilde{P}_x$ are polynomial functions in k^2 and R'^2. By examining the expressions for k_x and R_x, one can easily see that for $x < \mu_0$, k_x and R_x have largest values when x = 1, and for $x > \mu_0$, k_x and R_x have largest values when $x = N_B^*$. This indicates, therefore, that among all exchange terms, the one-exchange term and the core-exchange term are the most important. In fact, this finding has been amply verified by explicit resonating-group calculations. For example, in $^3He + \alpha$ scattering [180] where $\mu_0 = 12/7$, the two-exchange term was found to be rather unimportant, and in $\alpha + {}^{16}O$ scattering [181] where $\mu_0 = 3.2$, the one-, two-, and three-exchange terms were found to yield progressively weaker contribution.

The effective potentials $\tilde{V}_l$ corresponding to the one-exchange term and $\tilde{V}_c$ corresponding to the core-exchange term have the following expressions:

$$\tilde{V}_l(\underline{R}') = \tilde{P}_l \exp\left[-(k/k_l)^2\right] \exp\left[-(R'/R_l)^2\right] \tag{165}$$

with

$$k_l = \left[\mu_0(2\mu_0 - 1)\alpha\right]^{1/2}, \tag{166}$$

*In the case where $N_A = N_B$, such as $^{40}Ar + {}^{40}Ca$ scattering, the largest value of x will be somewhat smaller than N_B.

$$R_1 = \left[\frac{4(\mu_0 - 1)}{2\mu_0 - 1} \frac{1}{\alpha} \right]^{1/2} , \tag{167}$$

and

$$\tilde{V}_c(\underset{\sim}{R}') = \tilde{P}_c \exp\left[-(k/k_c)^2\right] \exp\left[-(R'/R_c)^2\right] P^{R'} \tag{168}$$

with

$$k_c = \left(\frac{N_A N_B}{N_A - N_B} \alpha \right)^{1/2} , \tag{169}$$

$$R_c = \left(\frac{4}{N_A - N_B} \frac{1}{\alpha} \right)^{1/2} \tag{170}$$

For comparison, we also give here the direct nuclear potential V_N which, in the limit of a zero-range nucleon-nucleon potential, has the form*

$$V_N(\underset{\sim}{R}') = \tilde{P}_N \exp\left[-(R'/R_N)^2\right] \tag{171}$$

with

$$R_N = \left(\frac{2\mu_0 - 1}{\mu_0} \frac{1}{\alpha} \right)^{1/2} . \tag{172}$$

*With a finite-range nucleon-nucleon potential, the direct nuclear potential V_N will have a range longer than that given by eq. (172).

In addition, it is important to note that in the polynomial factors $\tilde{P}_I$ and $\tilde{P}_N$, the highest powers of R'^2 are both given by $n_A + n_B$, with n_A and n_B being, respectively, the principal quantum numbers, in oscillator wells A and B, of the last shells to be filled. For example, in $\alpha + {}^{16}O$ scattering, the value of n_A is 1 and the value of n_B is 0 when the cluster internal functions are assumed to have the lowest configurations in their respective oscillator wells. As for the polynomial factor $\tilde{P}_C$, its highest power of R'^2 is somewhat more difficult to determine; however, it has been derived in ref. [178] , where it was shown that for those interesting cases in which N_A and N_B have nearly equal values, this highest power is again approximately given by $n_A + n_B$ [182] . Therefore, since the polynomial factors in $\tilde{V}_I$, $\tilde{V}_C$, and V_D have similar values for their highest powers in R'^2 , it is appropriate to simply examine the exponential factors in order to decide the situations under which the effective potentials $\tilde{V}_I$ and $\tilde{V}_C$ make important contributions.

Let us first study the spatial dependence of $\tilde{V}_I$ and $\tilde{V}_C$. By comparing the values of R_I and R_C with the value of R_N , we can make the following remarks:

(i) The ratio R_I / R_N is given by

$$\frac{R_I}{R_N} = \left[1 - \frac{1}{(2\mu_0 - 1)^2} \right]^{1/2} , \tag{173}$$

which is smaller than but close to 1, indicating that the one-exchange term is always important. This is consistent with the result, stated in subsection 5.2a, that the values of $C_{a\lambda}$ in eq. (152) are appreciably larger than 1 for all investigated systems. In addition, the fact that

$R_I < R_N$ is also in agreement with an empirical finding [183], obtained by potential-model analyses of p, ^{3}He, and α scattering on ^{16}O, that the range of the Wigner-type effective potential is somewhat shorter than that of the direct nuclear potential.

(ii) The characteristic range R_C decreases with increasing value of the difference between the nucleon numbers in clusters A and B. This means that one expects the core-exchange effect to become less important as (N_A-N_B) increases. Indeed, as is discussed in subsection 5.2a, we have reached a similar conclusion from explicit resonating-group calculations. There it was shown that the degree of odd-even ℓ-dependence is quite strong in scattering systems involving two s-shell nuclei where the values of $(N_A - N_B)$ are small, and weak in systems such as $\alpha + ^{16}$O and n + ^{40}Ca where $(N_A - N_B)$ takes on rather large values. Similarly, of course, the finding that core-exchange effects are important in ^{12}C + ^{13}C [171] and ^{12}C + ^{16}O [77] scattering but not in α + ^{40}Ca scattering [80, 114] supports the assertion reached by our present analysis.

Next, we examine the energy dependence of exchange effects by studying the expressions for the characteristic wave numbers k_I and k_C given by eqs. (166) and (169). To do this, we make the reasonable assumption that the effective potentials $\tilde{V}_I$ and $\tilde{V}_C$ become unimportant when their energy-dependent exponential factors acquire a value less than e^{-4}. Adopting this criterion, one can then easily find that the one-exchange term has a significant influence when $E/\mu_0 < \tilde{E}_I^*$ where

---

*It is interesting to note that E/μ_0 is also the incident energy per nucleon in the laboratory system, regardless of whether A or B is the incident nucleus.

$$\tilde{E}_1 = \frac{\hbar^2}{2M} \frac{4(2\mu_0 - 1)}{\mu_0} \alpha \qquad (174)$$

with M being the nucleon mass, and the core-exchange term has a significant influence when $E/\mu_0 < \tilde{E}_c$ where

$$\tilde{E}_c = \frac{\hbar^2}{2M} \frac{4(N_A + N_B)^2}{N_A N_B} \frac{1}{N_A - N_B} \alpha \qquad (175)$$

In table 2, we list the values of $\tilde{E}_1$ and $\tilde{E}_c$ calculated for various systems. Here it is seen that the one-exchange term is important over a wide energy range for all systems. On the other hand, because of the factor $(N_A - N_B)$ occurring in eq. (175), the core-exchange term has a slow energy dependence only when $(N_A - N_B)$ is relatively small.

Finally, it should be emphasized that the considerations given here are made in the Born approximation and based mainly on the features of the normalization kernel. Therefore, the results obtained have only semi-quantitative significance at relatively high energies. However, we do believe that especially the dependence of the core-exchange effect on the factor $(N_A - N_B)$ is very likely a realistic prediction and this particular finding should be very useful when one attempts to construct potential models for the analyses of experimental scattering results.

5.3. Direct-reaction mechanisms

Since resonating-group calculations employ totally antisymmetric wave functions, all exchange effects are explicitly included. Thus it is

possible to use these calculations for a study of direct-reaction mechanisms. In this subsection, we shall carefully examine the $\alpha(p,d)^3He$ reaction using the plane-wave Born approximation (PWBA) [184], in the hope of obtaining a transparent picture concerning the roles played by different direct-reaction processes which are represented by various coupling-kernel terms in the resonating-group formulation.

5.3a. Brief description of the method of analysis

The formulation of the two-channel $\alpha(p,d)^3He$ problem is briefly given in subsection 4.3a and, hence, will not be further described here. For our present purpose, it suffices to say that the transition from the $p + \alpha$ channel to the $d + {}^3He$ channel is effected by the coupling kernel K_{fg} (hereafter simply written as K) which has the form

$$K = K^a + K^b \tag{176}$$

with

$$K^a(\underset{\sim}{R}'_f, \underset{\sim}{R}''_g) = (N_f N_g)^{-1/2} \Big\langle \Phi_3(123)\Phi_d(45)\xi_f \delta(\underset{\sim}{R}_f - \underset{\sim}{R}'_f) Z(\underset{\sim}{R}_{cm})$$

$$|H - E_T| (1 - P_{45}) \mathcal{A}_\alpha \left[\Phi_\alpha(1234)\xi_g \delta(\underset{\sim}{R}_g - \underset{\sim}{R}''_g)\right] Z(\underset{\sim}{R}_{cm}) \Big\rangle \tag{177}$$

and

$$K^b(\underline{R}'_f, \underline{R}''_g) = (N_f N_g)^{-1/2} \langle \phi_3(123)\phi_d(45)\xi_f \delta(\underline{R}_f - \underline{R}'_f) Z(\underline{R}_{cm})$$

$$|H - E_T|(-P_{15} - P_{25} - P_{35}) \mathcal{A}_\alpha [\phi_\alpha(1234)\xi_g \delta(\underline{R}_g - \underline{R}''_g)] Z(\underline{R}_{cm})\rangle, \quad (178)$$

where P_{ij} is an operator interchanging the spatial, spin, and isospin coordinates of nucleons i and j, and $\mathcal{A}_\alpha$ is the antisymmetrization operator for the α cluster. In the above equations, it should be noted that the arguments of the internal functions of the clusters indicate which nucleons are involved in these clusters; such a labelling is permissible, because the wave function is totally antisymmetrized.

From eqs. (177) and (178), one can clearly see that K^a corresponds to a process in which the incident proton is contained in the outgoing deuteron, while K^b corresponds to a process in which the incident proton is contained in the outgoing ^{3}He. In other words, K^a describes a one-nucleon pickup process, while K^b describes a two-nucleon pickup process.

Since our sole purpose in the present study is to gain an understanding of reaction mechanisms, we simplify the formulation in the following way: (i) a single-Gaussian deuteron function ϕ_d yielding the same rms radius as the three-Gaussian function of subsection 4.3a is used, (ii) a simplified nucleon-nucleon potential with a Serber mixture is employed; this potential is described in a previous publication [8], and (iii) the Coulomb interaction is neglected. These simplifications do not change the essential features of the results obtained in subsection 4.3a, but they do allow a

more straightforward interpretation.

By summing over spin and isospin coordinates, the kernel functions K^a and K^b become [22]

$$K^a = K^a_T + K^a_E + K^a_{12} + K^a_{14} + K^a_{15} + K^a_{45} \tag{179}$$

and

$$K^b = K^b_T + K^b_E + K^b_{12} + K^b_{14} + K^b_{23} + K^b_{24} + K^b_{45} \ . \tag{180}$$

In these equations, the functions K^a_T, K^b_T , K^a_E, and K^b_E arise from the kinetic-energy operator T and the total energy E_T. The remaining functions come from the potential-energy operator; they have the forms

$$K^a_{ij} = C^a_{ij} \int \left[\psi_f(123;45)\right]^* v_{ij}\, \psi_g(1234;5)\, d\tau \tag{181}$$

and

$$K^b_{ij} = C^b_{ij} \int \left[\psi_f(123;45)\right]^* v_{ij}\, \psi_g(5234;1)\, d\tau \ , \tag{182}$$

where we have introduced the notation

$$\psi_f(123;45) = \phi_3(123)\phi_d(45)\delta(\underline{R}_f - \underline{R}'_f)\mathcal{Z}(\underline{R}_{cm}) \ , \tag{183}$$

$$\psi_g(1234;5) = \phi_\alpha(1234)\delta(\underline{R}_g - \underline{R}''_g)\mathcal{Z}(\underline{R}_{cm}) \ , \tag{184}$$

and

$$\psi_g'(5234;1) = P_{15}^r \psi_g(1234;5) \tag{185}$$

Also, in eqs. (181) and (182), C_{ij}^a and C_{ij}^b are constant factors unimportant for our present consideration, v_{ij} is the form factor of the nucleon-nucleon potential given by

$$v_{ij} = \exp(-K r_{ij}^2), \tag{186}$$

and $d\tau$ signifies the integration over all spatial variables.

Next, we compute the PWBA reaction amplitude for each of the terms in K^a and K^b. For example, the Born amplitude corresponding to K_{ij}^a is

$$B_{ij}^a = -\frac{\mu_f}{2\pi\hbar^2}\int \exp(-i\underline{k}_f\cdot\underline{R}_f')K_{ij}^a(\underline{R}_f',\underline{R}_g'')\exp(i\underline{k}_g\cdot\underline{R}_g'')d\underline{R}_f' d\underline{R}_g'', \tag{187}$$

where $\underline{k}_g$ and $\underline{k}_f$ are propagation vectors in channels g and f, respectively. By carrying out the spatial integrations in eqs. (181) and (182), analytic expressions for the various amplitudes can be obtained [22]. The differential reaction cross section is then given by

$$\frac{d\sigma}{d\Omega} = \frac{v_f}{v_g}|B^a + B^b|^2, \tag{188}$$

where v_g and v_f are, respectively, the relative velocities of the clusters at large separation in the incident and reaction channels.

5.3b. Result and discussion

The validity of the PWBA at relatively high energies can be tested by making a comparison between the differential reaction cross section computed by solving the resonating-group coupled integrodifferential equations and that computed by using the PWBA. This comparison is shown in fig. 19 at an energy of E_g = 130 MeV (the corresponding value of E_f is 104.88 MeV). From this figure it is seen that, even though the over-all agreement is only fair, the Born result does reproduce the essential features, i.e., the occurrence of large peaks at forward and backward directions and a sharp minimum at around 100^o. Thus, we feel that a study using the PWBA should be useful in yielding a qualitative understanding of the importance of various direct-reaction processes.

From the explicit expressions for the Born amplitudes, one finds that all terms contained in B^a (i.e., B^a_T, B^a_E, and B^a_{ij}) are peaked in the forward direction, while all terms contained in B^b (i.e., B^b_T, B^b_E, and B^b_{ij}) are peaked in the backward direction. This is shown in fig. 20, where the solid curves represent the amplitudes B^a and B^b at E_g = 130 MeV. Here it is seen that, at such a relatively high energy, the cross-section behaviour in the forward angular region can be accounted for by a one-nucleon pickup process, while the cross-section behaviour in the backward angular region can be accounted for by a two-nucleon pickup process. In fact, it is evident that there is effectively no interference between these two processes. We should point out, however, that this lack of interference is strictly a high-energy phenomenon; already at a lower energy of E_g = 70 MeV (E_f = 44.88 MeV), our calculation shows that interference effects become fairly important in the intermediate angular region (see also ref. [140]).

A detailed examination shows that, even though many individual terms in B^a and B^b have appreciable magnitudes, the following approximate relations hold at relatively high energies:

$$B^a_{45} \approx B^a ,$$

$$B^b_{12} \approx B^b . \qquad (189)$$

This is also shown in fig. 20, where the dashed curves represent the amplitudes B^a_{45} and B^b_{12} at E_g = 130 MeV. At lower energies of E_g = 100 and 70 MeV, these relations are still reasonably valid; for example, at $\theta = 0^o$ the ratios B^a_{45}/B^a are equal to 0.83 and 0.80 at these two energies, while at $\theta = 180^o$ the ratios B^b_{12}/B^b are equal to 1.09 and 1.12. Thus, referring to eqs. (181) and (182), one sees that, for an approximate description of the two pickup processes, it is only necessary to consider the interaction between the incident nucleon and the nucleons which are removed from the target (note that the spatial integrals involved in K^b_{12} and K^b_{13} yield the same result). This seems to be intuitively reasonable, but does require to be further examined. At present, our feeling is that this particular cancellation among the various Born amplitudes is related to the presence of redundant solutions in our resonating-group formulation.

In summary, this investigation shows that, at relatively high energies, the cross-section behaviour of the $\alpha(p,d)^3$He reaction at forward angles can be explained as arising from a one-nucleon pickup process, while that at backward angles can be explained as arising from a two-nucleon pickup

process. In addition, it is found that for an approximate description of these pickup processes, one needs only to consider the interaction between the incident nucleon and the nucleons removed from the target. This is an important finding, because if it should turn out to be generally true, then antisymmetrized direct-reaction calculations can be simplified to a considerable extent.

5.4. Concluding remarks

The discussion in this section shows that the Pauli principle is always important in determining the behaviour of scattering and reaction processes. This means that, for a proper description of these processes, it is generally necessary to employ totally antisymmetric wave functions in the calculations. However, there are relatively simple ways which can be used to approximately represent the major effects of antisymmetrization. In scattering problems, one may adopt as intercluster interaction an energy-dependent effective potential which possesses an odd-even dependence on the orbital angular momentum and which contains possibly also a Pauli repulsive-core component. In reaction problems, the situation becomes comparatively simple at relatively high energies, where a careful examination of the resonating-group calculation shows that a complete antisymmetrization between the nucleons in the incident and target nuclei may not need to be carried out and the differential reaction cross section in either the forward or the backward angular region may be reasonably described by a single direct-reaction process.

6. Conclusion

The resonating-group method is a microscopic method to solve nuclear many-body problems. Its formulation is based on the idea that relatively long-range correlations, manifested through the formation of nucleon clusters such as ^{3}He, α, and ^{16}O clusters, are important in determining the properties of nuclear systems. In this method, one first chooses an appropriate trial-function space, and then studies bound-state, scattering, and reaction problems by solving the Schrödinger equation, formulated as a projection equation, in this space. As the examples discussed in sect. 4 show, this type of approach does lead to successful conclusions, and improved results can be obtained by systematically enlarging the function space employed.

The important features of the resonating-group method are the utilization of a fully antisymmetric wave function, the use of a reasonable nucleon-nucleon potential, and a correct treatment of the total center-of-mass motion. Because of these features, resonating-group calculations can frequently become quite complicated from a computational viewpoint when the number of nucleons involved is relatively large. Indeed, it is primarily for this reason that earlier studies have been restricted to systems containing no more than about ten nucleons. Recently, however, with the development of various generator-coordinate techniques, the computational difficulty has been substantially alleviated, and even relatively heavy systems such as ^{16}O + ^{40}Ca and α + ^{18}O scattering can be considered. In sect. 3, we have described how one of these techniques, the complex-generator-coordinate technique, works. This particular technique is chosen for a detailed description, because it is especially flexible in the sense that its application is not limited to cases where the

choice of equal oscillator width parameters for the cluster internal functions is a reasonable approximation. In fact, as is shown in that section, it can be generally used to obtain matrix elements in scattering and reaction problems where the internal functions of the various clusters are flexibly described by translationally-invariant, antisymmetrized products of single-particle wave functions generated from any potential well which is appropriate, although the use of oscillator wells does lead to further simplification in computation.

Because of the use of totally antisymmetrized wave functions, resonating-group calculations can be employed to investigate the effects of the Pauli principle (see also ref. [185]). In sect. 5, it is shown that in scattering problems the essential result of antisymmetrization is to introduce an odd-even ℓ-dependent component into the effective internuclear potential, the importance of which seems to decrease with increasing value of the difference between the nucleon numbers in the incident and target nuclei. This means that one would expect this odd-even component to be generally important in those cases where the nuclei involved have similar mass, but to have a comparatively minor influence when the nucleon-number difference is large. Indeed, it is precisely this latter feature which enables the conventional optical model to yield a reasonable description, over a large angular region, of light-ion scattering by medium and heavy-weight nuclei.

Also, in sect. 5, we have discussed the role played by the Pauli principle in antisymmetrized direct-reaction calculations. There it was shown that, under certain circumstances, one may simplify the calculation by carrying out only a partial antisymmetrization, corresponding to the adoption of a single direct-reaction process, between the nucleons in the incident

and target nuclei. For example, in the $^{6}Li(p,^{3}He)\alpha$ reaction at relatively high energies [5,142], the behaviour in the forward angular region may be satisfactorily explained by employing only the process in which the incident proton picks up a deuteron cluster from the target, while that in the backward angular region may be adequately described by considering the incident proton to pick up a triton cluster from ^{6}Li.

Even though resonating-group calculations have so far always yielded satisfactory results, there is a somewhat undesirable feature which should be mentioned. That is, two-nucleon potentials of relatively simple form have generally been employed. In particular, the presence of a strong repulsive component in the nucleon-nucleon potential has usually not been explicitly considered and the saturation property has been taken into account only in a relatively crude manner by mostly fixing the rms radii of the clusters involved. We emphasize, however, that although the use of more refined forces will undoubtedly influence the numerical results to a certain extent, the general features of nuclear processes will be essentially unchanged. This must be so since, for scattering and reaction problems in which the incident energy per nucleon is less than about 50 MeV, these general features are determined mainly by the fact that nucleons are fermions and nuclear forces are short-ranged, saturating, and on the average attractive.

At present, there exist many resonating-group bound-state, scattering, and reaction calculations involving s-shell clusters. Consequently, an impressive amount of information has been obtained concerning cluster states in very light nuclei. For heavier systems, the situation is rather different; here, essentially only scattering calculations involving doubly-closed-shell nuclei ^{16}O and ^{40}Ca have been attempted. Therefore, there are still many

interesting problems yet to be considered, and some of these problems which are well within our present-day capabilities are:

(i) A systematic study of light-ion scattering by ^{6}Li or ^{7}Li and the scattering of ^{16}O by ^{17}O, ^{18}O, ^{19}F, and ^{20}Ne. This will be a useful study, because the results obtained should give us further information concerning the dependence of the odd-even effect on the nucleon-number difference of the interacting nuclei.

(ii) Direct-reaction calculations involving relatively heavy clusters, such as $^{18}O(p,t)^{16}O$ reaction and so on.

Also, of course, it will be important to study the case of three or more-cluster decays. This is, however, a comparatively more difficult problem, the solution of which would probably require further advance in mathematical and computational techniques.

In conclusion, it is our opinion that the resonating-group method is a practical, microscopic method of solving nuclear many-body problems. Therefore, it should be extensively used in the future to study the properties of those nuclear systems which have heretofore been treated only by macroscopic, phenomenological means.

Appendix A

The direct potential V_D

In optical-model studies, one of the interesting developments was the discovery [18] that, in light-ion scattering by medium and heavy-weight nuclei, the experimental data may be fairly well represented by using an optical potential for which the real part is obtained by a folding procedure involving the matter distributions of the nuclei and the nucleon-nucleon force. In this Appendix, the purpose is to show that this folding potential is just the direct potential V_D given by eq. (34).

For simplicity in discussion, we shall assume that the nucleon-nucleon potential is purely central and consists of only a direct or spin-isospin-independent part V_d. Then, from eq. (34), we obtain

$$V_D(\underset{\sim}{R}) = \langle \Phi(A)\Phi(B)\mathcal{Z}(\underset{\sim}{R}_{cm}) \mid V' \mid \hat{\Phi}(A)\hat{\Phi}(B)\mathcal{Z}(\underset{\sim}{R}_{cm}) \rangle_{\underset{\sim}{R}}$$

$$= \frac{N_A N_B}{N_A!\, N_B!} \langle \hat{\Phi}(A)\hat{\Phi}(B)\mathcal{Z}(\underset{\sim}{R}_{cm}) \mid V_d(\underset{\sim}{r}_i - \underset{\sim}{r}_j) \mid \hat{\Phi}(A)\hat{\Phi}(B)\mathcal{Z}(\underset{\sim}{R}_{cm}) \rangle_{\underset{\sim}{R}} \quad \ldots.(190)$$

where i and j are nucleons in clusters A and B, respectively. Now, by defining internal spatial coordinates

$$\underset{\sim}{\rho}_i = \underset{\sim}{r}_i - \underset{\sim}{R}_A \quad , \qquad (i \in A)$$

$$\underset{\sim}{\rho}_j = \underset{\sim}{r}_j - \underset{\sim}{R}_B \quad , \qquad (j \in B) \qquad (191)$$

we can write $V_d(\underline{r}_i - \underline{r}_j)$ as

$$V_d(\underline{r}_i - \underline{r}_j) = V_d(\underline{\rho}_i - \underline{\rho}_j + \underline{R})$$

$$= \int V_d(\underline{\eta} - \underline{\xi} + \underline{R})\,\delta(\underline{\rho}_i - \underline{\eta})\,\delta(\underline{\rho}_j - \underline{\xi})\,d\underline{\eta}\,d\underline{\xi} \quad (192)$$

Substituting eq. (192) into eq. (190) yields

$$V_D(\underline{R}) = \frac{N_A N_B}{N_A!\,N_B!} \int \langle \hat{\Phi}(A)\hat{\Phi}(B)\mathcal{Z} \,|\, \delta(\underline{\rho}_i - \underline{\eta})\delta(\underline{\rho}_j - \underline{\xi}) \,|\, \hat{\Phi}(A)\hat{\Phi}(B)\mathcal{Z} \rangle_{\underline{R}}$$

$$\times\; V_d(\underline{\eta} - \underline{\xi} + \underline{R})\,d\underline{\eta}\,d\underline{\xi} \quad (193)$$

Using the expression

$$\rho_A(\underline{\eta}) = \frac{\langle \hat{\Phi}(A) \,|\, \sum_{i=1}^{N_A} \delta(\underline{\rho}_i - \underline{\eta}) \,|\, \hat{\Phi}(A) \rangle}{\langle \hat{\Phi}(A) \,|\, \hat{\Phi}(A) \rangle}$$

$$= \frac{N_A}{N_A!} \frac{\langle \hat{\Phi}(A) \,|\, \delta(\underline{\rho}_i - \underline{\eta}) \,|\, \hat{\Phi}(A) \rangle}{\langle \Phi(A) \,|\, \hat{\Phi}(A) \rangle} \quad (194)$$

for the matter distribution in cluster A and a similar expression for the matter distribution $\rho_B(\underline{\xi})$ in cluster B, we then find, by using further the normalization condition of eq. (26),

$$V_D(\underset{\sim}{R}) = \int \rho_A(\underset{\sim}{\eta})\, \rho_B(\underset{\sim}{\xi})\, V_d(\underset{\sim}{\eta} - \underset{\sim}{\xi} + \underset{\sim}{R})\, d\underset{\sim}{\eta}\, d\underset{\sim}{\xi} \quad , \tag{195}$$

which has the form of what is commonly referred to as a double-folding potential.

From the discussion presented in subsection 5.2b, one can understand why the double-folding procedure is useful in optical-model studies of light-ion scattering by medium and heavy-weight nuclei. The main reason is that, in such cases, the nucleon-number difference of the interacting nuclei is large. Consequently, the odd-even ℓ-dependence plays a comparatively minor role and its omission in the optical potential will essentially affect the features of the scattering cross section only at extreme backward angles.

Apendix B

Approximate treatment of the exchange-Coulomb interaction

In this Appendix, we discuss the exchange-Coulomb kernel in the case where the wave function is given by

$$\Psi = \mathcal{A}\bar{\Psi} = \mathcal{A}'\hat{\Psi} \quad , \tag{196}$$

with

$$\bar{\Psi} = \Phi(A)\Phi(B)F(\underset{\sim}{R})Z(\underset{\sim}{R}_{cm}) \tag{197}$$

and

$$\hat{\Psi} = \hat{\Phi}(A)\hat{\Phi}(B)F(\underset{\sim}{R})Z(\underset{\sim}{R}_{cm}) \quad . \tag{198}$$

As is evident from eq. (30), this particular kernel has the form

$$K_C(\underset{\sim}{R}',\underset{\sim}{R}'') = \langle \Phi(A)\Phi(B)\delta(\underset{\sim}{R}-\underset{\sim}{R}')Z \,|\, \mathcal{V}_C \,|\, \mathcal{A}''[\hat{\Phi}(A)\hat{\Phi}(B)\delta(\underset{\sim}{R}-\underset{\sim}{R}'')Z] \rangle \quad , \tag{199}$$

where

$$\mathcal{V}_C = \sum_{i<j=1}^{N} V_{ij}^{C} \tag{200}$$

with V_{ij}^{C} being the Coulomb potential between nucleons i and j. Due to the fact that the Coulomb potential does not have a Gaussian spatial

dependence, the evaluation of the exchange-Coulomb kernel frequently requires a considerable amount of computational effort. Therefore, it is desirable to devise a simple procedure by which this kernel can be approximately evaluated but is still accurate enough for practical purposes. Here we propose such a procedure which is based on the recognition that, because of the long-range nature of the Coulomb potential, the total Coulomb energy of a bound system, described by the wave function of eqs. (196) - (198) with

$$F(\underline{R}) = \frac{1}{R} f_{\ell}(R) P_{\ell}(\cos\theta) \tag{201}$$

may be computed in an approximate manner by using only the unantisymmetrized part of the wave function (see chapter 6 of ref.[5]). That is, one can obtain a good estimate of the Coulomb energy, given exactly by

$$E^{C}_{T\ell} = \frac{\langle \bar{\Psi} | \mathcal{V}_C | \Psi \rangle}{\langle \bar{\Psi} | \Psi \rangle} = \frac{\langle \bar{\Psi} | \mathcal{V}_C | \hat{\Psi} \rangle + \langle \bar{\Psi} | \mathcal{V}_C | \mathcal{A}'' \hat{\Psi} \rangle}{\langle \bar{\Psi} | \hat{\Psi} \rangle + \langle \bar{\Psi} | \mathcal{A}'' \hat{\Psi} \rangle} \tag{202}$$

from the approximate expression

$$E^{C}_{T\ell} \approx \frac{\langle \bar{\Psi} | \mathcal{V}_C | \hat{\Psi} \rangle}{\langle \bar{\Psi} | \hat{\Psi} \rangle} \tag{203}$$

By equating these two expressions for $E^{C}_{T\ell}$, one then finds

$$\langle \bar{\Psi} | \mathcal{V}_C | \mathcal{A}'' \hat{\Psi} \rangle = E^{C}_{T\ell} \langle \bar{\Psi} | \mathcal{A}'' \hat{\Psi} \rangle . \tag{204}$$

Using eqs. (197) - (199) and eq. (204) thus yields

$$\int F^*(\underline{R}')\, K_C(\underline{R}',\underline{R}'')\, F(\underline{R}'')\, d\underline{R}'\, d\underline{R}''$$

$$= E^C_{T\ell} \int F^*(\underline{R}')\, \mathcal{N}_E(\underline{R}',\underline{R}'')\, F(\underline{R}'')\, d\underline{R}'\, d\underline{R}'' \,, \tag{205}$$

where the normalization kernel $\mathcal{N}_E(\underline{R}',\underline{R}'')$ is given by eq. (24). If one now makes partial-wave expansions for K_C and $\mathcal{N}_E$, i.e.,

$$K_C(\underline{R}',\underline{R}'') = \frac{1}{R'R''} \sum_\ell \sum_m k^C_\ell(R',R'')\, Y_{\ell m}(\theta',\phi')\, Y^*_{\ell m}(\theta'',\phi'') \tag{206}$$

$$\mathcal{N}_E(\underline{R}',\underline{R}'') = \frac{1}{R'R''} \sum_\ell \sum_m \mathcal{N}_{E\ell}(R',R'')\, Y_{\ell m}(\theta',\phi')\, Y^*_{\ell m}(\theta'',\phi'') \,, \tag{207}$$

then one obtains from eqs. (201) and (205) the following equation:

$$\int_0^\infty \int_0^\infty f^*_\ell(R')\, k^C_\ell(R',R'')\, f_\ell(R'')\, dR'\, dR''$$

$$= E^C_{T\ell} \int_0^\infty \int_0^\infty f^*_\ell(R')\, \mathcal{N}_{E\ell}(R',R'')\, f_\ell(R'')\, dR'\, dR'' \tag{208}$$

Since $f_\ell(R)$ is an arbitrary function, eq. (208) therefore implies that

$$k^C_\ell(R',R'') = E^C_{T\ell}\, \mathcal{N}_{E\ell}(R',R'') \,, \tag{209}$$

which is a very simple, though approximate, expression for the partial-wave exchange-Coulomb kernel.

In an actual calculation, one further expresses $E^C_{T\ell}$ in eq. (209) as

$$E^C_{T\ell} = E^C_A + E^C_B + E^C_{R\ell} \ , \tag{210}$$

where E^C_A and E^C_B are, respectively, the internal Coulomb energies of clusters A and B, and $E^C_{R\ell}$ is the relative Coulomb energy between the clusters. The energies E^C_A and E^C_B may be easily computed by using the expressions for the cluster internal functions $\hat{\phi}(A)$ and $\hat{\phi}(B)$. On the other hand, the energy $E^C_{R\ell}$ is an a priori unknown quantity, but may be determined by the use of a self-consistent procedure to be discussed below.

If one of the clusters, say cluster B, is composed solely of neutrons, then the exchange-Coulomb kernel is just given by

$$k^C_\ell(R',R'') = E^C_A \, \mathcal{N}_{E\ell}(R',R'') \ . \tag{211}$$

In this special case, it is interesting to note that the above expression for k^C_ℓ is in fact exact, as can be easily verified by an explicit calculation.

There is another important point which should be mentioned. For states in which the clusters penetrate into each other strongly, the mutual antisymmetrization between the nucleons in different clusters is important. In such cases, there will be substantial cancellations between the individual terms in both the numerator and the denominator of eq. (202), and the consequence may be quite severe if one omits exchange-Coulomb contributions entirely by simply setting k^C_ℓ equal to zero in the calculation.

We shall now discuss how to determine the value of $E^C_{R\ell}$ in a

self-consistent manner. For this, let us consider a bound or a sharp resonance state which has a certain definite value for the relative orbital angular-momentum quantum number ℓ . What we do is to first choose an arbitrary but reasonable value for $E^C_{R\ell}$ and then calculate the cluster separation energy by solving the integrodifferential equation

$$\left\{ \frac{\hbar^2}{2\mu} \left[\frac{d^2}{dR'^2} - \frac{\ell(\ell+1)}{R'^2} \right] + E - V_N(R') - V_C(R') \right\} f_\ell(R')$$

$$= \int_0^\infty \left[k_\ell^N(R',R'') + k_\ell^C(R',R'') \right] f_\ell(R'')\, dR'' \qquad (212)$$

Two separate calculations will be performed, one for the actual case in which both clusters are charged and the other for the hypothetical case in which the charges of the clusters are assumed to be zero (i.e., we set all charge-dependent quantities in eq. (212) as zero). These calculations will yield separation energies E_S and E_S^o in the charged and uncharged cases, respectively. The difference $\Delta E_S = E_S^o - E_S$ is then a good estimate of the relative Coulomb energy. In general, the value of ΔE_S so determined will, of course, not be equal to the value of $E^C_{R\ell}$ chosen initially. Thus, the procedure is to systematically repeat the calculation with different choices of $E^C_{R\ell}$ until self-consistency, i.e., $E^C_{R\ell} = \Delta E_S$, is finally obtained. This self-consistent value of $E^C_{R\ell}$ will then be used in eqs. (209) and (210) to calculate binding energies and phase shifts in all states which are characterized by this particular value of ℓ .

In principle, one should determine the self-consistent values of $E^C_{R\ell}$ for all values of ℓ . In practice, however, this does not seem necessary and it is a good approximation to use the value determined for $\ell = 0$

in all even-ℓ states and the value determined for $\ell = 1$ in all odd-ℓ states.* The reason why this simplification does yield satisfactory results is that in all states of a rotational band the relative Coulomb energies are similar, and for those values of ℓ for which no bound or sharp resonance states exist, the calculated values of the phase shifts are not expected to be greatly sensitive to the choice of $E^C_{R\ell}$ appearing in the approximate expression for the exchange-Coulomb kernel.

Next, we illustrate the procedure described above in the $\alpha+\alpha$ case where the exact expression for the exchange-Coulomb kernel has been derived. In this case, the trial function has the form of eq. (196) with the α-particle spatial wave function given by eqs. (144) and (146). The nucleon-nucleon potential used is that of eq. (117), with the depth and range parameters specified in eq. (150). The exchange-mixture parameter u is chosen to be 0.93, which yields a ^{8}Be, $\ell = 0$ bound state having an α-particle separation energy of 0.748 MeV.

Using the self-consistent procedure for the $\ell = 0$ ground state, we obtain a value of $E^C_{R\ell}$ equal to 1.63 MeV. The corresponding value for the

---

*For example, in the $\alpha + {}^{16}$O system, the self-consistent values are obtained by performing calculations on the $\ell = 0$ ground state and the $\ell = 1$ excited state at 5.79 MeV. These values turn out to be equal to 6.12 and 5.19 MeV for $\ell = 0$ and 1, respectively. In a case such as the ^{3}H + α system where the ground state has $\ell = 1$ and no bound or sharp resonance states exist for $\ell = 0$, one can simply use the value determined for $\ell = 1$ in all orbital-angular-momentum states.

α-particle separation energy is 0.709 MeV, which is very close to the above-mentioned value obtained with the exact exchange-Coulomb kernel. Also, as a comparison, we have computed the separation energy in the case where the exchange-Coulomb interaction is neglected by setting $k_\ell^c = 0$. This results in a value of 0.246 MeV, which is appreciably smaller than the correct value of 0.748 MeV quoted above.

In fig. 21, we show a comparison of $\ell = 0, 2, 4$ phase shifts calculated with the exact exchange-Coulomb kernel (solid dots), with the approximate but self-consistent exchange-Coulomb kernel (solid curves), and with k_ℓ^c set as zero (dashed curves). Here it is seen that the approximation of omitting exchange-Coulomb effects leads to significant deviations from the exact result especially at energies near resonances. On the other hand, the use of our proposed simple, self-consistent procedure to take these effects into account does yield satisfactory phase-shift values in all orbital angular-momentum states.

References

[1] J. A. Wheeler, Phys. Rev. 52 (1937) 1083, 1107.

[2] Proceedings of the International Conference on Nuclear Forces and the Few-Nucleon Problem, edited by T. C. Griffith and E. A. Power (Pergamon, London, 1960), vol. II.

[3] K. Wildermuth and Th. Kanellopoulos, Nucl. Phys. 7 (1958) 150, 9 (1958/59) 449.

[4] K. Wildermuth and W. McClure, Cluster Representation of Nuclei (Springer-Verlag, Berlin, 1966).

[5] K. Wildermuth and Y. C. Tang, A Unified Theory of the Nucleus (Vieweg, Braunschweig, 1977).

[6] K. Wildermuth and Th. Kanellopoulos, CERN-Report 59-23 (1959).

[7] R. K. Sheline and K. Wildermuth, Nucl. Phys. 21 (1960) 196.

[8] Y. C. Tang, in Proceedings of the International Conference on Clustering Phenomena in Nuclei, Bochum (IAEA, Vienna, 1969), p. 109.

[9] A. Arima, H. Horiuchi, K. Kubodera, and N. Takigawa, in Advances in Nuclear Physics, edited by M. Baranger and E. Vogt (Plenum, New York, 1972), vol. 5, p. 345.

[10] D. M. Brink, in Proceedings of the International Conference on Clustering Phenomena in Nuclei, Bochum (IAEA, Vienna, 1969), p. 147.

[11] W. Sünkel and K. Wildermuth, Phys. Lett. 41B (1972) 439.

[12] D. R. Thompson and Y. C. Tang, Phys. Rev. C12 (1975) 1432, C13 (1976) 2597; Y. C. Tang, Fizika (Suppl. 3) 9 (1977) 91.

[13] A. Weiguny, in Proceedings of the INS-IPCR Symposium on Cluster Structure of Nuclei and Transfer Reactions Induced by Heavy Ions, Tokyo, 1975 (IPCR Cyclotron Progress Report Supplement 4), p. 203.

[14] H. Friedrich, K. Langanke, and A. Weiguny, Phys. Lett. 63B (1976) 125.

[15] W. Sünkel, Phys. Lett. 65B (1976) 419.

[16] D. R. Thompson, M. LeMere, and Y. C. Tang, Phys. Lett. 69B (1977) 1.

[17] I. Reichstein and Y. C. Tang, Nucl. Phys. A158 (1970) 529.

[18] G. W. Greenlees, G. J. Pyle, and Y. C. Tang, Phys. Rev. 171 (1968) 1115.

[19] E. W. Schmid, preprint (1977).

[20] H. Jacobs, K. Wildermuth, and E. Wurster, Phys. Lett. 29B (1969) 455.

[21] D. R. Thompson and Y. C. Tang, Phys. Rev. C8 (1973) 1649.

[22] F. S. Chwieroth, University of Minnesota Report COO-1764-180 (1973).

[23] H. Horiuchi, Progr. Theoret, Phys. 47 (1972) 1058.

[24] M. LeMere, Y. C. Tang, and D. R. Thompson, Phys. Rev. C14 (1976) 23; Phys. Lett. 63B (1976) 1; Phys. Rev. C14 (1976) 1715.

[25] D. L. Hill and J. A. Wheeler, Phys. Rev. 89 (1953) 1102.

[26] J. J. Griffin and J. A. Wheeler, Phys. Rev. 108 (1957) 311.

[27] D. M. Brink, in Proceedings of the International School of Physics "Enrico Fermi", course 36 (ed. by C. Bloch, Academic Press, New York, 1966), p. 247.

[28] C. W. Wong, Phys. Reports 15C (1975) 283.

[29] M. V. Mihailovic and M. Rosina, Editors, Generator-Coordinate Method for Nuclear Bound States and Reactions, Fizika Suppl. 5 (1973).

[30] H. Horiuchi, K. Ikeda, M. Kamimura, S. Saito, T. Tamagaki, and A. Tohsaki, Progr. Theoret. Phys. Suppl. no. 62 (1977).

[31] H. Horiuchi, Progr. Theoret. Phys. 43 (1970) 375.

[32] D. M. Brink and A. Weiguny, Nucl. Phys. A120 (1968) 59.

[33] D. Zaikin, Nucl. Phys. A170 (1971) 584.

[34] Y. Yukawa, Phys. Lett. 38B (1972) 1.

[35] F. Tabakin, Nucl. Phys. A182 (1972) 497.

[36] A. Tohsaki, F. Tanabe, and R. Tamagaki, Progr. Theoret. Phys. 53 (1975) 1022.

[37] R. Beck, J. Borysowicz, D. M. Brink, and M. V. Mihailovic, Nucl. Phys. A244 (1975) 45, 58.

[38] L. F. Canto and D. M. Brink, Nucl. Phys. A279 (1977) 85.

[39] B. Giraud, J. C. Hocquenghem and A. Lumbroso, Phys. Rev. C7 (1973) 2274.

[40] B. Giraud, J. LeTourneux, and E. Osnes, Ann. Phys. (N. Y.) 89 (1975) 359.

[41] N. de Takacsy, Phys. Rev. C5 (1972) 1883.

[42] H. Friedrich, H. Husken, and A. Weiguny, Nucl. Phys. A220 (1974) 125.

[43] M. Mihailovic, L. Goldfarb, and M. Nagarajan, Nucl. Phys. A273 (1976) 207.

[44] Y. Mito and M. Kamimura, Progr. Theoret. Phys. 56 (1976) 583.

[45] D. Baye and P. H. Heenen, Nucl. Phys. A233 (1974) 304.

[46] B. Giraud and J. LeTourneux, Nucl. Phys. A240 (1975) 365.

[47] A. Tohsaki-Suzuki, K. Naito, T. Ando, and K. Ikeda, in Proceedings of the International Pre-Symposium on Clustering Phenomena in Nuclei, Tokyo, Japan (1977).

[48] M. LeMere, Ph.D. Thesis, University of Minnesota (1977).

[49] D. R. Thompson, M. LeMere, and Y. C. Tang, Nucl. Phys. A270 (1976) 211.

[50] S. Hochberg, H. S. W. Massey, and L. H. Underhill, Proc. Phys. Soc. (London) A67 (1954) 957.

[51] Y. C. Tang, E. Schmid, and K. Wildermuth, Phys. Rev. 131 (1963) 2631.

[52] H. Horiuchi, Progr. Theoret. Phys. 58 (1977) 204.

[53] F. S. Chwieroth, Y. C. Tang, and D. R. Thompson, Nucl. Phys. A189 (1972) 1.

[54] S. Saito, S. Okai, R. Tamagaki, and M. Yasuno, Progr. Theoret. Phys. 50 (1973) 1561.

[55] D. Clement and E. Schmid, in Proceedings of the 2nd International Conference on Clustering Phenomena in Nuclei, College Park, Maryland, 1975 (National Technical Information Service, U. S. Department of Commerce, Springfield, Virginia) p. 148.

[56] E. W. Schmid, Nuovo Cim. 18A (1973) 771.

[57] J. Schwager, Nuovo Cim. 18A (1973) 787.

[58] F. S. Chwieroth, Y. C. Tang, and D. R. Thompson, Phys. Lett. 46B (1973) 301.

[59] D. R. Thompson, R. E. Brown, M. LeMere, and Y. C. Tang, Phys. Rev. C16 (1977) 1.

[60] D. R. Thompson, M. LeMere, and Y. C. Tang, Nucl. Phys. A286 (1977) 53.

[61] F. Ajzenberg-Selove, Nucl. Phys. A190 (1972) 1.

[62] W. E. Hunt, M. K. Mehta and R. H. Davis, Phys. Rev. 160 (1967) 782.

[63] C. Bergman and R. K. Hobbie, Phys. Rev. C3 (1971) 1729.

[64] B. Buck and A. A. Pilt, Nucl. Phys. A280 (1977) 133.

[65] N. F. Mangelson, B. G. Harvey, and N. K. Glendenning, Nucl. Phys. A119 (1968) 79.

[66] F. Ajzenberg-Selove, Nucl. Phys. A166 (1971) 1.

[67] T. Matsuse, M. Kamimura, and Y. Fukushima, Progr. Theoret. Phys. 53 (1975) 706.

[68] Y. Fukushima, M. Kamimura, and T. Matsuse, Progr. Theoret. Phys. 55 (1976) 1310.

[69] T. Tomoda and A. Arima, in Proceedings of the INS-IPCR Symposium on Cluster Structure of Nuclei and Transfer Reactions Induced by Heavy Ions, Tokyo, 1975 (IPCR Cyclotron Progress Report Supplement 4), p. 90.

[70] H. T. Fortune, R. Middleton, and R. R. Betts, Phys. Rev. Lett. 29 (1972) 738.

[71] E. W. Schmid, Y. C. Tang, and K. Wildermuth, Phys. Lett. 7 (1963) 263.

[72] H. Stöwe, H. H. Hackenbroich, and H. Hutzelmeyer, Z. Phys. 247 (1971) 95.

[73] M. Kamimura and T. Matsuse, Progr. Theoret. Phys. 51 (1974) 438.

[74] H. Friedrich and K. Langanke, Nucl. Phys. A252 (1975) 47.

[75] F. Nemoto, Y. Yamamoto, H. Horiuchi, Y. Suzuki, and K. Ikeda, Progr. Theoret. Phys. 54 (1975) 104.

[76] D. Baye and P. H. Heenan, Nucl. Phys. A276 (1977) 354.

[77] D. Baye, Nucl. Phys. A272 (1976) 445.

[78] D. Baye and P. H. Heenan, Nucl. Phys. A283 (1977) 176.

[79] T. Sakuda, S. Nagata, and F. Nemoto, Progr. Theoret. Phys. 56 (1976) 1126.

[80] H. Friedrich, K. Langanke, A. Weiguny, and R. Santo, Phys. Lett. 55B (1975) 345.

[81] D. Baye and G. Reidemeister, Nucl. Phys. A258 (1976) 157.

[82] M. Kamimura, T. Matsuse, and K. Takada, Progr. Theoret. Phys. 47 (1972) 1537.

[83] Y. Fukushima and M. Kamimura, in Proceedings of the International Conference on Nuclear Structure, Tokyo (1977).

[84] A. B. Volkov, Nucl. Phys. 74 (1965) 33.

[85] F. Ajzenberg-Selove, Nucl. Phys. A248 (1975) 1.

[86] H. Morinaga, Phys. Lett. 21 (1966) 78.

[87] H. Horiuchi, in Proceedings of the International Conference on Nuclear Structure, Tokyo (1977).

[88] N. Takigawa and A. Arima, Nucl. Phys. A168 (1971) 593.

[89] H. Hutzelmeyer and H. H. Hackenbroich, Z. Phys. 232 (1970) 356.

[90] N. Gabr and H. H. Hackenbroich, Acta. Phys. Austr., to be published.

[91] H. H. Hackenbroich, T. H. Seligman, and W. Zahn, Nucl. Phys. A259 (1976) 445.

[92] E. Uegaki, S. Okabe, Y. Abe, and H. Tanaka, Progr. Theoret. Phys. 57 (1977) 1262.

[93] S. Okabe, Y. Abe, and H. Tanaka, Progr. Theoret. Phys. 57 (1977) 866.

[94] H. Stöwe and W. Zahn, Nucl. Phys. A289 (1977) 317, A286 (1977) 89.

[95] W. Zahn, Nucl. Phys. A269 (1976) 138.

[96] N. de Takacsy, Nucl. Phys. A178 (1972) 469.

[97] P. Kramer and D. Schenzle, Nucl. Phys. A204 (1973) 593.

[98] R. W. Bauer, J. D. Anderson, and L. J. Christensen, Nucl. Phys. 47 (1963) 241.

[99] A. A. Cowley, G. Heymann, R. L. Keizer and M. J. Scott, Nucl. Phys. 86 (1966) 363.

[100] W. S. McEver, T. B. Clegg, J. M. Joyce, E. J. Ludwig, and R. L. Walter, Nucl. Phys. A178 (1972) 529.

[101] C. Bergman, Ph.D. Thesis, University of Minnesota (1968).

[102] H. Oeschler, H. Schröter, H. Fuchs, L. Baum, G. Paul, H. Lüdecke, R. Santo, and R. Stock, Phys. Rev. Lett. 28 (1972) 694.

[103] R. D. Furber, Ph.D. Thesis, University of Minnesota (1976).

[104] P. Heiss and H. H. Hackenbroich, Phys. Lett. 30B (1969) 373.

[105] D. R. Thompson and Y. C. Tang, Phys. Rev. C11 (1975) 1473.

[106] D. Clement, E. J. Kanellopoulos, and K. Wildermuth, Phys. Lett. 55B (1975) 19.

[107] W. Sünkel and K. Wildermuth, in Proceedings of the 2nd International Conference on Clustering Phenomena in Nuclei, College Park, Maryland, 1975 (National Technical Information Service, U. S. Department of Commerce, Springfield, Virginia), p. 156.

[108] H. Friedrich, Nucl. Phys. A224 (1974) 357.

[109] L. F. Canto, Nucl. Phys. A279 (1977) 97.

[110] P. H. Heenan, Nucl. Phys. A272 (1976) 399.

[111] D. J. Stubeda, M. LeMere, and Y. C. Tang, Phys. Rev. C17 (1978) 447.

[112] W. Laskar and B. Remaud, J. de Phys. 34 (1973) 783.

[113] R. J. Philpott, Nucl. Phys. A289 (1977) 109.

[114] D. Frekers and K. Langanke, Fizika (Suppl. 2) 9 (1977) 17.

[115] F. S. Chwieroth, R. E. Brown, Y. C. Tang, and D. R. Thompson, Phys. Rev. C8 (1973) 938.

[116] M. LeMere, Y. C. Tang, and D. R. Thompson, Nucl. Phys. A266 (1976) 1.

[117] D. R. Thompson and Y. C. Tang, Nucl. Phys. A106 (1968) 591.

[118] J. A. Koepke, R. E. Brown, Y. C. Tang, and D. R. Thompson, Phys. Rev. C9 (1974) 823.

[119] H. Kihara, M. Kamimura,and A. Tohsaki-Suzuki, in Proceedings of the International Conference on Nuclear Structure (contributed papers), Tokyo (1977), p. 235.

[120] D. R. Thompson, Y. C. Tang, and F. S. Chwieroth, Phys. Rev. C10 (1974) 987.

[121] R. Nilsson, W. K. Jentschke, G. R. Briggs, R. O. Kerman, and J. N. Snyder, Phys. Rev. 109 (1958) 850.

[122] H. Werner and J. Zimmerer, in Proceedings of the International Conference on Nuclear Physics, Paris, 1964 (Editions du Centre National de la Recherche Scientifique, Paris, 1965), p. 241.

[123] T. A. Tombrello and L. S. Senhouse, Phys. Rev. 129 (1963) 2252.

[124] N. P. Heydenberg and G. M. Temmer, Phys. Rev. 104 (1956) 123.

[125] W. S. Chien and R. E. Brown, Phys. Rev. C10 (1974) 1767.

[126] R. E. Brown and Y. C. Tang, Phys. Rev. 176 (1968) 1235.

[127] M. LeMere, R. E. Brown, Y. C. Tang, and D. R. Thompson, Phys. Rev. C12 (1975) 1140.

[128] R. E. Shamu and J. G. Jenkin, Phys. Rev. 135 (1964) B99.

[129] W. J. McDonald and J. M. Robson, Nucl. Phys. 59 (1964) 321.

[130] A. J. Frasca, R. W. Finlay, R. D. Koshel, and R. L. Cassola, Phys. Rev. 144 (1966) 854.

[131] W. Sünkel and K. Wildermuth, Phys. Lett. 26B (1968) 655.

[132] L. C. Niem, P. Heiss, and H. H. Hackenbroich, Z. Phys. 244 (1971) 346.

[133] P. Heiss and H. H. Hackenbroich, Nucl. Phys. A182 (1972) 522.

[134] H. H. Hackenbroich and P. Heiss, Z. Phys. 242 (1971) 352.

[135] H. H. Hackenbroich, P. Heiss, and L. C. Niem, Nucl. Phys. A221 (1974) 461.

[136] F. S. Chwieroth, Y. C. Tang, and D. R. Thompson, Phys. Rev. C9 (1974) 56.

[137] G. R. Satchler, L. W. Owen, A. J. Elwyns, G. L. Morgan, and R. L. Walter, Nucl. Phys. A112 (1968) 1.

[138] M. Ivanovich, P. G. Young, and G. G. Ohlsen, Nucl. Phys. A110 (1968) 441.

[139] L. G. Volta, P. G. Roos, N. S. Chant, and R. Woody, III, Phys. Rev. C10 (1974) 520.

[140] F. S. Chwieroth, Y. C. Tang, and D. R. Thompson, Phys. Rev. C10 (1974) 406.

[141] P. Heiss and H. H. Hackenbroich, Nucl. Phys. A202 (1973) 353; Z. Phys. 251 (1972) 168; Phys. Lett. 61B (1976) 339.

[142] R. Hub, D. Clement, and K. Wildermuth, Z. Phys. 252 (1972) 324.

[143] K. Schenk, M. Mörike, G. Staudt, P. Turek, and D. Clement, Phys. Lett. 52B (1974) 36.

[144] T. Kaneko and H. Kanada, Progr. Theoret. Phys. 57 (1977) 1277.

[145] H. Kanada, T. Kaneko, and M. Nomoto, Progr. Theoret. Phys. 52 (1974) 725, 55 (1976) 471.

[146] D. Baye, P. H. Heenan, and M. Libert-Heinemann, Fizika (Suppl. 2) 9 (1977) 5.

[147] P. Heiss, H. H. Hackenbroich, and K. Prescher, Phys. Lett. 52B (1974) 411.

[148] W. Schütte, H. H. Hackenbroich, H. Stöwe, P. Heiss, and H. Aulenkamp, Phys. Lett. 65B (1976) 214.

[149] S. Barshay and G. M. Temmer, Phys. Rev. Lett. 12 (1964) 728.

[150] M. Simonius, Phys. Lett. 37B (1971) 446.

[151] G. Schrieder, H. Genz, and A. Richter, Nucl. Phys. A247 (1975) 203, and references contained therein.

[152] H. Eikemeier and H. H. Hackenbroich, Nucl. Phys. A169 (1971) 407; Z. Phys. 195 (1966) 412.

[153] E. E. Gross, E. Newman, M. B. Greenfield, R. W. Rutkowski, W. J. Roberts, and A. Zucker, Phys. Rev. C5 (1972) 602.

[154] W. Dahme et al , in Proceedings of the 4th International Symposium on Polarization Phenomena in Nuclear Reactions, Zürich (1975).

[155] H. H. Hackenbroich, in Proceedings of the 2nd International Conference on Clustering Phenomena in Nuclei, College Park, Maryland, 1975 (National Technical Information Service, U. S. Department of Commerce, Springfield, Virginia), p. 107.

[156] H. H. Hackenbroich, in Proceedings of the 4th International Symposium on Polarization Phenomena in Nuclear Reactions, Zürich (1975).

[157] J. K. Perring and T. H. R. Skyrme, Proc. Phys. Soc. (London) A69 (1956) 600.

[158] N. Austern, Direct Nuclear Reaction Theories (Wiley, New York, 1970).

[159] R. E. Brown, F. S. Chwieroth, Y. C. Tang, and D. R. Thompson, Nucl. Phys. A230 (1974) 189.

[160] S. Saito, Progr. Theoret. Phys. 41 (1969) 705.

[161] R. E. Brown, W. S. Chien, and Y. C. Tang, in Proceedings of the International Conference on Few-Body Problems in Nuclear and Particle Physics, Quebec, Canada (1974).

[162] P. Swan, Phys. Rev. Lett. 19 (1967) 245.

[163] R. A. Partridge, Y. C. Tang, D. R. Thompson, and R. E. Brown, Nucl. Phys. A273 (1976) 341.

[164] D. R. Thompson and Y. C. Tang, Phys. Rev. C4 (1971) 306.

[165] Y. C. Tang and R. E. Brown, Phys. Rev. C4 (1971) 1979.

[166] G. W. Greenlees, W. Makofske, Y. C. Tang, and D. R. Thompson, Phys. Rev. C6 (1972) 2057.

[167] P. E. Frisbee, Ph.D. Thesis, University of Maryland (1972).

[168] B. Buck, H. Friedrich, and C. Wheatley, Nucl. Phys. A275 (1977) 246.

[169] H. Bohlen, N. Marquardt, W. von Oertzen, and Ph. Gorodetzky, Nucl. Phys. A179 (1972) 504.

[170] W. von Oertzen, in Proceedings of the INS-IPCR Symposium on Cluster Structure of Nuclei and Transfer Reactions Induced by Heavy Ions, Tokyo, 1975 (IPCR Cyclotron Progress Report Supplement 4), p. 337.

[171] W. von Oertzen, Nucl. Phys. A148 (1970) 529.

[172] P. Charles, F. Auger, I. Badawy, B. Berthier, M. Dost, J. Gastebois, B. Fernandez, S. M. Lee and E. Plagnol, in Proceedings of the European Conference on Nuclear Physics with Heavy Ions, Caen (1976) p. 68; also, J. Gastebois, preprint (1977).

[173] R. Stock, U. Jahnke, D. L. Hendrie, J. Mahoney, C. F. Maquire, W. F. W. Schneider, D. K. Scott and G. Wolschin, Phys. Rev. C14 (1976) 1823.

[174] Y. Kondo, S. Nagaka, S. Ohkubo, and O. Tanimura, Progr. Theoret. Phys. 53 (1975) 1006.

[175] F. Michel and R. Vanderpoorten, Phys. Rev. C16 (1977) 142.

[176] N. S. Wall, Phys. Rev. C14 (1976) 2326.

[177] M. LeMere and Y. C. Tang, to be published.

[178] D. Baye, J. Deenan, and Y. Salmon, Nucl. Phys. A289 (1977) 511.

[179] G. W. Greenlees and Y. C. Tang, Phys. Lett. 34B (1971) 359.

[180] R. E. Brown and Y. C. Tang, unpublished result.

[181] T. Matsuse, M. Kamimura, and Y. Fukushima, in Proceedings of the 2nd International Conference on Clustering Phenomena in Nuclei, College Park, Maryland, 1975 (National Technical Information Service, U. S. Department of Commerce, Springfield, Virginia), p. 163.

[182] D. Baye and P. H. Heenen, Fizika (Suppl. 3) 9 (1977) 1.

[183] M. LeMere, R. E. Brown, Y. C. Tang, and D. R. Thompson, Phys. Rev. C15 (1977) 1191.

[184] F. S. Chwieroth, Y. C. Tang, and D. R. Thompson, Fizika (Suppl. 2) 9 (1977) 13.

[185] Y. C. Tang and D. R. Thompson, in Proceedings of the 2nd International Conference on Clustering Phenomena in Nuclei, College Park, Maryland, 1975 (National Technical Information Service, U. S. Department of Commerce, Springfield, Virginia), p. 119.

Table 1

Values of $C_{a\lambda}$ and $C_{b\lambda}$

System	$C_{a\lambda}$	$C_{b\lambda}$
$n + {}^{6}Li$ ($\lambda = 2$)	1.13	-0.05
$n + {}^{6}Li$ ($\lambda = 4$)	1.20	0.05
${}^{3}H + \alpha$	1.16	-0.14
$\alpha + {}^{16}O$	1.25	≈ 0
$n + {}^{40}Ca$	1.35	≈ 0

Table 2

Values of $\tilde{E}_1$ and $\tilde{E}_c$ in various systems

System	N_A-N_B	α (fm^{-2})	$\tilde{E}_1$ (MeV/nucleon)	$\tilde{E}_c$ (MeV/nucleon)
$^3H + \alpha$	1	0.45	53	152
$\alpha + {}^{16}O$	12	0.36	50	16
$^{16}O + {}^{17}O$	1	0.32	50	106
$^{16}O + {}^{20}Ne$	4	0.30	47	25
$^{16}O + {}^{40}Ca$	24	0.27	43	5

Figure Captions

Figure 1: Demonstration, in the n + ^{40}Ca system, of the existence of redundant solutions in $\ell = 2$ states and the nonexistence of redundant solutions in $\ell = 3$ states.

Figure 2: Comparison of calculated and experimental energy spectra of ^{17}O, ^{18}F, ^{19}F, and ^{20}Ne. The levels shown are those which have predominantly n, d, ^{3}H, and α plus ^{16}O cluster configurations.

Figure 3: Calculated phase shifts for α + ^{16}O scattering.

Figure 4: Comparison of calculated and experimental energy spectra of ^{12}C. The levels shown are those which have predominantly a 3α cluster configuration. (Adapted from ref. [83]).

Figure 5: Comparison of calculated and experimental differential cross sections for n, d, ^{3}He, and α scattering by ^{16}O at indicated energies.

Figure 6: Comparison of calculated and experimental differential cross sections for α + ^{16}O scattering at 19.2 MeV.

Figure 7: $\alpha + \alpha$ scattering with and without specific distortion effect.

Figure 8: Comparison of calculated and experimental differential cross sections for n + α , n + ^{16}O, and n + ^{40}Ca scattering at indicated energies.

Figure 9: Comparison of coupled-channel (solid curve) and single-channel (dashed curve) differential cross sections for d + ^{3}H scattering at 2.02 MeV with experimental data (solid dots).

Figure 10: Comparison of calculated and experimental differential reaction cross sections for the process α (p,d) ^{3}He.

Figure 11: Comparison of calculated and experimental differential reaction cross sections for the process $^4He(d,t)^3He$ at indicated energies. (Adapted from ref. [148]).

Figure 12: Comparison of calculated and experimental analyzing powers for the reaction $^4He(d,t)^3He$ at E_f = 21.33 MeV. (Adapted from ref. [148]).

Figure 13: Phase shifts as a function of ℓ for various systems, all calculated at a wave number of 1.52 fm^{-1}.

Figure 14: Calculated $^3H + ^3He$ and $d + ^3He$ phase shifts as a function of ℓ in various channel-spin states.

Figure 15: The parameter C_ℓ as a function of ℓ for $n + ^{40}Ca$ and $^3H + \alpha$ scattering at indicated energies.

Figure 16: Calculated $n + ^6Li$ phase shifts at 30 MeV as a function of ℓ.

Figure 17: Comparison of resonating-group and potential-model results for $^3He + \alpha$ scattering at 44.5 MeV.

Figure 18: Comparison of resonating-group and potential-model results for $n + ^{40}Ca$ scattering at 30 MeV.

Figure 19: Comparison of RGM and PWBA results for the differential reaction cross section of the process $\alpha(p,d)^3He$ at E_g = 130 MeV.

Figure 20: Various Born amplitudes for the reaction $\alpha(p,d)^3He$ at E_g = 130 MeV.

Figure 21: Comparison of $\alpha + \alpha$ phase shifts calculated with the exact exchange-Coulomb kernel, with the approximate but self-consistent exchange-Coulomb kernel, and with k_ℓ^C set as zero.

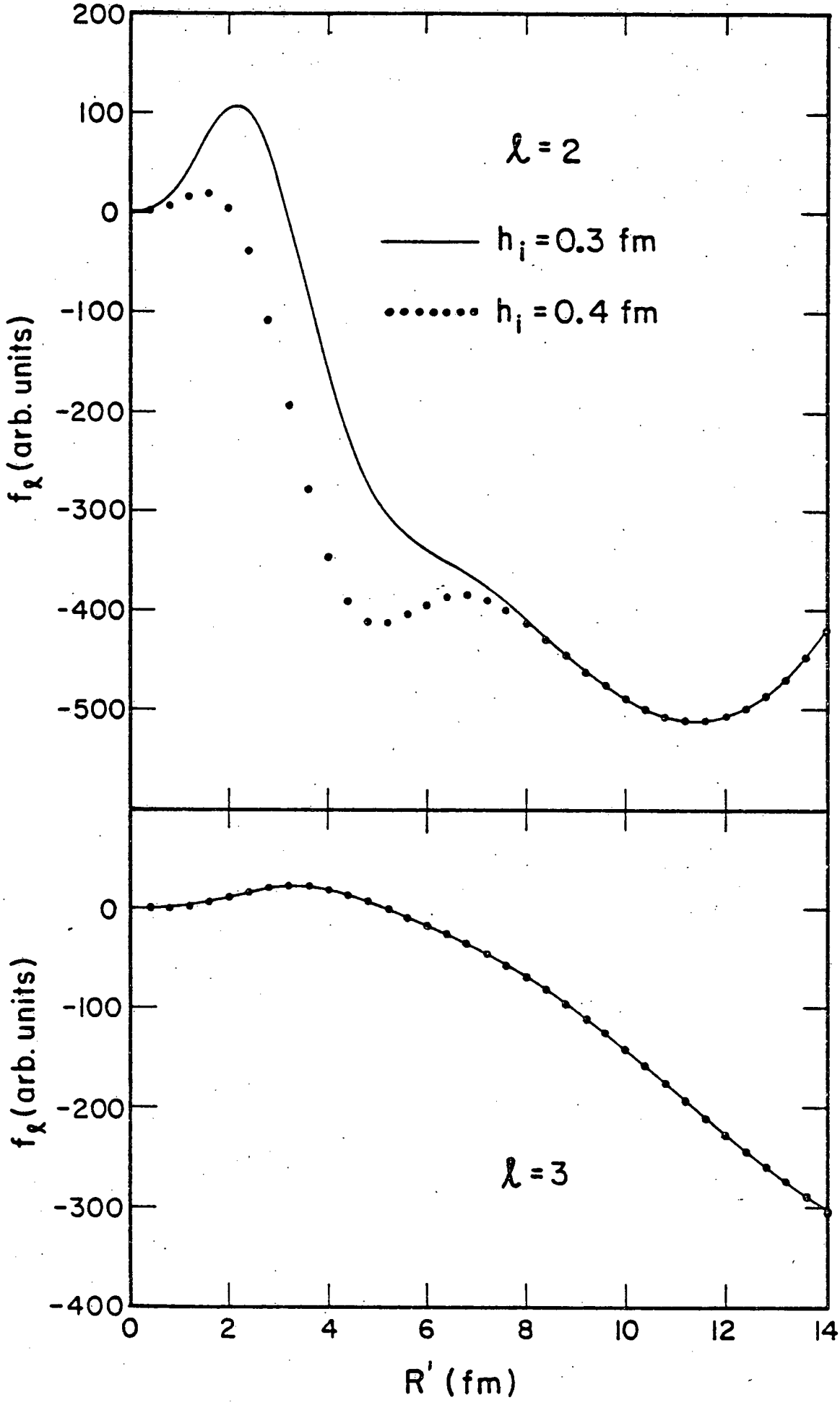
200
100
0
-100
-200
-300
-400
-500
f_ℓ (arb. units)
$\ell = 2$
$h_i = 0.3$ fm
$h_i = 0.4$ fm
0
-100
-200
-300
-400
f_ℓ (arb. units)
$\ell = 3$
0
2
4
6
8
10
12
14
R' (fm)

Fig. 1

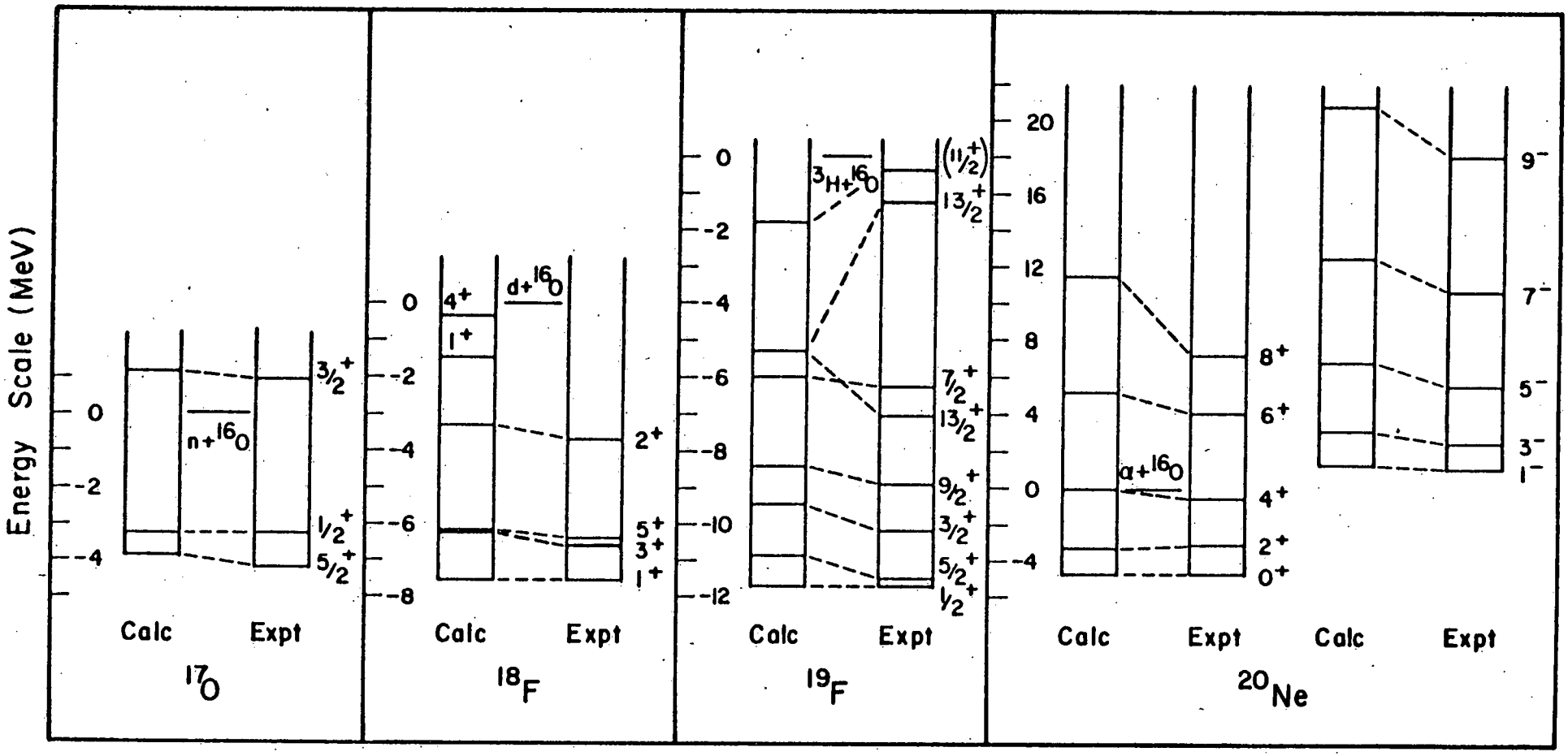
Energy Scale (MeV)
0
-2
-4
n+16O
3/2+
1/2+
5/2+
Calc
Expt
17O
0
-2
-4
-6
-8
4+
1+
d+16O
2+
5+
3+
1+
Calc
Expt
18F
0
-2
-4
-6
-8
-10
-12
3H+16O
(11/2+)
13/2+
7/2+
13/2+
9/2+
3/2+
5/2+
1/2+
Calc
Expt
19F
20
16
12
8
4
0
-4
α+16O
8+
6+
4+
2+
0+
Calc
Expt
9-
7-
5-
3-
1-
Calc
Expt
20Ne

Fig 2

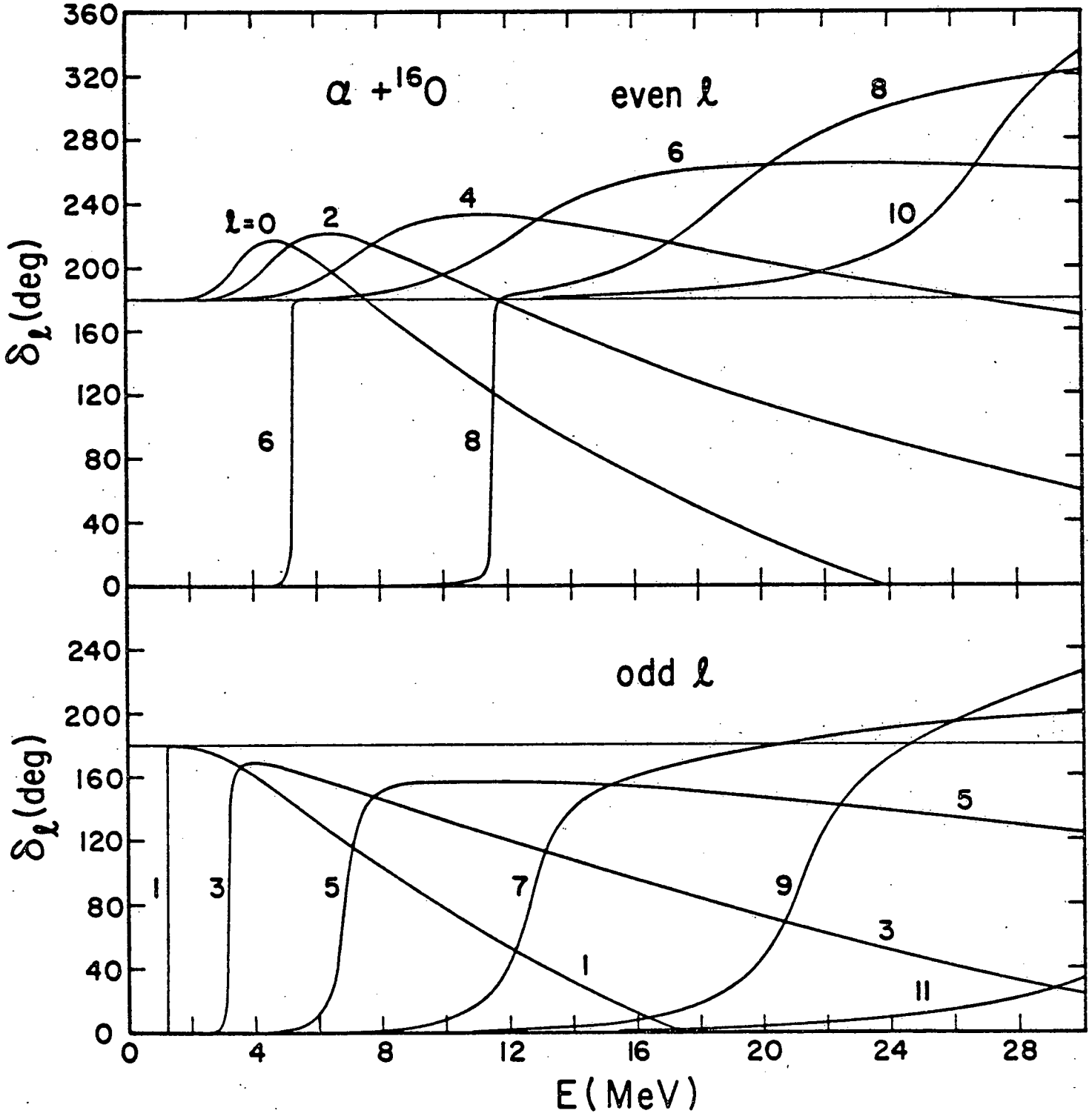
α + 16O
even ℓ
odd ℓ
ℓ=0
2
4
6
8
10
1
3
5
7
9
11
δℓ (deg)
E (MeV)
0
40
80
120
160
200
240
280
320
360
4
8
12
16
20
24
28

Fig. 3

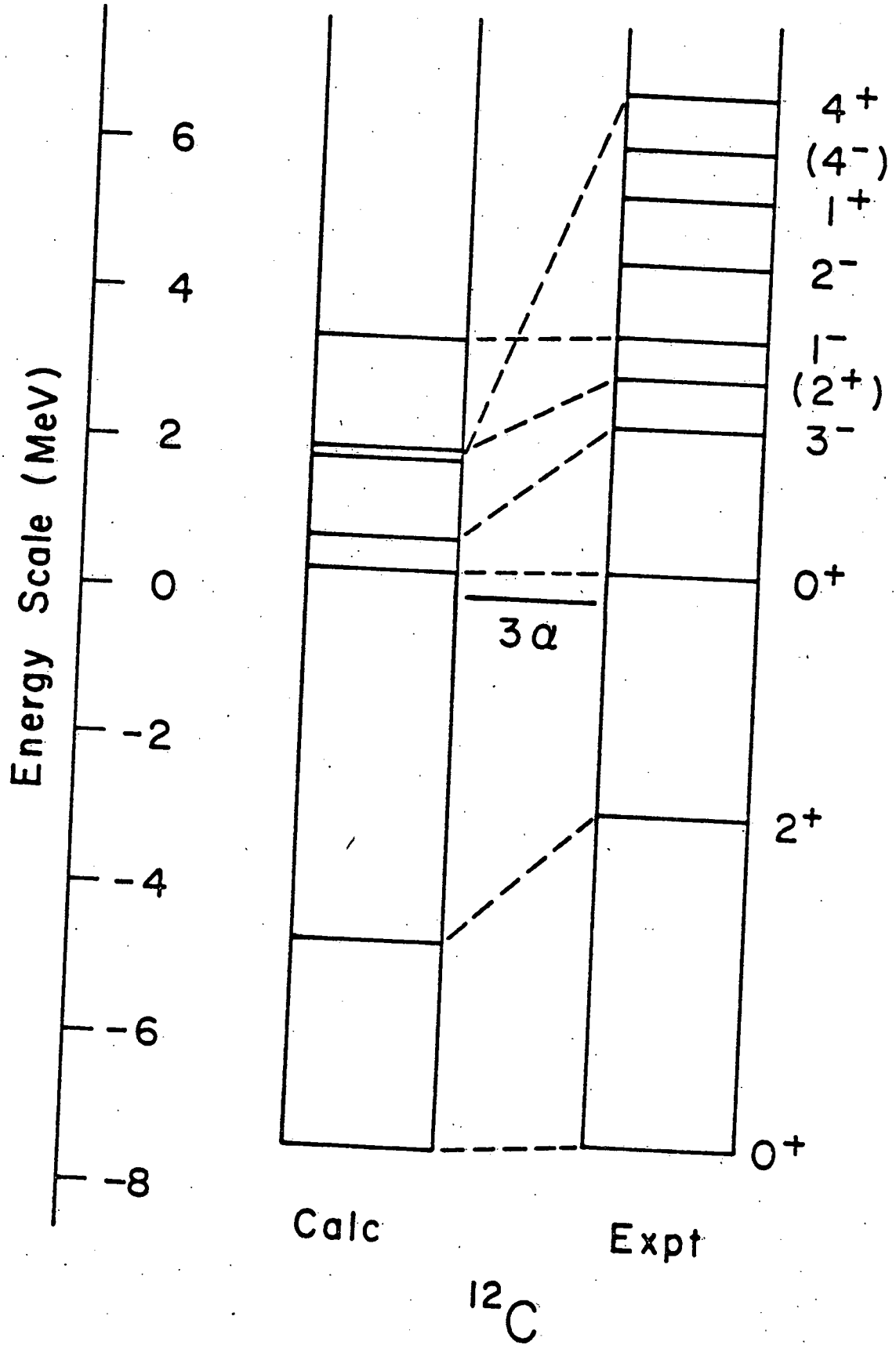

Fig. 4

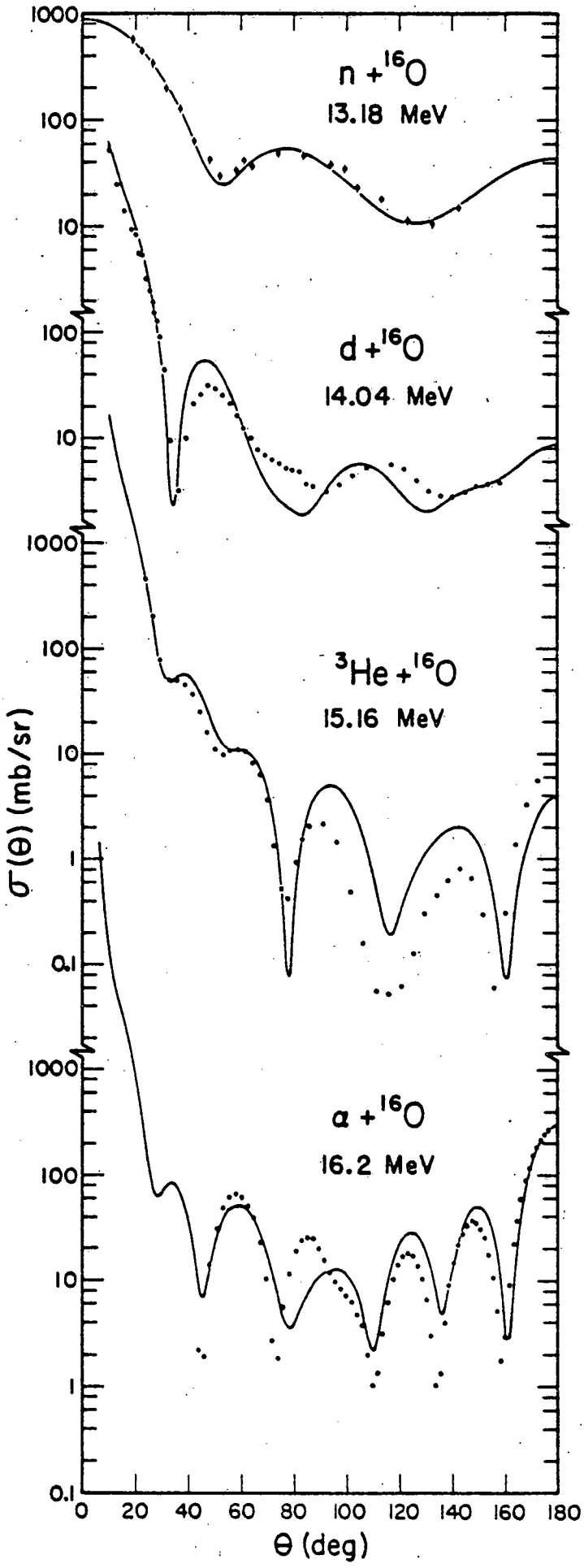
n + 16O
13.18 MeV
d + 16O
14.04 MeV
3He + 16O
15.16 MeV
α + 16O
16.2 MeV
σ(θ) (mb/sr)
θ (deg)
1000
100
10
1
0.1
0
20
40
60
80
100
120
140
160
180

Fig. 5

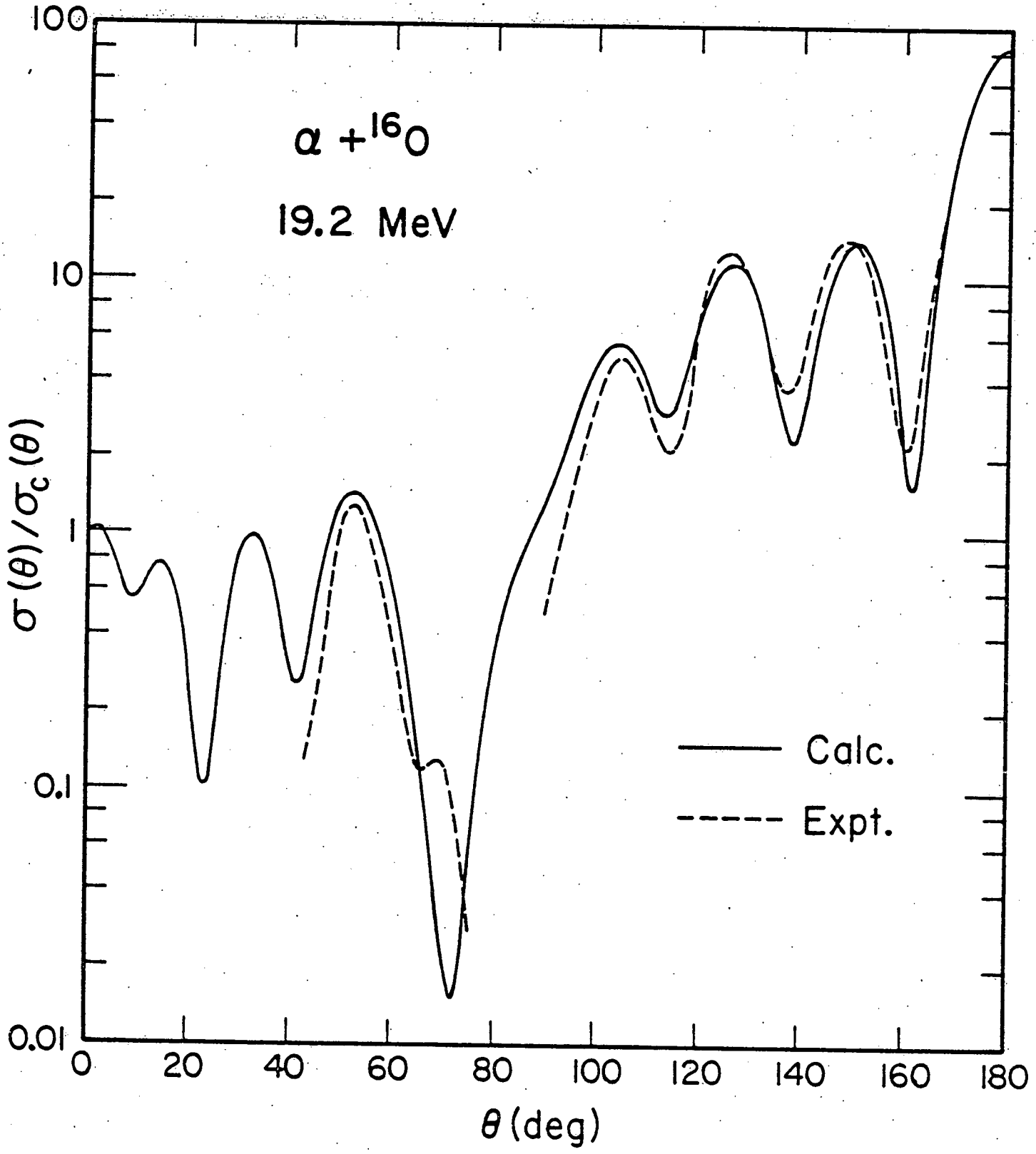
α + 16O
19.2 MeV
100
10
1
0.1
0.01
σ(θ)/σc(θ)
0
20
40
60
80
100
120
140
160
180
θ (deg)
Calc.
Expt.

Fig. 6

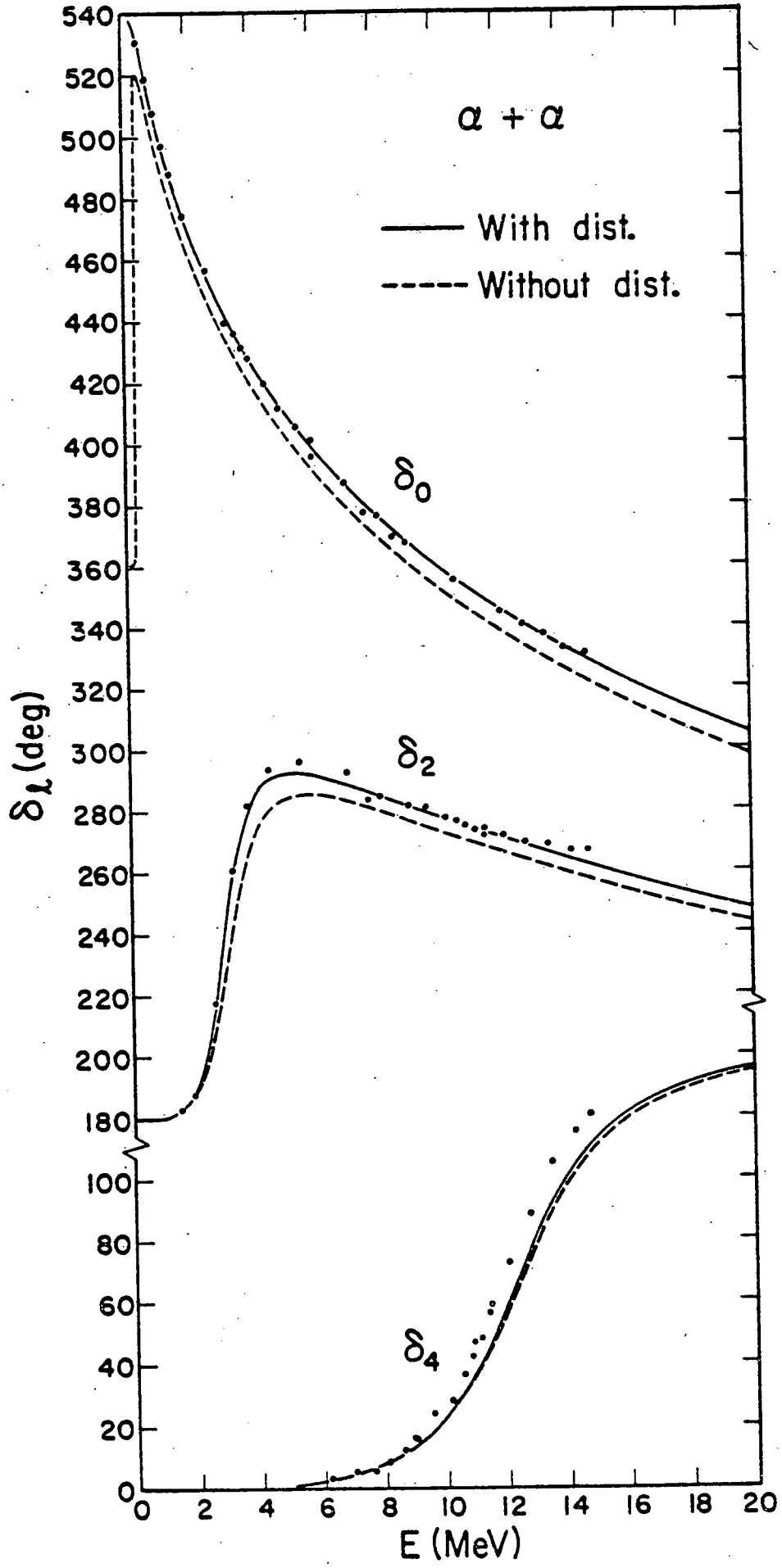
α + α
With dist.
Without dist.
δ_0
δ_2
δ_4
δ_ℓ (deg)
E (MeV)
540
520
500
480
460
440
420
400
380
360
340
320
300
280
260
240
220
200
180
100
80
60
40
20
0
0
2
4
6
8
10
12
14
16
18
20

Fig. 7

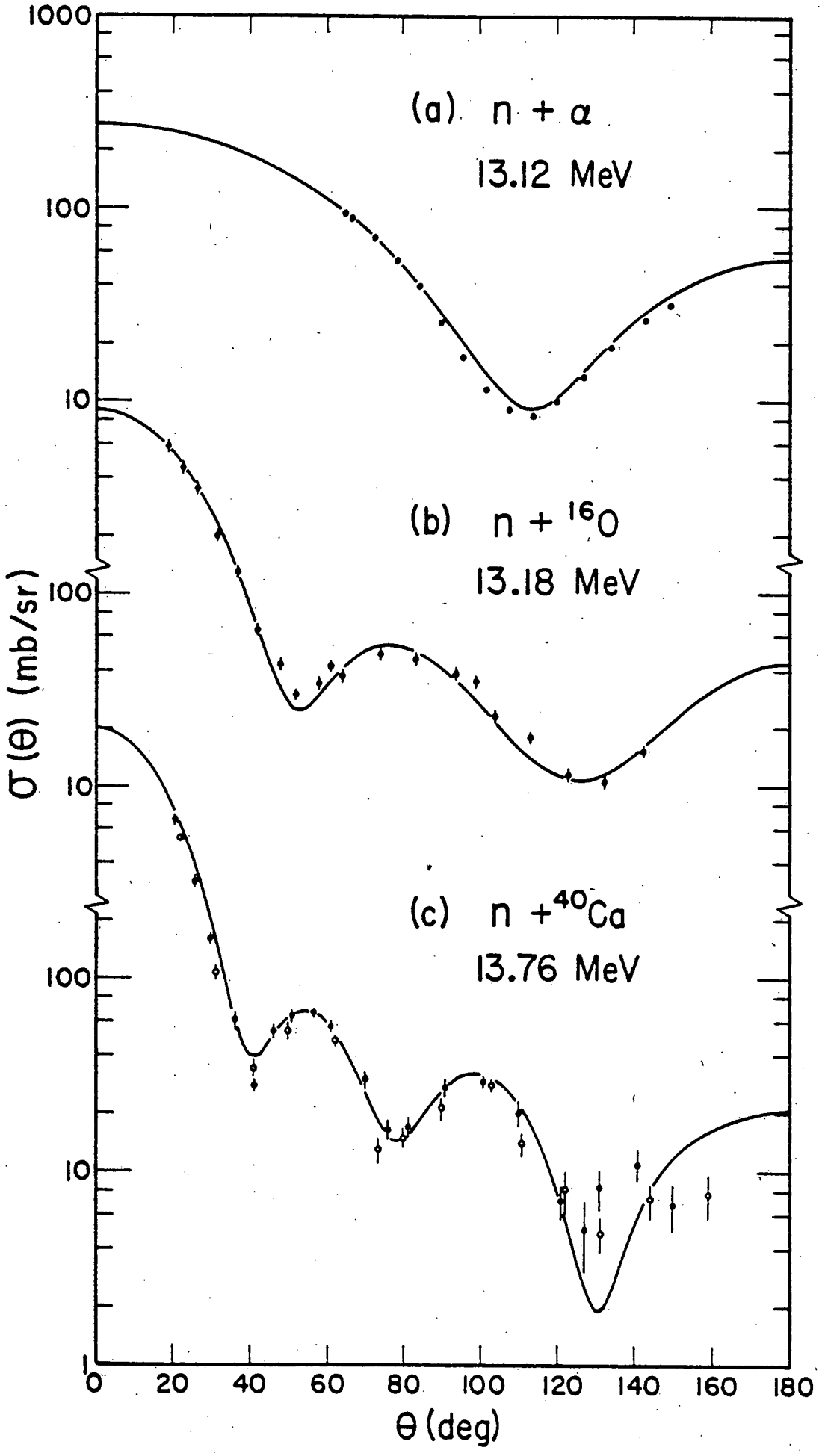
(a) n + α
13.12 MeV
(b) n + 16O
13.18 MeV
(c) n + 40Ca
13.76 MeV
σ(θ) (mb/sr)
θ (deg)
1000
100
10
1
0
20
40
60
80
100
120
140
160
180

Fig. 8

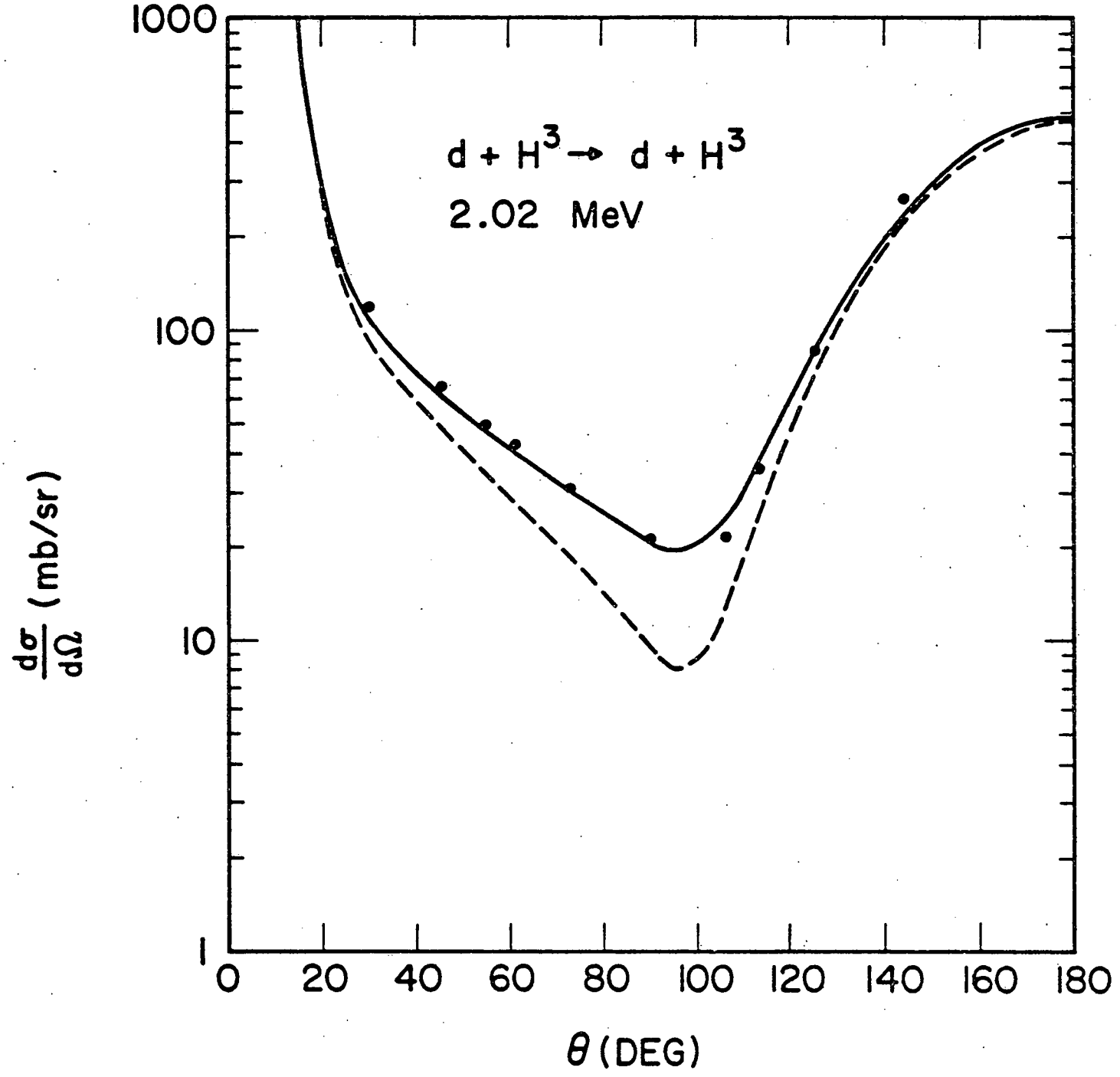
1000
100
10
1
$d + H^3 \rightarrow d + H^3$
2.02 MeV
$\frac{d\sigma}{d\Omega}$ (mb/sr)
0
20
40
60
80
100
120
140
160
180
θ (DEG)

Fig. 9

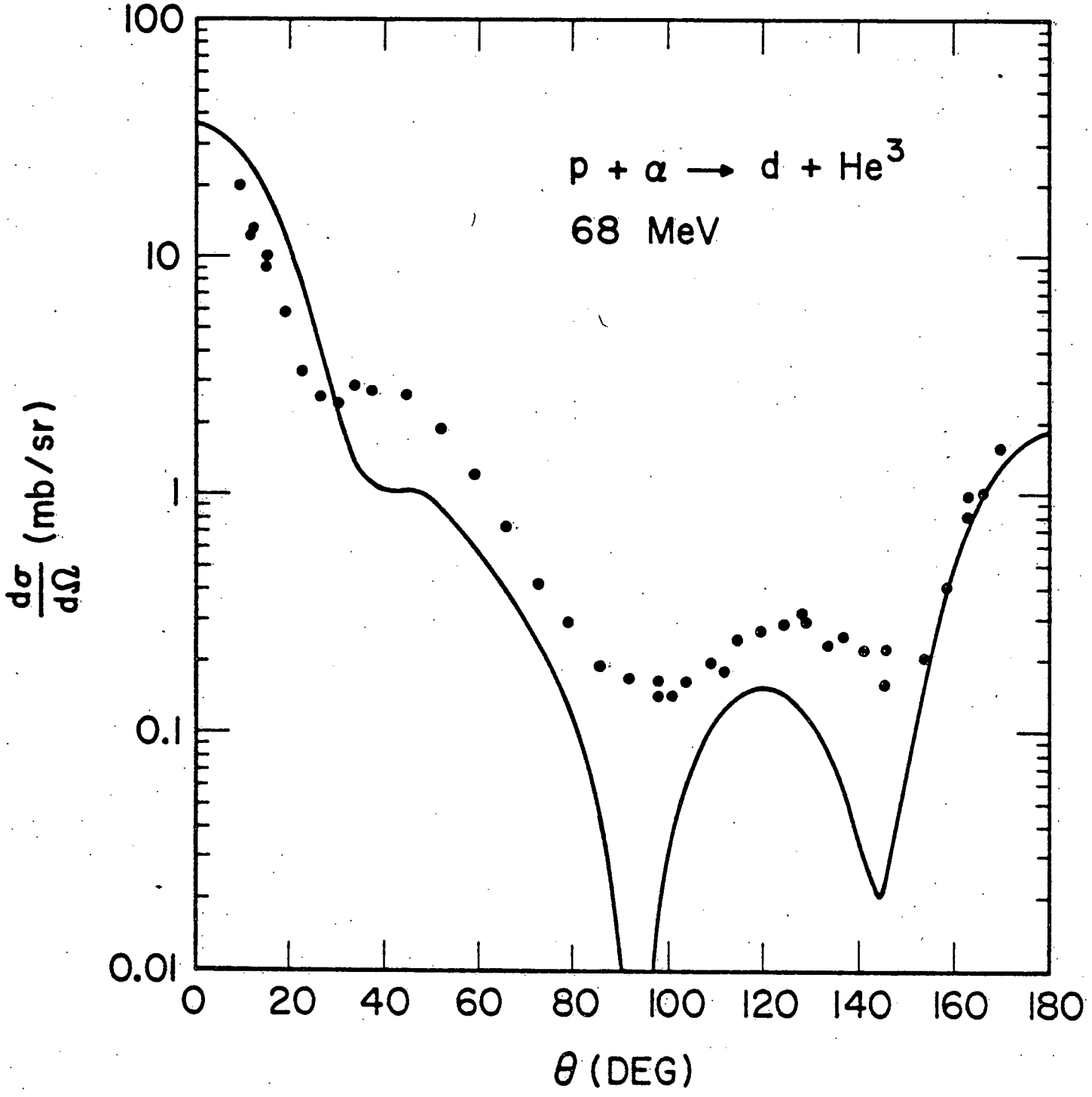
100
10
1
0.1
0.01
$\frac{d\sigma}{d\Omega}$ (mb/sr)
p + α → d + He³
68 MeV
0
20
40
60
80
100
120
140
160
180
θ (DEG)

Fig 10

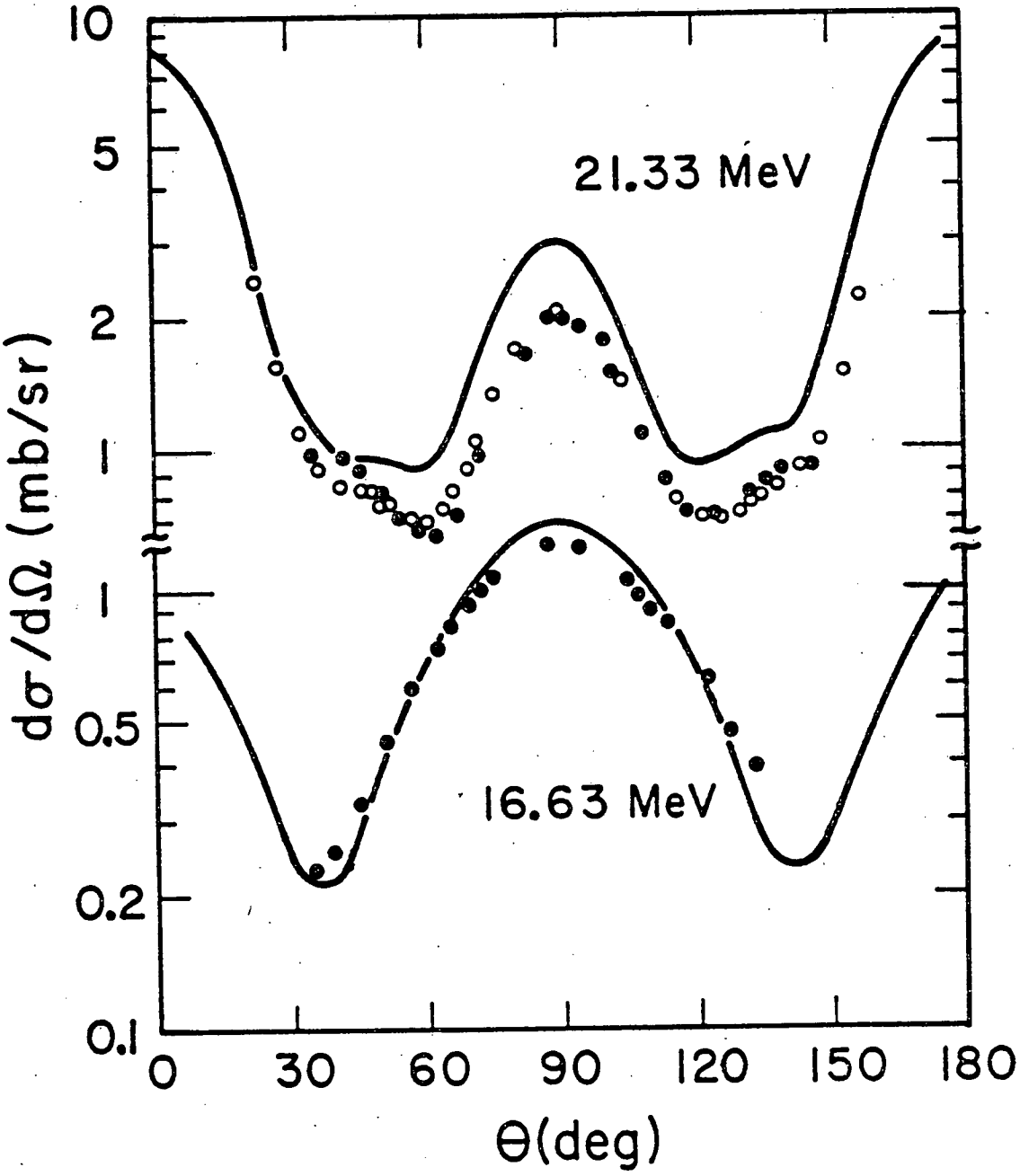
10
5
2
1
1
0.5
0.2
0.1
21.33 MeV
16.63 MeV
dσ/dΩ (mb/sr)
0
30
60
90
120
150
180
θ(deg)

Fig 11

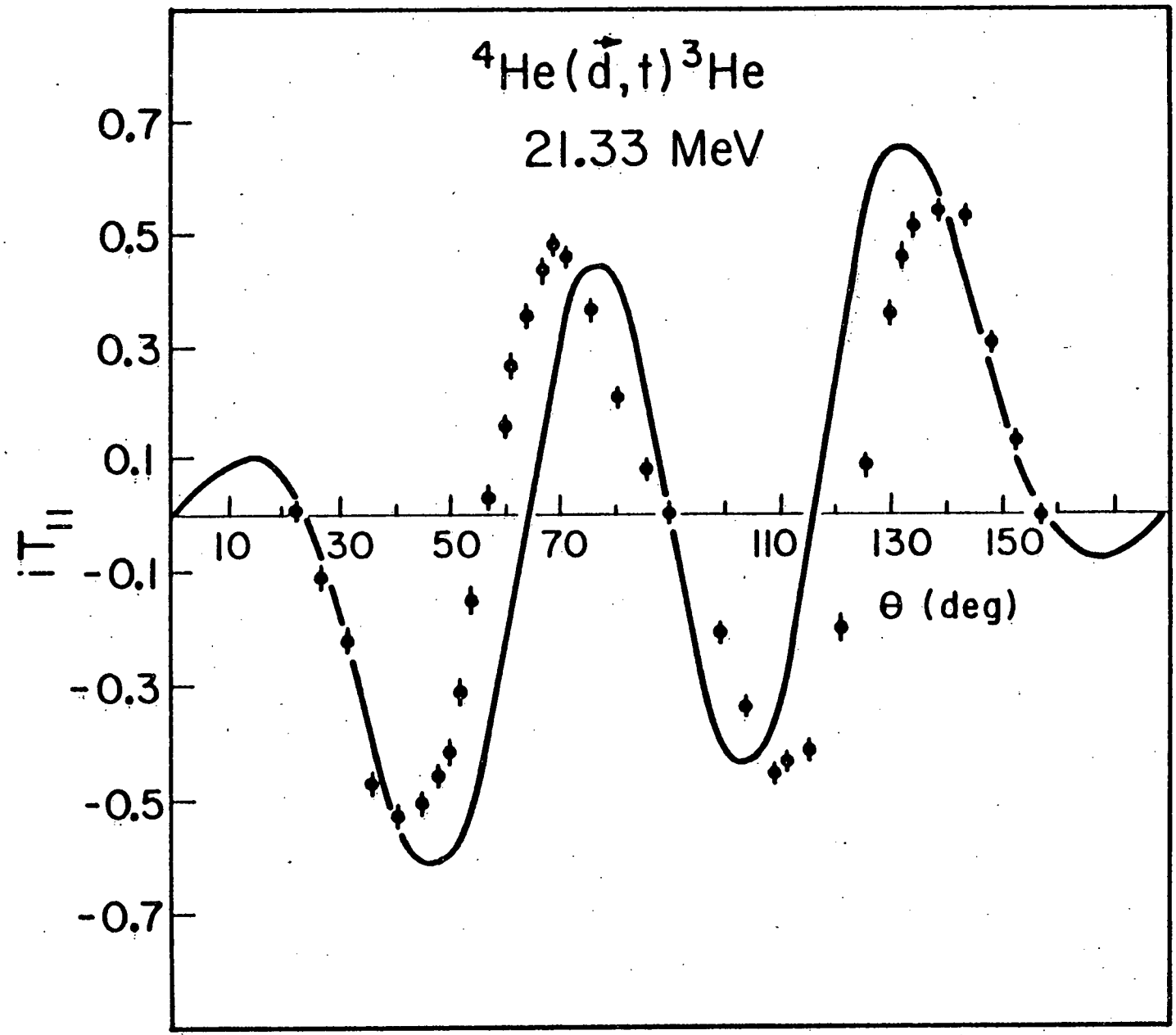
$^4He(\vec{d},t)^3He$
21.33 MeV
0.7
0.5
0.3
0.1
-0.1
-0.3
-0.5
-0.7
T_{11}
10
30
50
70
110
130
150
θ (deg)

Fig. 12

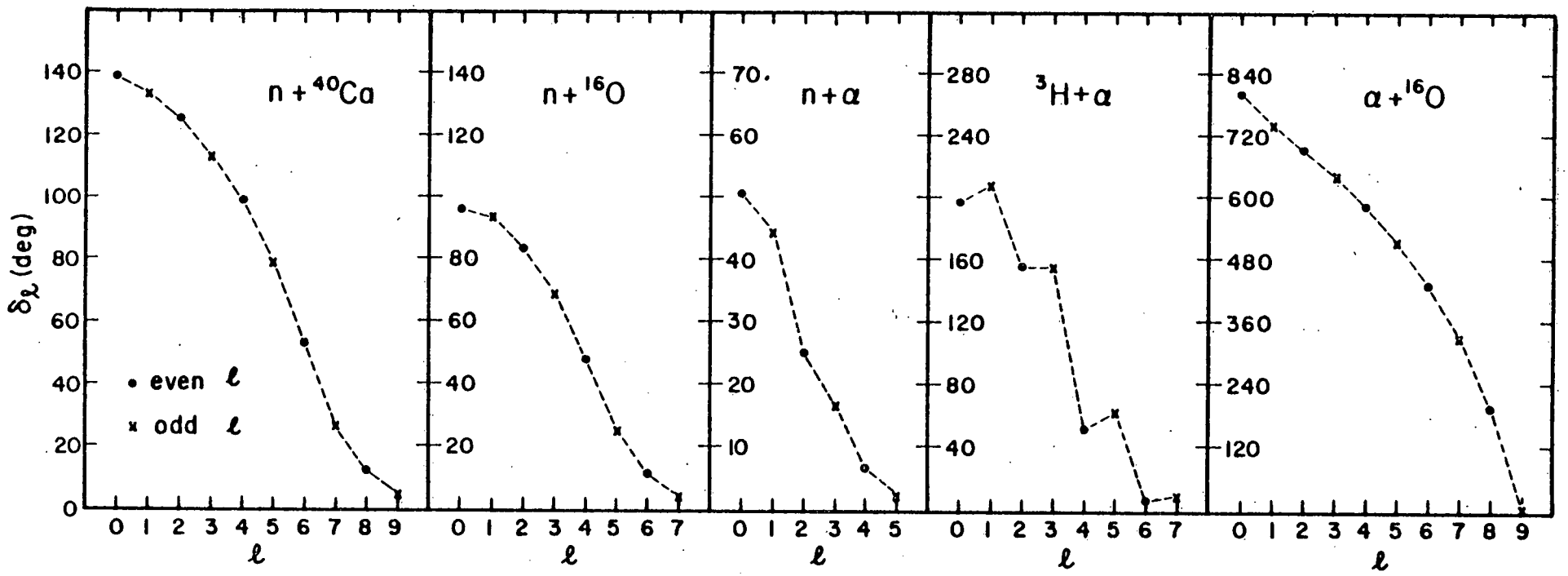

Fig. 13

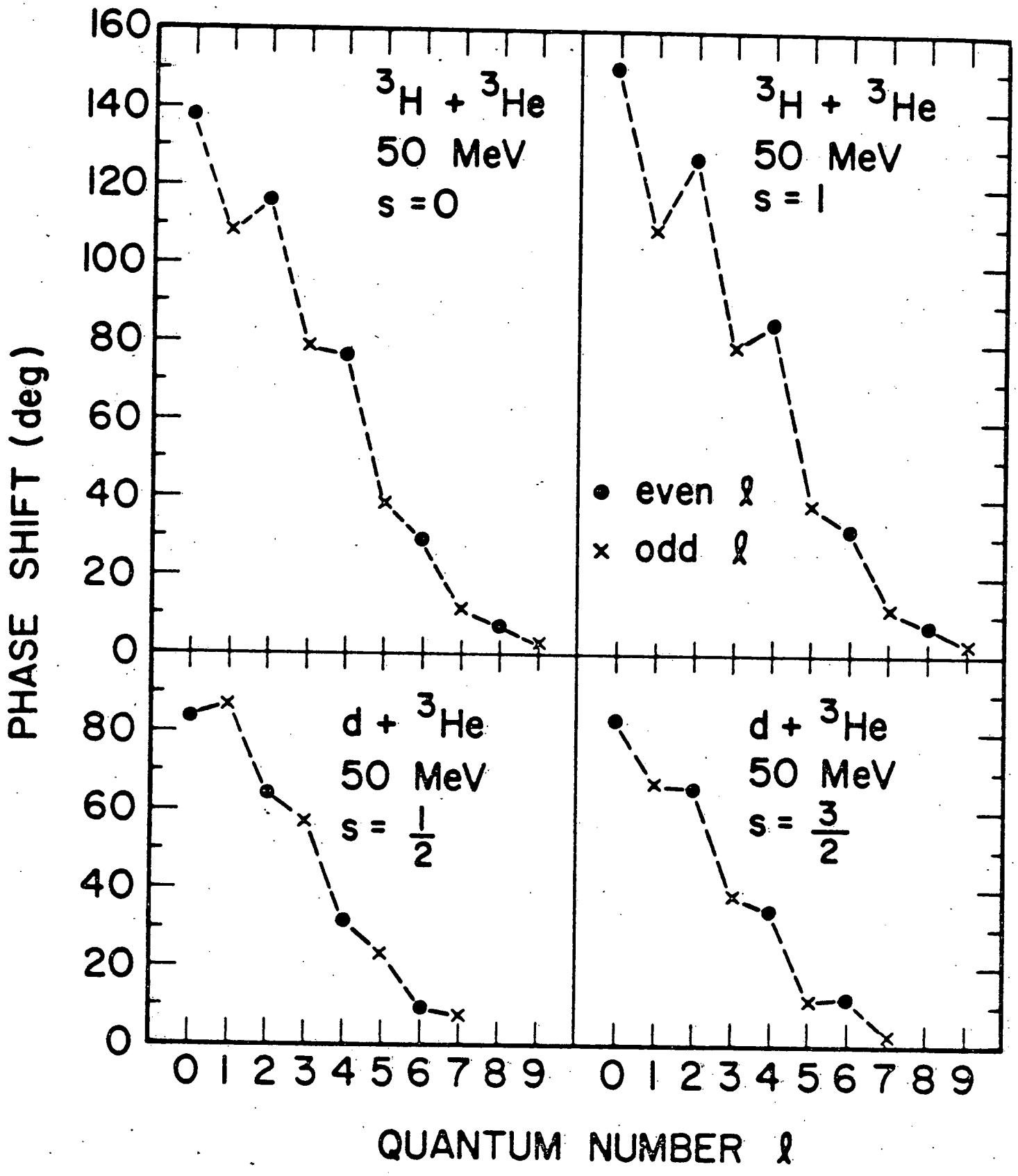
PHASE SHIFT (deg)
160
140
120
100
80
60
40
20
0
$^3H + ^3He$
50 MeV
s = 0
$^3H + ^3He$
50 MeV
s = 1
• even ℓ
× odd ℓ
d + ^3He
50 MeV
s = 1/2
d + ^3He
50 MeV
s = 3/2
0 1 2 3 4 5 6 7 8 9
0 1 2 3 4 5 6 7 8 9
QUANTUM NUMBER ℓ

Fig. 14

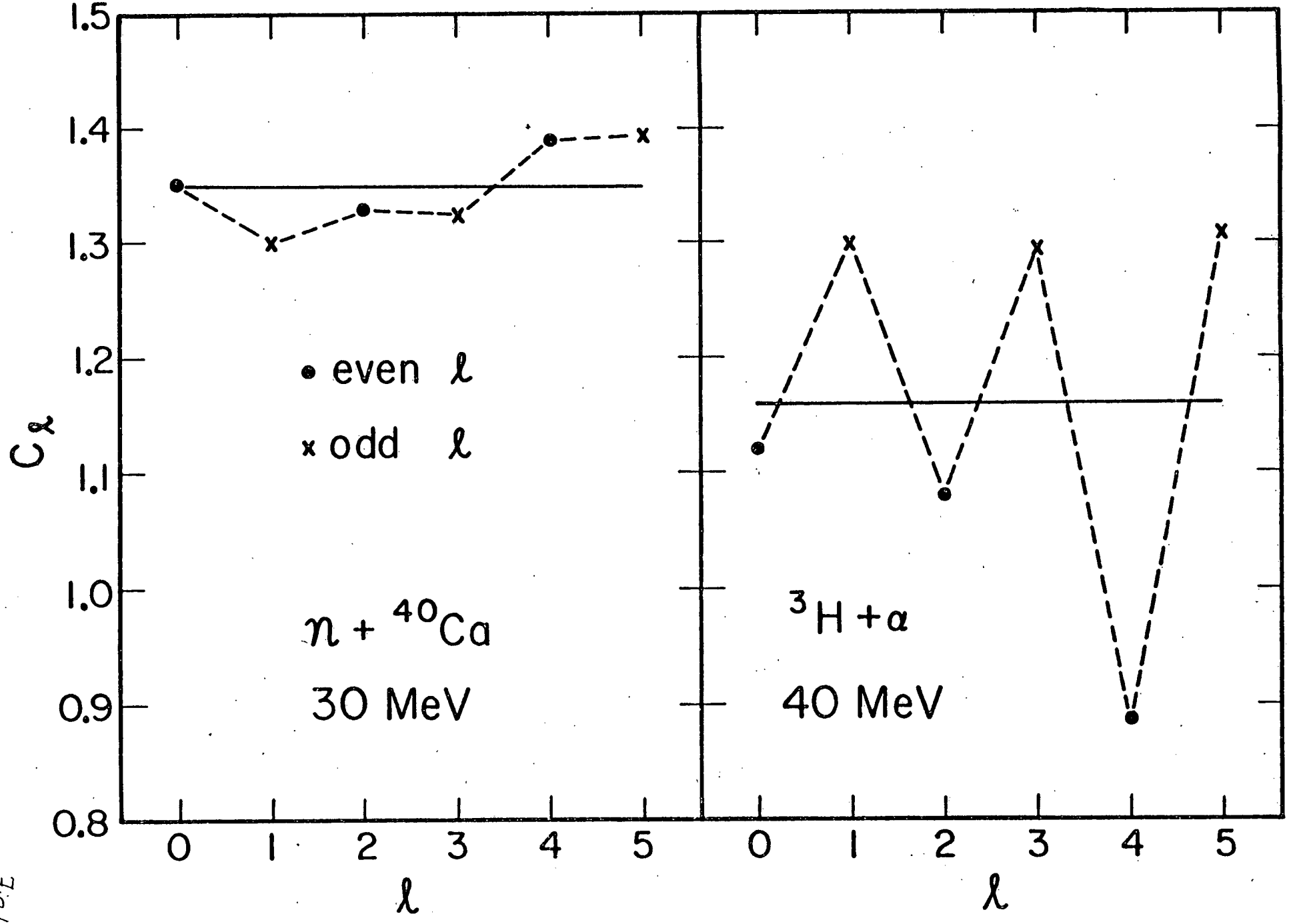
1.5
1.4
1.3
1.2
1.1
1.0
0.9
0.8
C_ℓ
• even ℓ
× odd ℓ
n + ^{40}Ca
30 MeV
^{3}H + α
40 MeV
0 1 2 3 4 5
ℓ
0 1 2 3 4 5
ℓ

Fig 15

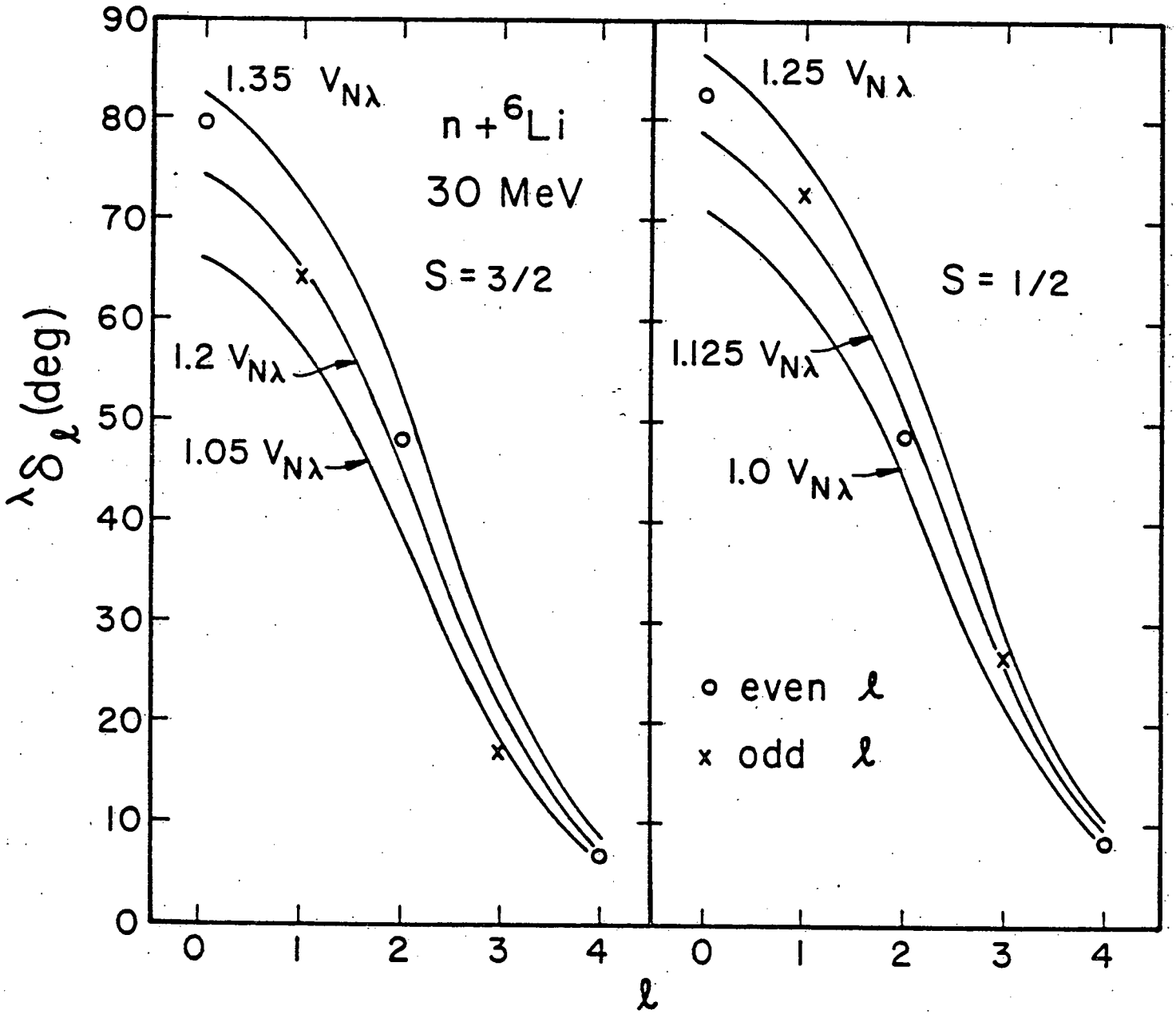
90
80
70
60
50
40
30
20
10
0
0
1
2
3
4
$\lambda\delta_\ell$ (deg)
ℓ
1.35 $V_{N\lambda}$
1.2 $V_{N\lambda}$
1.05 $V_{N\lambda}$
$n + {}^6Li$
30 MeV
S = 3/2
1.25 $V_{N\lambda}$
1.125 $V_{N\lambda}$
1.0 $V_{N\lambda}$
S = 1/2
o even ℓ
x odd ℓ

Fig 16

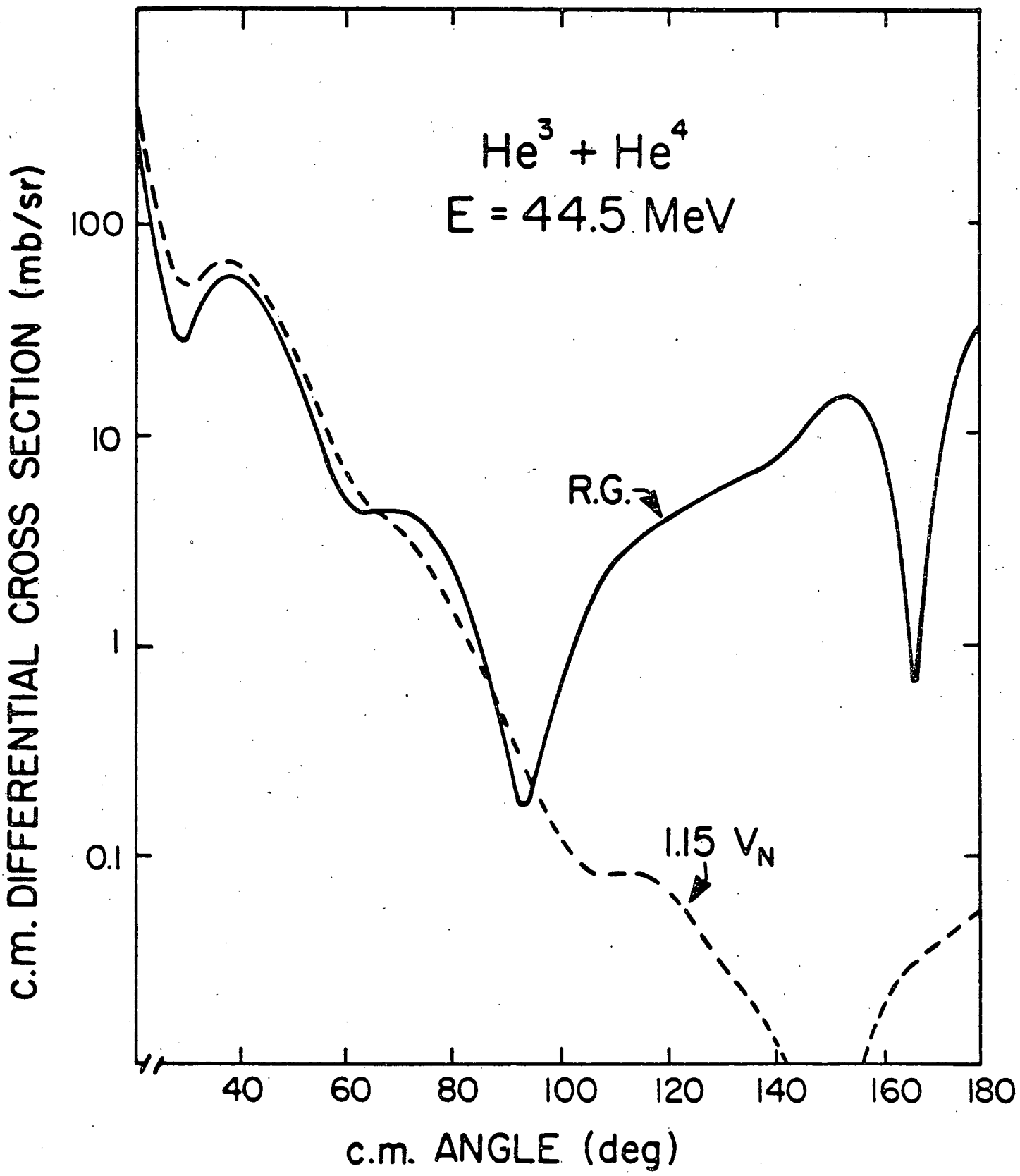
$He^3 + He^4$
E = 44.5 MeV
R.G.
1.15 V_N
c.m. DIFFERENTIAL CROSS SECTION (mb/sr)
100
10
1
0.1
40
60
80
100
120
140
160
180
c.m. ANGLE (deg)

Fig. 17

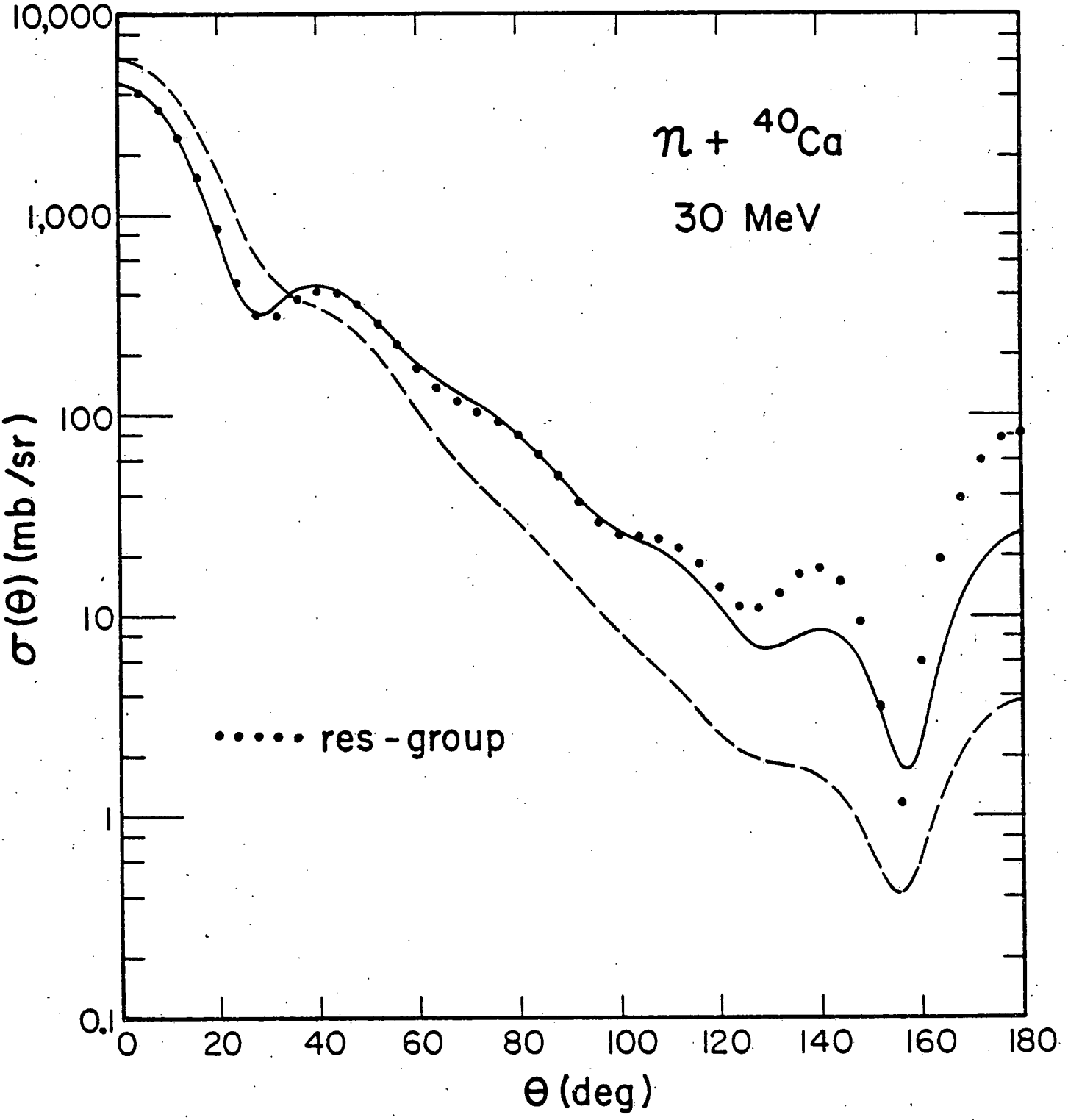
10,000
1,000
100
10
1
0.1
σ(θ) (mb/sr)
n + 40Ca
30 MeV
res - group
0
20
40
60
80
100
120
140
160
180
θ (deg)

Fig. 18

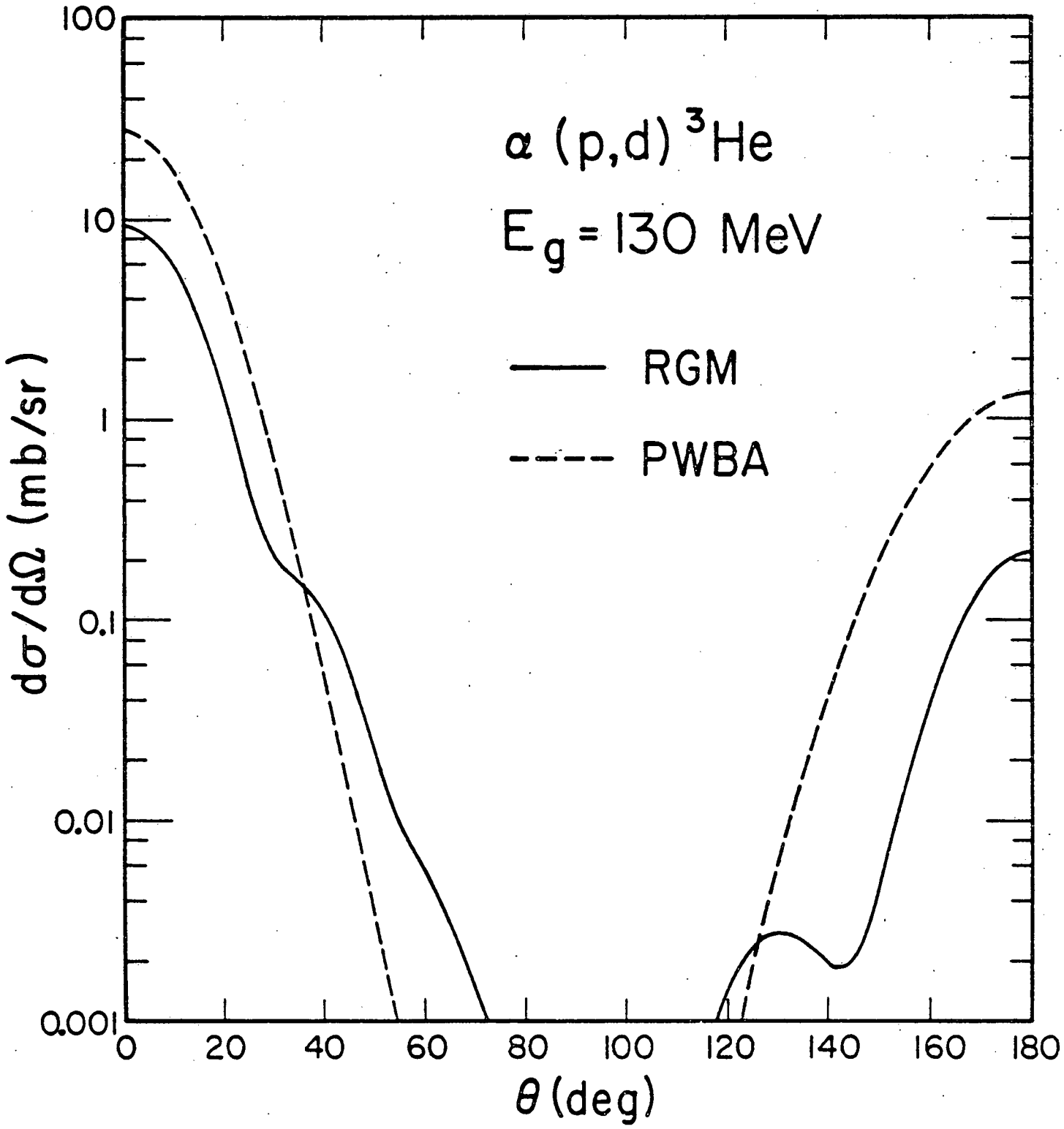
α (p,d) ³He
E_g = 130 MeV
RGM
PWBA
dσ/dΩ (mb/sr)
θ (deg)
100
10
1
0.1
0.01
0.001
0
20
40
60
80
100
120
140
160
180

Fig. 19

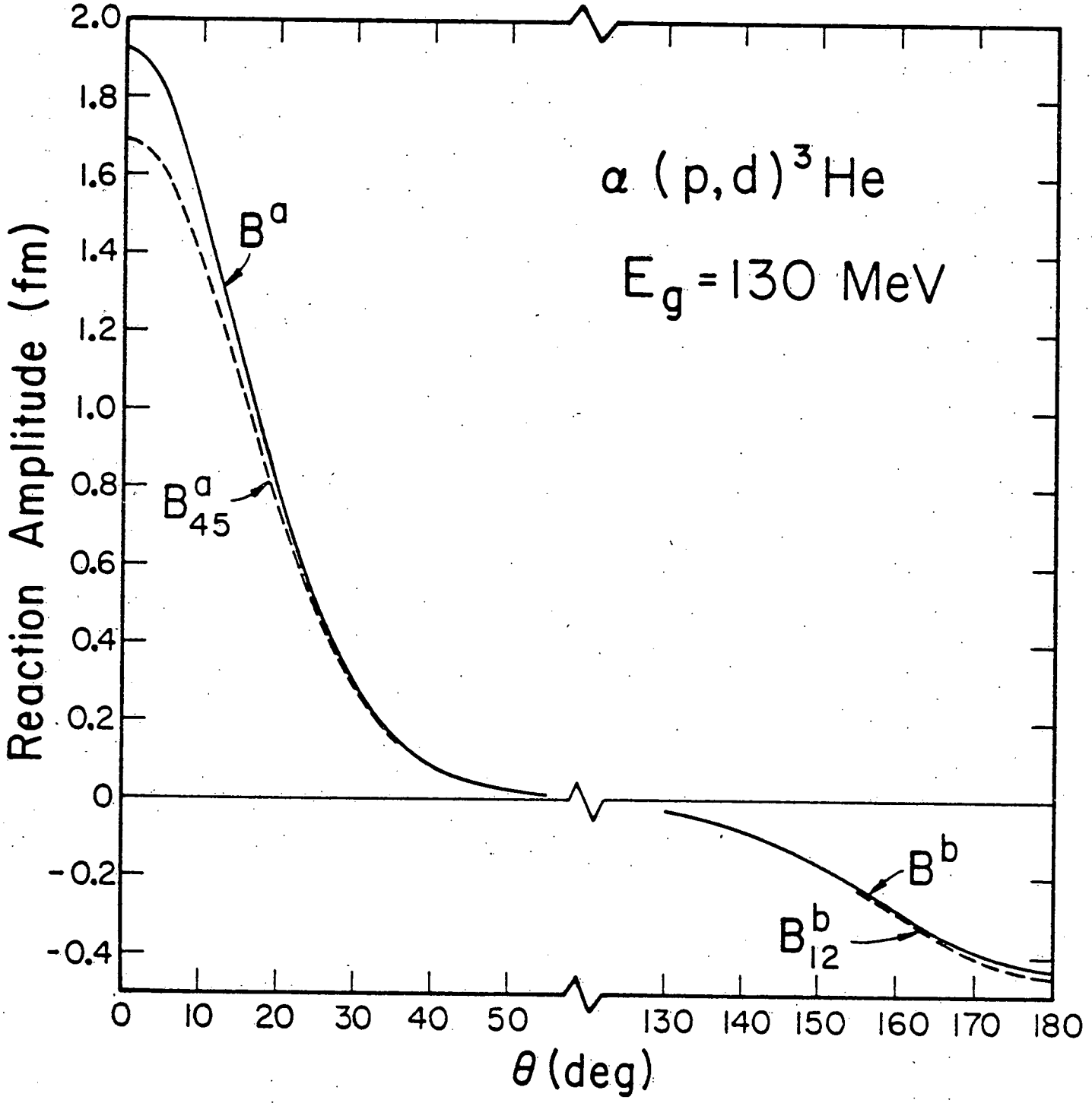
α (p,d)³He
E_g = 130 MeV
B^a
B^a_45
B^b
B^b_12
Reaction Amplitude (fm)
θ (deg)
2.0
1.8
1.6
1.4
1.2
1.0
0.8
0.6
0.4
0.2
0
-0.2
-0.4
0
10
20
30
40
50
130
140
150
160
170
180

Fig. 20

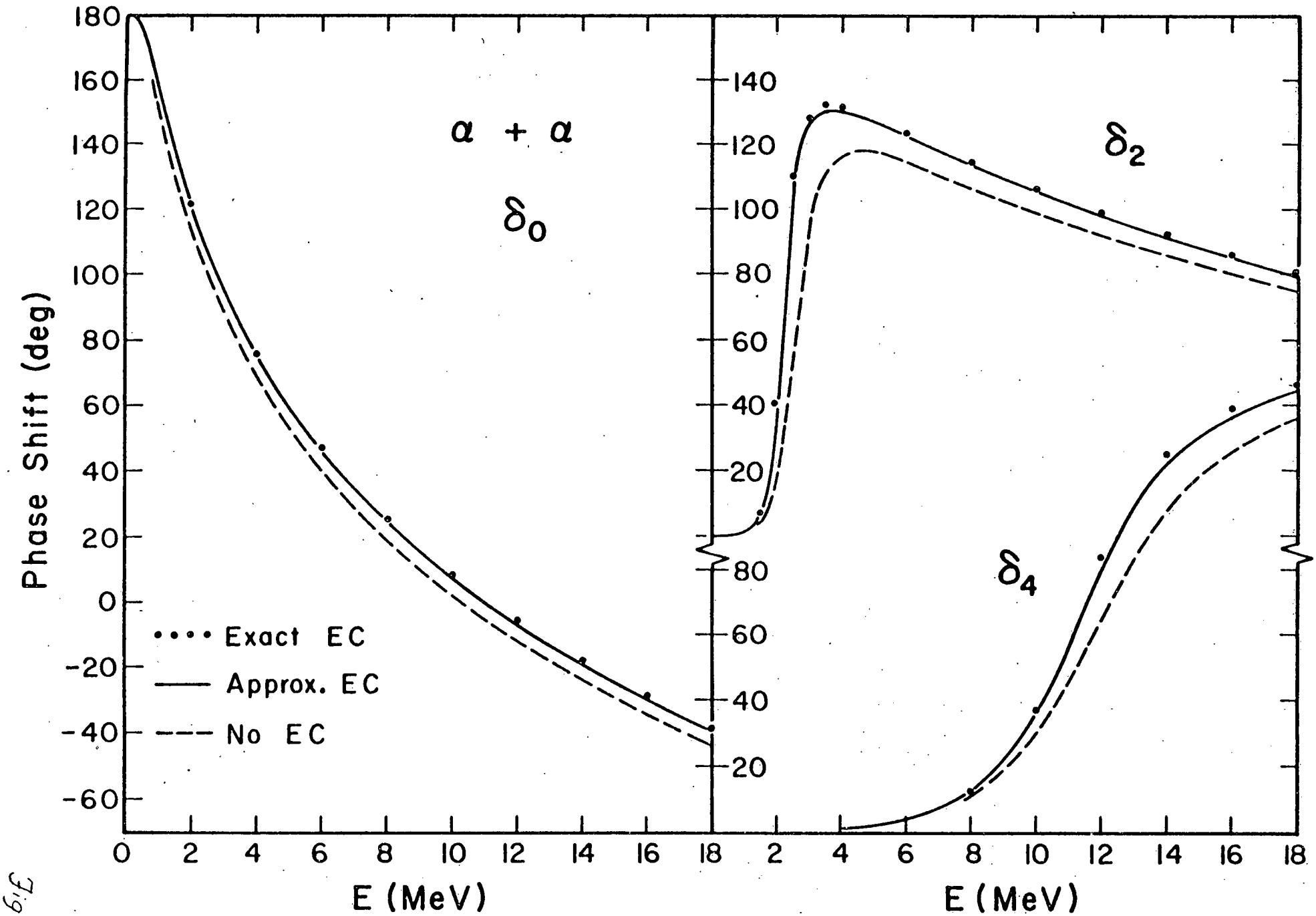

Fig 21